The Thesis Committee for Serdar Bender
Certifies that this is the approved version of the following thesis:

Co-optimization of CO_2 Sequestration and Enhanced Oil Recovery and Co-optimization of CO_2 Sequestration and Methane Recovery in Geopressured Aquifers

APPROVED BY
SUPERVISING COMMITTEE:

Supervisors:

Kamy Sepehrnoori

Christopher Jablonowski

Co-optimization of CO_2 Sequestration and Enhanced Oil Recovery and Co-optimization of CO_2 Sequestration and Methane Recovery in Geopressured Aquifers

by

Serdar Bender, B.S.

Thesis

Presented to the Faculty of the Graduate School of

The University of Texas at Austin

in Partial Fulfillment

of the Requirements

for the Degree of

MASTER OF SCIENCE IN ENGINEERING

The University of Texas at Austin

August 2011

Dedication

This thesis is dedicated to Mustafa Kemal Ataturk, who is the founder of the Turkish Republic. It is also dedicated to my father, Kaplan Bender, my mother, Sati Bender, my sister, Simay Bender, and my fiancé, Cansu Bender, who have been a great source of motivation and inspiration.

Acknowledgements

First of all, I am heartily thankful to my supervisors, Kamy Sepehrnoori and Christopher Jablonowski for their guidance, support and patience during this thesis. This was a very valuable experience for my future career. I also would like to thank my colleagues, Reza Ganjdanesh, Luiz Schmall, and Abdoljalil Varavei for their advice and suggestions.

Finally, I am grateful to the Turkish Petroleum Corporation for their full financial support.

August 2011

Abstract

Co-optimization of CO_2 Sequestration and Enhanced Oil Recovery and Co-optimization of CO_2 Sequestration and Methane Recovery in Geopressured Aquifers

Serdar Bender, M.S.E.

The University of Texas at Austin, 2011

Supervisors: Kamy Sepehrnoori and Christopher Jablonowski

In this study, the co-optimization of carbon dioxide sequestration and enhanced oil recovery and the co-optimization of carbon dioxide sequestration and methane recovery studies were discussed. Carbon dioxide emissions in the atmosphere are one of the reasons of global warming and can be decreased by capturing and storing carbon dioxide. Our aim in this study is to maximize the amount of carbon dioxide sequestered to decrease carbon dioxide emissions in the atmosphere and maximize the oil or methane recovery to increase profit or to make a project profitable. Experimental design and response surface methodology are used to co-optimize the carbon dioxide sequestration and enhanced oil recovery and carbon dioxide sequestration and methane recovery. At

the end of this study, under which circumstances these projects are profitable and under which circumstances carbon dioxide sequestration can be maximized, are given.

Table of Contents

List of Tables

List of Figures

Chapter 1: Introduction

In recent years, there has been concern about global warming and carbon dioxide is one of the greenhouse gasses. Among greenhouse gases, the global radioactive forcing of carbon dioxide is almost sixty percent, which means that carbon dioxide emissions have more effect on climate change when compared with others (McCarthy et al., 2001). Capture and storage of carbon dioxide is one of the methods that will prevent the carbon dioxide emissions in to the atmosphere (Hoffert et al., 2002). According to Ghomian (2008), carbon dioxide injection into coal seams, mature or depleted oil and gas reservoirs and deep aquifers are the ways to store carbon dioxide in geological sinks. The aim of enhanced oil recovery projects is to increase the oil recovery and decrease the amount of carbon dioxide injected. However, today in developed countries the aim is to increase the oil recovery and the amount of carbon dioxide sequestered because of its greenhouse effect. According to Petrusak et al. (2009), 29.7-34.7 gigatonnes of carbon dioxide can be sequestered while producing 24 million barrels of oil from depleted oil and gas fields. Sequestration of carbon dioxide in deep saline aquifers seems a non-economic investment when compared to enhanced oil recovery projects because there is no production of energy from such aquifers. According to Lee and Kyonggi (2000), dissolved natural gas can be found in geopressured-geothermal aquifers, most of which is methane. Dissolved methane can be produced while sequestering the carbon dioxide; in addition, these aquifers have long-term storage capability because of their size. These aspects of deep saline aquifers should render it quite economical.

This study is divided into two main parts. The first part is the co-optimization of carbon dioxide sequestration and enhanced oil recovery for depleted oil reservoirs, and the second part is the co-optimization of carbon dioxide sequestration and methane

recovery from geopressured-geothermal aquifers. In the first part, the aim is to find the best strategy to maximize the carbon dioxide storage and oil recovery. The water alternating solvent injection method is performed and compared with the water alternating pure carbon dioxide injection method. In the second part, the goal is to understand under which circumstances the carbon dioxide storage and methane recovery process can be profitable. Different scenarios are built by using well location, well configuration, and economical parameters. In these scenarios, the water enriched carbon dioxide injection method is applied.

This thesis consists of five chapters:

Chapter 1 gives information about the aim of this study and provides general information about each chapter. Chapter 2 presents the literature review. In the second chapter, the literature review about the applications of carbon dioxide sequestration and enhanced oil recovery by using different injection methods, the methane extraction from saline aquifers by injecting carbon dioxide, experimental and response surface methodologies are discussed.

Chapter 3 discusses the co-optimization of carbon dioxide storage and oil recovery. In this chapter, the water alternating solvent gas injection process is applied and co-optimized by using experimental design and response surface methodologies. Sensitivity analysis is performed to understand the effect of the most important parameters on carbon dioxide flooding. In the design, the aim is set as maximizing both amount of carbon dioxide sequestered and profit.

In Chapter 4, carbon dioxide sequestration and the methane extraction process are discussed. The carbon dioxide enriched water injection and methane extraction method is applied and co-optimized by using experimental design and response surface methodologies. In this project, the aim is to maximize the methane production and carbon

dioxide sequestration by changing well coordinates, well configuration, and economical parameters. The final chapter summarizes this study and presents the conclusion and recommendations for future work.

Chapter 2: Literature Review

Fossil fuel burning is the predominant reason for increasing the concentrations of the leading greenhouse gas, carbon dioxide (Bachu, 2000). Because of the carbon dioxides greenhouse effect, developed countries are searching for ways to decrease the carbon dioxide concentration in the atmosphere. One of the ways suggested by the Kyoto Protocol to decrease the carbon dioxide emission is the sequestration of carbon dioxide in underground (Gallo, Couillens, & Manai, 2002).

Coal seams, deep saline formations, depleted oil, and gas reservoirs are good candidates for geological sequestration of carbon dioxide. Also, these formations can be evaluated by producing oil and methane (Ennis-King & Lincoln, 2002). The major advantage of depleted oil reservoirs is that residual oil can be produced while injecting carbon dioxide, which should make the project profitable. According to Freund, et al. (2000), 0.3% of the world oil production originates from carbon dioxide enhanced oil recovery. There are many economical parameters affecting the cost of the sequestration process. The most important parameter is reservoir properties which will affect the amount of CO_2 that can be sequestered, the amount of oil that can be recovered, and the duration of the project. Depending on these properties and other parameters, the sequestration process costs between five and twenty dollars per tonne (Nguyen, 2003).

There are different methods for carbon dioxide sequestration and enhanced oil recovery. Pure carbon dioxide injection and water alternating gas injection are the methods that have shown great success for sequestration and economic aspects. Forooghi, et al. (2009) showed that water alternating gas injection and water alternating solvent gas injection methods are better for enhanced oil recovery and carbon dioxide sequestration when compared with the continuous carbon dioxide injection method for their reservoir

under study. They also concluded that the continuous carbon dioxide injection method is more efficient, if the aim of the project is to sequester the maximum amount of carbon dioxide.

Water alternating gas injection and continuous gas injection methods are used to improve oil recovery. These methods can be modified by changing the gas content, water alternating gas (WAG) ratios, etc. The aim of the water alternating gas injection method is to increase oil recovery by decreasing the mobility ratio between gas and oil. While the sweep efficiency for gas injection is 60%, it becomes 90% for simultaneous water gas injection (Rogers and Grigg, 2001). WAG ratio, slug size, injection-production rates, and bottomhole pressure are the variables which have great impact on the success of the water alternating gas injection method (Chen, et al., 2009). In this method, it is important to decide the best ratio of water and gas to increase oil recovery. According to Wu, et al. (2004), the water alternating gas injection method will act as a water flooding method when the WAG ratio is increased. In addition, if the gas amount is very high compared with the water amount, the water alternating gas injection method will act as a continuous gas injection method.

In the literature, there are several studies about the water alternating gas injection method. This method shows great success in field applications. The key to the success of the project is to determine the optimum values for the parameters. Water alternating gas ratio, injection rates, slug size, and type of the displacement are the parameters which have great impact on the water alternating gas injection method (Sanchez, 1999).

The water alternating gas injection method was used in Siiri-A which is a well-known as, offshore producing field (Taheri and Sajjadian, 2006). The well configuration included both horizontal producers and injectors. Different water alternating gas ratios, slug sizes and three-phase relative permeability models were used. It was concluded that

the water alternating gas injection method with a horizontal well configuration was the most attractive scenario in the way of oil recovery and economics for this low permeability and low porosity reservoir (Taheri and Sajjadian, 2006). Also, horizontal wells were used in an offshore field which is located in the Middle East. Different well configurations and injection methods were used to increase the oil recovery in that field. Among these, it was shown that oil recovery increased four-fold by using the water alternating gas injection method and that horizontal wells better increased oil recovery (Schneider and Shi, 2005).

Experimental studies show that oil viscosity has a greater impact than injection rate and permeability on heavy oil production. Also, the level of oil viscosity affects the injection method used to increase oil production. If oil viscosity is not low, the water flooding method is optional to increase oil recovery. However; if oil viscosity is low, the water alternating gas injection method is optional to increase oil recovery (Torabi, et al., 2010). The water flooding method was compared with the immiscible water alternating gas injection method. Results showed that the water alternating gas injection method provided better recovery from core flooding experiments. It was concluded that displacement is not only affected by the viscosity, but also by interfacial tension and swelling of the oil (Righi, et al., 2004).

The most important tasks in the water alternating gas injection method are optimizing the parameters that affect the recovery, the amount of carbon dioxide, and the economics of the project. There is a significant difference in recovery and economics between optimized and un-optimized processes. In the literature, several papers show the success of optimization. Optimization was performed using the proper injection rate and bottomhole pressure for producers as well as checking the results of water flooding, carbon dioxide flooding, and water alternating gas injection with and without

optimization. Results show that an additional 6.4% of oil was recovered by optimizing the water alternating gas injection method (Chen et al., 2010). Another study used the filtering Ensemble Kalman approach. This approach is used to optimize the water alternating gas injection process by using carbon dioxide injection rate, water injection rate and water alternating gas cycles as parameters. Storage of carbon dioxide and oil recovery is chosen as objective functions that need to be maximized. It has been observed that oil recovery is increased by 11%, showing the success of the optimization (Odi and Gupta, 2010).

As discussed before the effect of carbon dioxide emissions have a significant impact on global warming. The use of carbon dioxide to increase the oil recovery began in the 1960s. Today, because of its effects on global warming, geological storage of carbon dioxide is being performed. Aquifers, depleted reservoirs, and oil reservoirs are options to store carbon dioxide (Vidiuk and Cunha, 2007). Geopressured aquifers are good candidates for CO_2 injection due to its contributions to the economics of the project. Geopressured aquifers can be used to produce energy as hot pressured brine with natural gas exists in these aquifers. By using turbines, electricity can be generated from the high flow rates and geothermal energy can be produced by using the hot brine. In addition, natural gas can be produced from geopressured-geothermal aquifers (Hawkins and Parmigiano, 1973).

Several studies regarding the economics of methane production and energy generation from geopressured geothermal reservoirs exist. One such study used geopressured reservoir only for methane production and produced brine was not reinjected into the reservoir. They showed that the project was not profitable due to the size of the reservoir and other expenses (Doscher et al., 1979). Another study about geopressured aquifers showed that by injecting the produced brine into the aquifer could

improve the methane production and reinjecting costs can be decreased by using the energy from the heat and flowrate (Hammershaimb and Kuuskraa, 1984). Reinjecting the produced brine is an important process while producing from the geopressured reservoirs to obstruct the sudden pressure drops, which affect the amount of gas production and energy generation from flow and heat. The reinjection process should improve the recovery by 3% to 50% (Matthews, 1981).

There are lots of parameters affecting the methane production and electricity generation from geopressured geothermal reservoirs, and carbon dioxide sequestration in geopressured geothermal reservoirs. Due to the effect of carbon dioxide on global warming, it needs to be stored safely. The amount of carbon dioxide sequestered can be increased by dissolving it in brine. This can be improved by increasing the migration way of the carbon dioxide (Kartikasurja et al., 2008). Dissolving the carbon dioxide in brine will make it immobile and also keep it in the reservoir (Kumar et al., 2004). Keeping the carbon dioxide in the reservoir is one of the most important tasks due to environmental concerns. Permeability and porosity are important parameters affecting the amount of carbon dioxide storage as a residual gas. It is stated that this amount decreases with an increase in porosity and permeability (Ozah et al., 2006). Another concern about carbon dioxide sequestration is increasing the reservoir pressure due to the injection of large amounts of carbon dioxide. This can be solved by producing the brine, purifying it, and injecting again (Akinnikawe et al., 2010). Another study showed that saturating the produced brine with carbon dioxide and reinjecting it into the same reservoir could prevent the carbon dioxide from escaping the reservoir (Burton and Steven, 2007).

Geothermal energy is provided from the heat of the center of earth. Water at certain depths is hot and should be utilized to produce geothermal energy. For instance, the heat from the produced water can be used to generate electricity. There are two kinds

of geothermal reservoirs which are named as “steam type” (e.g.; geysers) and “hot water reservoirs” (Bayliss, 1972). As stated before, the current study considers carbon dioxide sequestration and methane extraction; therefore; we focus on hot water reservoirs. Geothermal energy can be used to offset the costs due to carbon dioxide sequestration and methane extraction. Temperature and pressure are the important parameters to generate electricity efficiently. Facilities need to be chosen according to temperature and pressure of the reservoir. Binary cycle power plants are good candidates for generating electricity from fluids whose temperature is not high (Budd, 1984).

Chapter 3: Co-optimization of CO_2 Sequestration and Enhanced Oil Recovery

3.1 INTRODUCTION

Carbon dioxide injection into oil reservoirs is a traditional method to increase oil recovery. In this respect, the aim is to increase oil recovery by using a minimum amount of CO_2, because companies need to purchase the CO_2 to be used for such a process. However, our aim in this work is to increase both oil recovery and the amount of CO_2 sequestered. The earth's temperature is affected by greenhouse gases in the atmosphere, such as CO_2. The concentration of CO_2 in the atmosphere is increasing each day. According to Keeling CD et al. (1995), the concentration of CO_2 in the atmosphere was 270 parts per million two hundred and fifty years ago; today, it is 370 parts per million. The concentration of CO_2 in the atmosphere can be reduced by capturing it and injecting it into geological formations. These geological formations can be depleted by oil and gas reservoirs, deep saline aquifers, coal seams, or mature oil and gas reservoirs (Ghomian, 2008).

In this chapter, experimental design and response surface methodology is used to co-optimize the recovery and storage by applying the water alternating solvent gas injection process. The aim of the water injection is to decrease the mobility of CO_2 in the reservoir. The solvent gas consists of CO_2 and light hydrocarbon gases. These light hydrocarbon gasses are injected with CO_2, to decrease the minimum miscibility pressure (MMP) so that residual oil can be produced. Kovcek et al. (2005) showed that injecting a mole fraction of 0.667 CO_2, 0.125 C2H6, 0.125 C3H8, and 0.083 C4H10 decreases the minimum miscibility pressure from 600 atm to below 250 atm for their reservoir under study. In this study, Kovcek et al.; (2005) method is modified and used to increase both CO_2 storage and oil recovery. Table 3-3 shows the modified version of the solvent.

Lastly, we perform the co-optimization of the CO_2 flooding and enhanced oil recovery by using experimental design and response surface methodology. Co-optimized results for water alternating solvent gas injection method are compared with those of the water alternating carbon dioxide injection method.

3.2 RESERVOIR DESCRIPTION AND DEVELOPMENT PLAN

3.2.1 Reservoir Description

This section of the study describes the properties of the reservoir model used to co-optimize carbon dioxide sequestration and recovery. The same model was used by Salazar (2009) and Ghomian (2008). This model is a sandstone oil reservoir. The three-dimensional corner point grid has the dimensions 90 ft x 87.5 ft x 10 ft with 16800 grid blocks given by 28 x 40 x 15 in the x, y, and z directions, respectively. In this model, there are two adjacent anticline domes at 6140 ft with a thickness of 150 ft. The depth of water-oil contact is 6400 ft and reservoir fluids are considered to be in a vertical equilibrium. There is no active power source for the reservoir. A summary of the reservoir properties is given in Table 3-1.The three-dimensional corner point reservoir model is shown in Figure 3-1. The fluid properties were modeled with a Peng-Robinson equation of state. The reservoir fluid description is presented in Table 3-2.

Table 3-1: Summary of the Reservoir Properties

Parameters	Values	Units
Number of cells in the x direction	28	
Number of cells in the y direction	40	
Number of cells in the z direction	15	
Number of gridblocks	28x40x15	

Table 3-1: Continued

Parameters	Values	Units
x gridblock size	90	ft
y gridblock size	87.5	ft
z gridblock size	10	ft
Width	2520	ft
Length	3500	ft
Thickness	150	ft
Depth	6140	ft
Pressure	3000	psia
Temperature	110	F
Average Horizontal Permeability	113	md
Average Vertical Permeability	11	md
Average Porosity	0.19	
kv/kh	0.1	
Depth of WOC	6400	ft
Bo	1.12	bbl/STB
Solution GOR	244	scf/STB
Soi	0.31	
OOIP	12.1	MMSTB

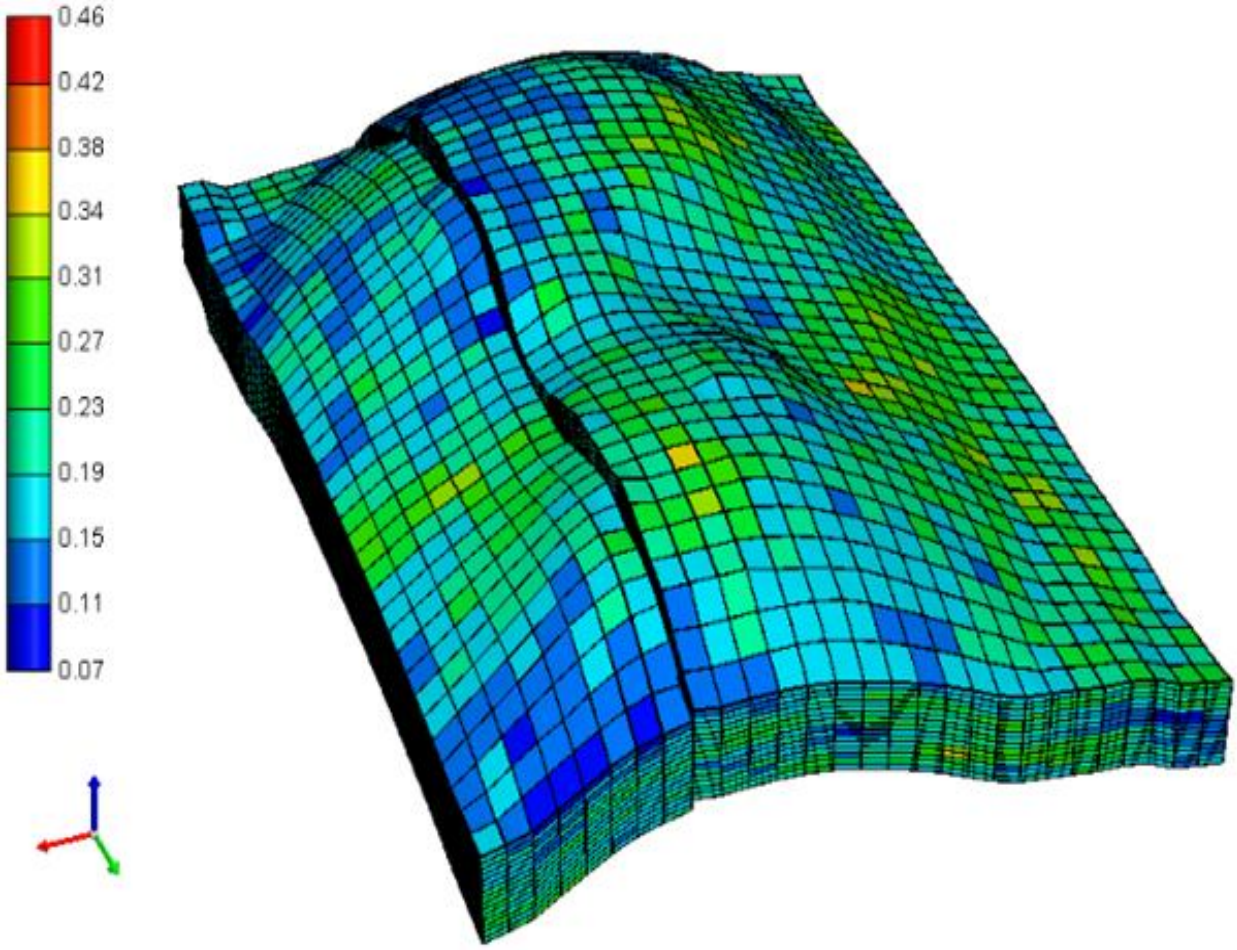

Figure 3-1: Three-Dimensional Corner Point Reservoir Model, Porosity

Table 3-2: Reservoir Fluid Description

Component	Mole Fraction	Pc (atm)	Tc (K)	Accentric factor	Molecular weight g/gmole
CO_2	0.0192	7.28E+01	303.8913	2.25E-01	4.40E+01
C1	0.069	4.54E+01	166.668	8.00E-03	1.60E+01
C2-3	0.174	4.49E+01	338.336	1.26E-01	3.60E+01
C4-6	0.1944	3.32E+01	466.1148	2.44E-01	7.05E+01
C7-16	0.314	2.07E+01	611.116	6.39E-01	1.47E+02
C17-29	0.155	1.57E+01	777.784	1.00E+00	3.01E+02
C30+	0.0742	1.56E+01	972.23	1.28E+00	5.63E+02

3.2.2 Development Plan

Before starting the solvent injection, oil production was carry out by thirteen vertical production wells for one hundred and forty days (See Figure 3-2). Then, six vertical injection wells were opened for water flooding (See Figure 3-3). Water flooding continued for ten years and ten months. Maximum flowing bottom hole pressure for the injection wells was 3300 psia and the water cut limit was 98%. During these periods 12.8 % of the original oil in place was produced, which was 1.553 MMSTB.

After the completion of the water flooding project, the water alternating solvent injection project began. In this project, all of the produced CO_2 and solvent was recycled and reused. If produced water was in excess the needs, excess produced water was re-injected into a disposal well. The composition of the solvent is given in Table 3-3. For this project six water injection wells were closed, two of them were converted to production wells and three new injection wells were opened (See Figure 3-4). Water and solvent were injected alternatively from the same coordinates. The maximum gas oil ratio was set to 30000 SCF/STB and the water cut limit was set to 98%. Operating properties for the production and injection wells during solvent injection are given in Table 3-4.

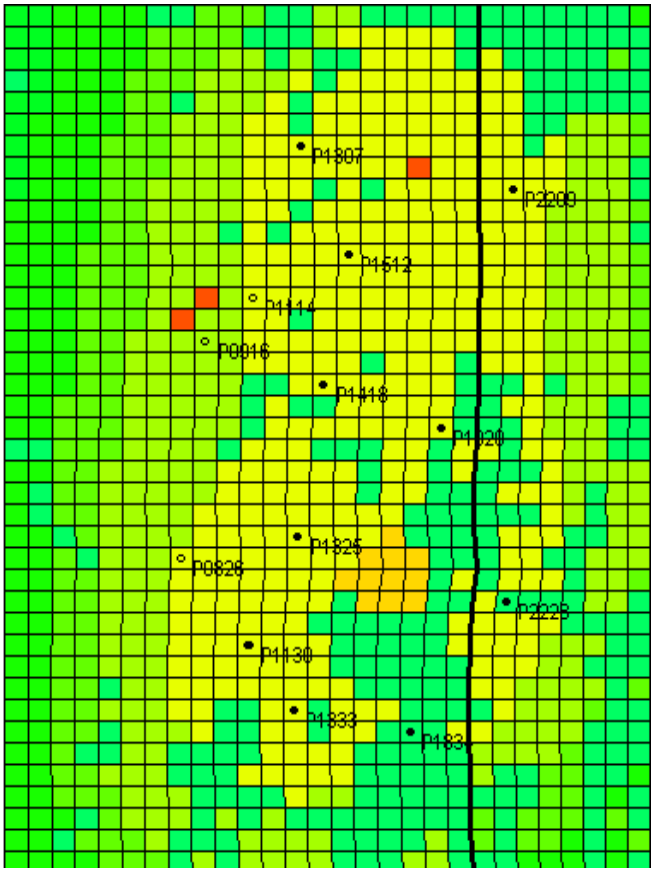

Figure 3-2: Oil Saturation Map of the Reservoir with Well Patterns (Primary Production)

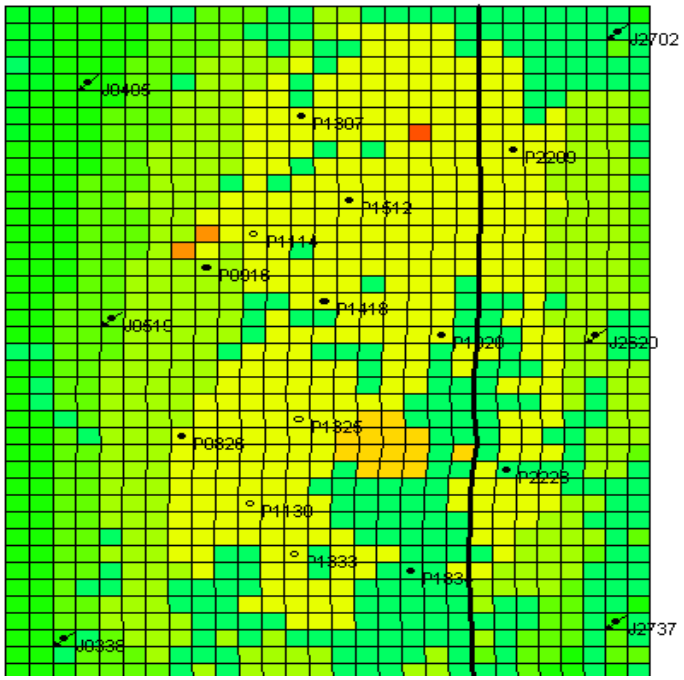

Figure 3-3: Oil Saturation Map of the Reservoir with Well Patterns (Water Flooding)

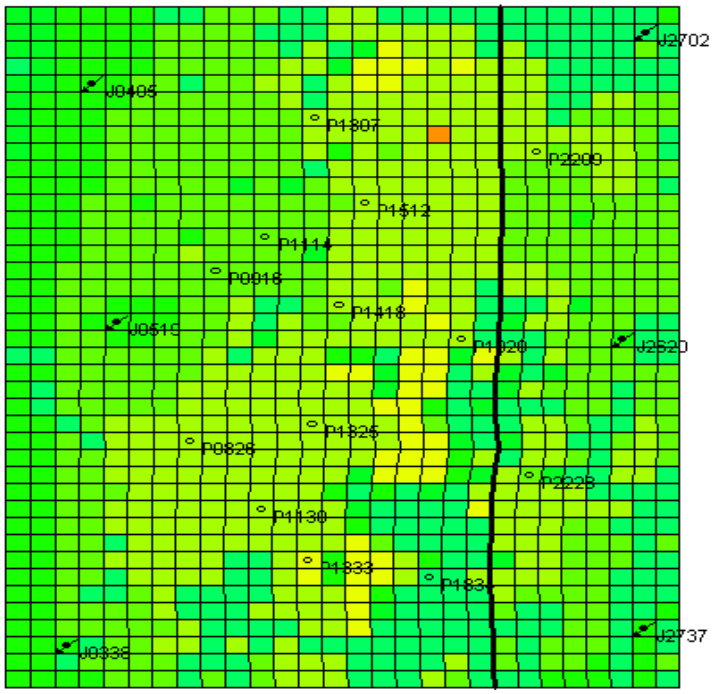

Figure 3-4: Oil Saturation Map of the Reservoir with Well Patterns (CO_2 Flooding)

Table 3-3: Composition of the Solvent (Mole Fraction)

Solvent	Values	Units
CO_2	0.667	%
C2-3	0.250	%
C4	0.083	%

Table 3-4: Operating Properties for the Production and Injection Wells During Solvent Injection

Production wells	Values	Units
Minimum flowing bottom hole pressure	1300	psia
Water cut limit	0.98	
Type	vertical	
Number	15	
Water injection wells		
Maximum flowing bottom hole pressure	3300	psia
Type	vertical	
Number	3	
Solvent Injection wells		
Maximum flowing bottom hole pressure	3300	psia
Type	vertical	
Number	3	

3.3 ENHANCED OIL RECOVERY ECONOMIC MODEL

In this section, the economic model used in this study is presented. To achieve this model, some of the equations used by Ghomian (2008) are modified to build a new model. To estimate the net cash flow, a code using Excel was written to post-process the reservoir and economic data to perform the economic analysis for this study. Table 3-5 shows the input data from the simulator and Table 3-6 shows the economic input data. Table 3-7 shows the calculated parameters to obtain the NPV. For the net cash flow calculations, an Excel spreadsheet was prepared and modified for each run.

Table 3-5: Input Data from the Simulator

	Units	Symbol
Oil Production	bbl/day	Opro
Water Production	bbl/day	Wpro
Water Injection	bbl/day	Winj
CO_2 Production	ft3/day	CO_2pro
CO_2 Injection	ft3/day	CO_2inj
Solvent Production	ft3/day	Spro
Solvent Injection	ft3/day	Sinj
Time	day	t

Table 3-6: Economic Input Data

	Units	Symbol	Low	Base	High
Total Investment	MM$	Tinv	7	14	21
Intangible Drilling Costs for Three Wells	MM$	IDC	4	8	12
Oil Price	$/bbl	OP	40	78	120
Oil Price Nominal Growth	fraction/year	OPI	0	0.02	0.05
Royalty	fraction	ROY		0.125	
Discount Rate	fraction/year	DR		0.08	
Fed Tax Rate	fraction	FTR	0.2	0.32	0.45
Local/State (Production) Taxes (sev)	$/STB	SEV	0	0.05	0.1
EOR Tax Credit Rate	fraction	EORTC	0	0.15	0.3
Lift Cost	$/bbl	LC	0.1	0.25	0.50
Lift Cost Nominal Growth	fraction/year	OCI	0	0.02	0.05
CO_2 Price	$/mcf	CO_2P	0	1	2
CO_2 Price Inflation	fraction/year		0	0.02	0.05
Recycle Cost for CO_2	$/mcf	RecCO_2	0.25	0.75	1.25
CO_2 Recycle Cost Inflation	fraction/year		0	0.02	0.05
CO_2 Injection Cost (compressor)	$/mcf	Included in Total Gas & Water Recycling & Operational Costs			
CO_2 Injection Cost Inflation	fraction/year				
Solvent Price	$/mcf	SP		7.5	

Table 3-6: Continued

	Units	Symbol	Low	Base	High
Solvent Price Inflation	fraction/year				
Recycle Cost for Solvent	$/mcf	RecS		0.02	
Solvent Recycle Cost Inflation	fraction/year				
Solvent Injection Cost (compressor)	$/mcf	Included in Total Gas & Water Recycling & Operational Costs			
Solvent Injection Cost Inflation	fraction/year				
Water Injection Cost	$/bbl	WIC		0.5	
Water Injection Cost Inflation	fraction/year		0	0.02	0.05

Table 3-7: Output Data

	Units	Symbol
Oil Revenue	mm$/yr	Orev
CO_2 Purchase Price	mm$/yr	CO_2PP
Solvent Purchase Price	mm$/yr	SolPP
Total Gas Recycling & Operational Cost	mm$/yr	TGROPC
Water Injection Cost	mm$/yr	WIC
Lift Cost	mm$/yr	LC
OC Income Before Tax	mm$/yr	OCIBT
Cumulative NCF Before Tax	mm$	CNCFBT
Depreciation	mm$/yr	Dep
Fed Income Tax	mm$/yr	FIT
EOR Tax Credit	mm$/yr	EORTC
OC Income After Tax	mm$/yr	OCIAT
Cumulative NCF After Tax	mm$	CNCFAT
Discounted Cumulative NCF After Tax	mm$	DCNCFAT

3.3.1 Calculation Algorithm

As mentioned previously, the aim of this project is to co-optimize the oil recovery and carbon dioxide storage. To perform the mentioned task, net income and CO_2 storage

are selected as response functions. Net income for water alternating and solvent gas injection enhanced oil recovery method is calculated for each run by the formulas given below. Oil production, water production, water injection, CO_2 production, CO_2 injection, solvent production, solvent injection, and time is obtained from the simulator on a daily basis; hence, in the equations we use a 365.25 to convert them to a yearly basis. Near the equations, it is written "Take Credit" and "No Credit". "Take Credit" means that credit is applied for the injected amount of CO_2 and "No Credit" means that credit is not applied for CO_2 injection. At the end of the calculations, NPV is determined for "Take Credit" and "No Credit" options.

Oil Revenue (mm$/yr) =

$$\frac{\text{Oil Production(mstb/day)} * 365.25 * \text{Oil Price(\$/stb)} * (1\text{-Royalty}) * \left((Oil\ \text{Price Inflation} + 1)^{t}\right)}{1000}$$

CO_2 Purchase Cost (mm$/yr) =

$$\frac{Max\left((CO2Inj(mmscf\ /\ day) - CO2\ \text{Pro(mmscf/day)}), 0\right) * 365.25 * CO2\ \text{Price(\$/mcf)}}{1000}$$

Solvent Purchase Cost (mm$/yr) =

$$\frac{Max\left((Solvent\ Inj(mmscf\ /\ day) - Solvent\ \text{Pro(mmscf/day)}), 0\right) * 365.25 * Solvent\ \text{Price(\$/mcf)}}{1000}$$

Total Gas & Water Recycling & Operational Cost (mm$/yr) =

$$\left(\frac{\left(\text{CO2 Pro(mmscf/day)} * \text{Recycle Cost}^{CO2}(\text{\$/mcf}) + \text{Solvent Pro(mmscf/day)} * \text{Recycle Cost}^{Solvent}(\text{\$/mcf})\right)}{1000} + \frac{\text{Water Pro(mbbl/day)} * \text{Recycle Cost}^{Water}(\$ / bbl)}{1000}\right) * \left((\text{Operational Cost Inflation}+1)^{t}\right) * 365.25$$

Water Injection Cost (mm$/yr) =

$$\frac{\left(\text{Water Inj(mstb/day)} * 365.25 * \text{Water Inj Cost(\$/stb)}\right) * \left((\text{Operational Cost Inflation}+1)^{t}\right)}{1000}$$

CO_2 Injection Cost (mm$/yr) =

$$\frac{\left(\text{CO2 Inj(mmscf/day)} * 365.25 * \text{CO2 Inj Cost(\$/mmscf)}\right) * \left((\text{Operational Cost Inflation}+1)^{t}\right)}{1000}$$

Solvent Injection Cost (mm$/yr) =

$$\frac{\left(\text{Solvent Inj(mmscf/day)} * 365.25 * \text{Solvent Inj Cost(\$/mmscf)}\right) * \left((\text{Operational Cost Inflation}+1)^{t}\right)}{1000}$$

Lift Cost (mm$/yr) =

$$\frac{\left(\text{Oil Pro(mstb/day)} + \text{ Water Pro(mstb/day)}\right) * 365.25 * \text{Lift Cost(\$/stb)} * \left((\text{Operational Cost Inflation}+1)^{t}\right)}{1000}$$

Production Taxes (state, Texas), (mm$/yr) =

Oil Revenue(mm$/yr)*Production Tax(fraction)

Taxable Income (Take Credit), (mm$) =

For the first calculation;

=

Oil Revenue(mm$/yr)*t(yr)-Intangible Drilling & Comp Costs(mm$)*(1-EOR Tax Credit Rate)

-Production Taxes(mm$/yr)*t(yr)

$$-\begin{pmatrix} \text{Lift Cost(mm\$/yr)+Solvent Injection Cost(mm\$/yr)+CO2 Injection Cost(mm\$/yr)} \\ +\text{Water Injection Cost(mm\$/yr)} + \text{Gas \& Water Recycle \& Operation Cost(mm\$/yr)} \\ +\text{Solvent Purchase Price(mm\$/yr)} + \text{CO2 Purchase Price(mm\$/yr)} + \text{Depreciation(mm\$/yr)} \end{pmatrix}$$

t(yr)(1-EOR Tax Credit Rate)

For other calculations (at time= t_i);

=

Oil Revenue(mm$/yr)*($t_i$(yr)-$t_{i-1}$(yr))

-Production Taxes(mm$/yr)*($t_i$(yr)-$t_{i-1}$(yr))

$$-\begin{pmatrix}\text{Lift Cost(mm\$/yr)+Solvent Injection Cost(mm\$/yr)+CO2 Injection Cost(mm\$/yr)}\\ +\text{Water Injection Cost(mm\$/yr)}+\text{Gas \& Water Recycle \& Operation Cost(mm\$/yr)}\\ +\text{Solvent Purchase Price(mm\$/yr)}+\text{CO2 Purchase Price(mm\$/yr)}+\text{Depreciation(mm\$/yr)}\end{pmatrix}$$

(t_i(yr)-t_{i-1}(yr))(1-EOR Tax Credit Rate)

Taxable Income (No Credit), (mm$) =

For the first calculation;

=

Oil Revenue(mm$/yr)*t(yr)-Intangible Drilling & Comp Costs(mm$)

-Production Taxes(mm$/yr)*t(yr)

$$-\begin{pmatrix}\text{Lift Cost(mm\$/yr)+Solvent Injection Cost(mm\$/yr)+CO2 Injection Cost(mm\$/yr)}\\ +\text{Water Injection Cost(mm\$/yr)}+\text{Gas \& Water Recycle \& Operation Cost(mm\$/yr)}\\ +\text{Solvent Purchase Price(mm\$/yr)}+\text{CO2 Purchase Price(mm\$/yr)}+\text{Depreciation(mm\$/yr)}\end{pmatrix}$$

*t(yr)

For other calculations (at time=t_i);

=

Oil Revenue(mm$/yr)*($t_i$(yr)-$t_{i-1}$(yr))

-Production Taxes(mm$/yr)*($t_i$(yr)-$t_{i-1}$(yr))

$$-\begin{pmatrix}\text{Lift Cost(mm\$/yr)+Solvent Injection Cost(mm\$/yr)+CO2 Injection Cost(mm\$/yr)}\\ +\text{Water Injection Cost(mm\$/yr)}+\text{Gas \& Water Recycle \& Operation Cost(mm\$/yr)}\\ +\text{Solvent Purchase Price(mm\$/yr)}+\text{CO2 Purchase Price(mm\$/yr)}+\text{Depreciation(mm\$/yr)}\end{pmatrix}$$

*(t_i(yr)-t_{i-1}(yr))

EOR Tax Credit We Get (mm$) =

Taxable Income (Take Credit), (mm$) - Taxable Income (No Credit), (mm$)

Federal Income Tax (for Credit Option) (mm$) =

Taxable Income (Take Credit), (mm$)*Federal Tax Rate

Federal Income Tax (for Non-Credit Option) (mm$) =

Taxable Income (No Credit), (mm$)*Federal Tax Rate

Previously Undeducted Operating Costs (mm$) =

For the first calculation;

EOR Tax Credit We Get (mm$) - Depreciation (mm$/yr)*t(yr)*EOR Tax Credit Rate

For other calculations (at time= t_i);

EOR Tax Credit We Get (mm$) - Depreciation (mm$/yr)* $(t_i(yr)-t_{i-1}(yr))$ *EOR Tax Credit Rate

After Tax Income (for Credit Option) (mm$)=

Taxable Income (Take Credit), (mm$) - Federal Income Tax (mm$)

-Previously Undeducted Operating Costs (mm$)

After Tax Income (for Non-Credit Option) (mm$)=

Taxable Income (No Credit), (mm$) - Federal Income Tax (mm$)

After Tax Cash Flow to Equity (mm$)=

For the first calculation;

=After Tax Income (mm$) + (Depreciation (mm$/yr)* t(yr)*(1-EOR Tax Credit Rate) + EOR Tax Credit We Get (mm$)

For other calculations (at time= t_i);

=After Tax Income (mm$) + (Depreciation (mm$/yr)* $(t_i(yr)-t_{i-1}(yr))$ *(1-EOR Tax Credit Rate) + EOR Tax Credit We Get (mm$)

After Tax Cash Flow to Equity (mm$) (for Non-Credit Option) =

For the first calculation;

=After Tax Income (for Non-Credit Option) (mm$) + (Depreciation (mm$/yr)* t(yr)

For other calculations (at time= t_i);

=After Tax Income (mm$) (for Non-Credit Option) + (Depreciation (mm$/yr)* ($t_i$(yr)-$t_{i-1}$(yr))

Discounted Cash Flow (for Non-Credit Option) (mm$) =

$$\frac{\text{AfterTax Cash Flow to Equity } (\text{mm\$}) \ (\text{for Non} - \text{Credit Option})}{(\text{Discount Rate}+1)^{t_i}}$$

Discounted Cash Flow (for Credit Option) (mm$) =

$$\frac{\text{AfterTax Cash Flow to Equity } (\text{mm\$}) \ (\text{for } C\text{redit Option})}{(\text{Discount Rate}+1)^{t_i}}$$

Cumulative Discounted Cash Flow (for Non-Credit Option) (mm$) =

For the first calculation;

= Discounted Cash Flow (for Non-Credit Option) (mm$) – Capital Investment (mm$)

For other calculations (at time= t_i);

$$= \text{Discounted Cash Flow } (\text{for Non} - \text{Credit Option})(\text{mm\$})_i$$

$$+ \text{Discounted Cash Flow } (\text{for Non} - \text{Credit Option})(\text{mm\$})_{i-1}$$

Cumulative Discounted Cash Flow (for Credit Option) (mm$)=

For the first calculation;

= Discounted Cash Flow (for Credit Option) (mm$) – Capital Investment (mm$)

For other calculations (at time= t_i);

$$= \text{Discounted Cash Flow } (\text{for Credit Option})(\text{mm\$})_i$$

$$+ \text{Discounted Cash Flow } (\text{for Credit Option})(\text{mm\$})_{i-1}$$

3.4 CO_2 SEQUESTRATION AND ENHANCED OIL RECOVERY CO-OPTIMIZATION

In this section, experimental design and response surface methodology is used to co-optimize the CO_2 sequestration and enhanced oil recovery. Factors which have great impact on the response functions were selected to make the design more accurate. These factors can be divided into two types: numerical and categorical factors. Total CO_2 slug

size, the ratio of water-gas, injection rate of the CO_2, coordinates of the injectors, and drilling time for the last injector were the numerical factors and well design was the categorical factor. NPV and the amount of CO_2 sequestered were selected as response functions. These design variables were also used by Salazar (2009). Design variables, their ranges, and response functions are shown in Table 3-8.

Table 3-8: Design Variables

Factors	Type	Min	Max	Factor Design Name
Total Slug Size, Pore Volume	Numerical	0.18	1	C
Ratio of water-gas	Numerical	0.4	1.6	A
Injection Rate of Gas, MMscfd	Numerical	4	16	B
Time for injector 3, yr	Numerical	1	10	K
Well Type	Categorical	Vertical	Horizontal	L
Well Coordinates				
Injector 1 (X)	Numerical	2	25	D
Injector 1 (Y)	Numerical	2	12	E
Injector 2 (X)	Numerical	2	25	F
Injector 2 (Y)	Numerical	12	25	G
Injector 3 (X)	Numerical	2	25	H
Injector 3 (Y)	Numerical	25	38	J

3.4.1 Design

Design variables, their ranges, and response functions used for the optimization are given and explained in this section. After determining the variables, their ranges, and response functions, D-optimal design is selected as an experimental design method to build the response surface. According to Ghomian (2008), the d-optimal design method can be used for the designs which have both categorical and numerical factors. The Design-Expert software, Version 6 (Stat-Ease Inc., 2005) was used to build the response

surface. To do this, we need to run eighty different cases and need to calculate the net present value and the amount of CO_2 sequestered for each run. Table 3-9 presents the D-optimal design with a quadratic model.

Table 3-9: D-optimal Design with Quadratic Model

Run	A	B	C	D	E	F	G	H	J	K	L
1	0.5	5	0.2	8	2	8	13	8	26	1	Vertical
2	1.5	15	1	23	2	8	26	8	26	1	Horizontal
3	1.5	15	0.2	8	13	23	26	8	39	1	Vertical
4	1.5	5	1	8	13	8	13	23	39	1	Horizontal
5	0.5	15	0.2	23	13	23	13	23	26	1	Horizontal
6	1.5	15	1	8	2	23	13	23	26	10	Vertical
7	0.5	15	0.2	8	2	8	26	23	39	10	Horizontal
8	0.5	5	1	23	2	23	26	23	39	1	Vertical
9	0.5	15	1	23	13	8	13	8	39	10	Vertical
10	0.5	5	0.2	23	2	8	26	8	39	10	Vertical
11	0.5	15	0.2	23	13	8	26	8	26	1	Vertical
12	0.5	5	0.2	8	13	8	26	23	39	1	Vertical
13	1.5	5	0.2	8	2	23	26	23	39	10	Vertical
14	0.5	15	0.2	23	13	23	26	23	39	10	Vertical
15	0.5	5	1	8	2	8	26	8	39	1	Horizontal
16	0.5	15	1	23	13	23	26	8	39	1	Horizontal
17	1.5	5	1	8	2	8	26	23	26	10	Horizontal
18	1.5	15	0.2	23	13	8	13	8	39	1	Horizontal
19	0.5	5	0.2	8	2	23	13	23	26	10	Horizontal
20	1.5	15	0.2	8	13	8	13	23	26	1	Vertical
21	1.5	15	0.2	23	2	8	13	8	26	10	Vertical
22	0.5	5	1	23	2	23	13	8	26	1	Horizontal
23	0.5	5	1	8	13	23	13	23	26	1	Vertical
24	0.5	15	1	8	2	8	13	23	26	1	Horizontal
25	1.5	5	0.2	8	13	8	26	8	39	10	Horizontal
26	1.5	15	1	8	2	8	13	8	39	10	Horizontal
27	0.5	15	1	23	2	23	13	23	39	10	Horizontal
28	1.5	5	0.2	8	13	23	13	8	26	10	Vertical
29	1.5	15	0.2	8	13	23	13	23	39	10	Horizontal
30	0.5	5	0.2	8	13	23	13	8	39	1	Horizontal
31	1.5	15	1	23	13	8	13	23	26	10	Horizontal

Table 3-9: Continued

Run	A	B	C	D	E	F	G	H	J	K	L
32	1.5	5	1	8	2	23	26	8	26	1	Vertical
33	0.5	15	0.2	8	2	23	26	8	26	1	Horizontal
34	1.5	15	1	8	2	23	26	23	39	1	Horizontal
35	1.5	5	0.2	23	2	8	13	23	26	1	Horizontal
36	1.5	15	1	8	13	23	13	8	26	1	Horizontal
37	1.5	5	1	23	2	23	13	23	26	10	Vertical
38	0.5	15	0.2	8	13	8	26	8	26	10	Vertical
39	0.5	15	1	23	13	23	26	8	26	10	Vertical
40	1.5	15	0.2	8	13	23	26	23	26	10	Horizontal
41	0.5	5	0.2	8	13	8	26	23	26	1	Horizontal
42	1.5	15	1	8	13	8	26	23	39	10	Vertical
43	1.5	15	0.2	23	13	8	26	23	39	1	Horizontal
44	0.5	5	0.2	23	2	23	13	23	39	1	Vertical
45	0.5	15	1	8	2	23	13	8	39	1	Vertical
46	1.5	5	1	8	13	8	13	8	26	10	Vertical
47	1.5	5	1	23	13	8	26	8	26	1	Horizontal
48	1.5	15	1	8	2	23	26	8	39	10	Horizontal
49	0.5	15	1	8	13	23	13	23	26	10	Horizontal
50	0.5	15	0.2	8	2	8	26	23	26	1	Vertical
51	0.5	15	0.2	23	13	23	13	8	39	10	Horizontal
52	1.5	5	1	23	13	23	26	23	26	10	Horizontal
53	1.5	5	1	8	2	23	13	23	39	1	Vertical
54	1.5	15	0.2	23	2	23	26	23	39	10	Vertical
55	0.5	5	0.2	8	2	8	13	8	39	10	Horizontal
56	1	10	0.6	15.5	7.5	15.5	19.5	15.5	32.5	1	Horizontal
57	1	10	0.6	15.5	7.5	15.5	19.5	15.5	26	5.5	Horizontal
58	1.5	10	0.6	15.5	7.5	15.5	19.5	15.5	32.5	5.5	Horizontal
59	1	15	0.6	15.5	7.5	15.5	19.5	15.5	32.5	5.5	Horizontal
60	1	10	0.6	15.5	13	15.5	19.5	15.5	32.5	5.5	Vertical
61	1	10	0.6	15.5	7.5	23	19.5	15.5	32.5	5.5	Horizontal
62	1	10	0.2	15.5	7.5	15.5	19.5	15.5	32.5	5.5	Vertical
63	0.5	5	1	8	2	8	13	15.5	39	10	Vertical
64	1.5	15	1	23	13	8	13	23	39	1	Vertical
65	0.5	15	1	15.5	2	8	26	23	39	1	Vertical
66	1.5	5	0.2	23	13	8	26	23	26	10	Vertical
67	0.5	5	1	23	13	8	19.5	23	39	10	Horizontal
68	1.5	5	0.2	23	7.5	8	13	23	39	10	Vertical

Table 3-9: Continued

Run	A	B	C	D	E	F	G	H	J	K	L
69	1.5	15	0.2	8	2	8	26	8	26	10	Horizontal
70	0.5	15	0.2	23	2	8	19.5	23	39	10	Vertical
71	0.5	15	1	8	2	8	19.5	8	26	10	Horizontal
72	1.5	5	0.2	23	2	23	26	8	39	1	Horizontal
73	0.5	10	1	23	13	8	26	23	26	1	Vertical
74	0.5	5	1	15.5	13	23	26	8	39	10	Vertical
75	0.5	5	0.2	23	2	23	26	23	26	10	Horizontal
76	1.5	15	0.2	15.5	13	8	13	8	39	10	Vertical
77	0.5	15	0.2	23	2	8	13	15.5	26	10	Horizontal
78	1.5	5	1	8	2	8	13	8	26	1	Horizontal
79	0.5	15	1	8	13	8	13	8	26	1	Vertical
80	0.5	5	0.2	23	13	8	13	8	26	1	Horizontal

3.4.2 Analysis of the Response Functions

In this section, analysis of the response functions is performed using the Design-Expert software, Version 6 (Stat-Ease Inc., 2005) outputs. First, by using sequential model sum of squares and model summary statistic tables, a suggested model is found. Secondly, an analysis of variance table is used to check insignificant model terms. Finally, Box-Cox and normal plot of residuals are plotted and need for transformation is checked. An equation for response functions is created and, by using this equation, response surfaces are generated. Daily production and injection data is obtained from the simulation result files. Then the data is post processed to make it usable in our NPV spreadsheet. This spreadsheet is built by using the economic model given in Section 3.3. Net present values for each run are calculated using this spreadsheet. The amount of CO_2 sequestered for each run is calculated by using the injected volume of CO_2 and the produced volume of CO_2, which are also obtained from the simulation result files. D-optimal design results and results of response functions are given in Table 3-10.

Table 3-10: D-optimal Design with Response Functions

Run	A	B	C	D	E	F	G	H	J	K	L	NPV (MM$)	CO_2 (Ton)
1	0.5	5	0.2	8	2	8	13	8	26	1	Vertical	69.558	162586.5
2	1.5	15	1	23	2	8	26	8	26	1	Horizontal	79.948	266152.2
3	1.5	15	0.2	8	13	23	26	8	39	1	Vertical	59.235	137207.2
4	1.5	5	1	8	13	8	13	23	39	1	Horizontal	49.627	108349.7
5	0.5	15	0.2	23	13	23	13	23	26	1	Horizontal	99.744	218855.3
6	1.5	15	1	8	2	23	13	23	26	10	Vertical	62.061	165733.5
7	0.5	15	0.2	8	2	8	26	23	39	10	Horizontal	79.458	192766.4
8	0.5	5	1	23	2	23	26	23	39	1	Vertical	65.363	105799.4
9	0.5	15	1	23	13	8	13	8	39	10	Vertical	55.538	258414.4
10	0.5	5	0.2	23	2	8	26	8	39	10	Vertical	85.044	159544.4
11	0.5	15	0.2	23	13	8	26	8	26	1	Vertical	63.949	185405.6
12	0.5	5	0.2	8	13	8	26	23	39	1	Vertical	63.723	115433.4
13	1.5	5	0.2	8	2	23	26	23	39	10	Vertical	92.185	192612.2
14	0.5	15	0.2	23	13	23	26	23	39	10	Vertical	57.161	151732.6
15	0.5	5	1	8	2	8	26	8	39	1	Horizontal	85.044	121577.4
16	0.5	15	1	23	13	23	26	8	39	1	Horizontal	63.591	124847.7
17	1.5	5	1	8	2	8	26	23	26	10	Horizontal	76.713	156810.9
18	1.5	15	0.2	23	13	8	13	8	39	1	Horizontal	56.388	104277.1
19	0.5	5	0.2	8	2	23	13	23	26	10	Horizontal	61.729	125267.3
20	1.5	15	0.2	8	13	8	13	23	26	1	Vertical	60.723	173397.2
21	1.5	15	0.2	23	2	8	13	8	26	10	Vertical	59.781	131561.2
22	0.5	5	1	23	2	23	13	8	26	1	Horizontal	70.96	362128.1
23	0.5	5	1	8	13	23	13	23	26	1	Vertical	65.363	582044.8
24	0.5	15	1	8	2	8	13	23	26	1	Horizontal	82.768	236725.1
25	1.5	5	0.2	8	13	8	26	8	39	10	Horizontal	51.487	111667.5
26	1.5	15	1	8	2	8	13	8	39	10	Horizontal	65.602	259771.9
27	0.5	15	1	23	2	23	13	23	39	10	Horizontal	68.46	184689.2
28	1.5	5	0.2	8	13	23	13	8	26	10	Vertical	62.077	126285.5
29	1.5	15	0.2	8	13	23	13	23	39	10	Horizontal	69.413	272982.9
30	0.5	5	0.2	8	13	23	13	8	39	1	Horizontal	96.823	201540.9
31	1.5	15	1	23	13	8	13	23	26	10	Horizontal	76.186	283639.4

Table 3-10: Continued

Run	A	B	C	D	E	F	G	H	J	K	L	NPV (MM$)	CO_2 (Ton)
32	1.5	5	1	8	2	23	26	8	26	1	Vertical	80.848	245653.8
33	0.5	15	0.2	8	2	23	26	8	26	1	Horizontal	48.837	126518.1
34	1.5	15	1	8	2	23	26	23	39	1	Horizontal	52.468	133609.2
35	1.5	5	0.2	23	2	8	13	23	26	1	Horizontal	53.776	112951.6
36	1.5	15	1	8	13	23	13	8	26	1	Horizontal	52.33	133850.5
37	1.5	5	1	23	2	23	13	23	26	10	Vertical	54.374	87265.1
38	0.5	15	0.2	8	13	8	26	8	26	10	Vertical	68.849	141867.8
39	0.5	15	1	23	13	23	26	8	26	10	Vertical	64.089	129969.2
40	1.5	15	0.2	8	13	23	26	23	26	10	Horizontal	74.316	278413
41	0.5	5	0.2	8	13	8	26	23	26	1	Horizontal	89.529	319150.6
42	1.5	15	1	8	13	8	26	23	39	10	Vertical	63.51	125088.4
43	1.5	15	0.2	23	13	8	26	23	39	1	Horizontal	64.986	124094.9
44	0.5	5	0.2	23	2	23	13	23	39	1	Vertical	61.614	113370.6
45	0.5	15	1	8	2	23	13	8	39	1	Vertical	80.366	255816.6
46	1.5	5	1	8	13	8	13	8	26	10	Vertical	52.86	113614.9
47	1.5	5	1	23	13	8	26	8	26	1	Horizontal	72.665	234602.4
48	1.5	15	1	8	2	23	26	8	39	10	Horizontal	58.792	97370.5
49	0.5	15	1	8	13	23	13	23	26	10	Horizontal	57.101	106749.7
50	0.5	15	0.2	8	2	8	26	23	26	1	Vertical	59.98	114834.2
51	0.5	15	0.2	23	13	23	13	8	39	10	Horizontal	61.723	106274.5
52	1.5	5	1	23	13	23	26	23	26	10	Horizontal	93.594	172878.9
53	1.5	5	1	8	2	23	13	23	39	1	Vertical	49.21	79725.9
54	1.5	15	0.2	23	2	23	26	23	39	10	Vertical	79.02	197597.9
55	0.5	5	0.2	8	2	8	13	8	39	10	Horizontal	67.467	301416.6
56	1	10	0.6	15.5	7.5	15.5	19.5	15.5	32.5	1	Horizontal	67.882	127322.1
57	1	10	0.6	15.5	7.5	15.5	19.5	15.5	26	5.5	Horizontal	75.08	190853.6
58	1.5	10	0.6	15.5	7.5	15.5	19.5	15.5	32.5	5.5	Horizontal	57.554	138422.8
59	1	15	0.6	15.5	7.5	15.5	19.5	15.5	32.5	5.5	Horizontal	87.936	175797.5
60	1	10	0.6	15.5	13	15.5	19.5	15.5	32.5	5.5	Vertical	55.694	89540.1
61	1	10	0.6	15.5	7.5	23	19.5	15.5	32.5	5.5	Horizontal	110.05	207699
62	1	10	0.2	15.5	7.5	15.5	19.5	15.5	32.5	5.5	Vertical	66.365	151923.9

Table 3-10: Continued

Run	A	B	C	D	E	F	G	H	J	K	L	NPV (MM$)	CO_2 (Ton)
63	0.5	5	1	8	2	8	13	15.5	39	10	Vertical	66.7	101831.8
64	1.5	15	1	23	13	8	13	23	39	1	Vertical	111.47	227284.2
65	0.5	15	1	15.5	2	8	26	23	39	1	Vertical	73.708	279184.3
66	1.5	5	0.2	23	13	8	26	23	26	10	Vertical	61.723	188039.8
67	0.5	5	1	23	13	8	19.5	23	39	10	Horizontal	58.758	88119.1
68	1.5	5	0.2	23	7.5	8	13	23	39	10	Vertical	60.847	141161.9
69	1.5	15	0.2	8	2	8	26	8	26	10	Horizontal	96.234	181900.2
70	0.5	15	0.2	23	2	8	19.5	23	39	10	Vertical	85.249	185349.5
71	0.5	15	1	8	2	8	19.5	8	26	10	Horizontal	89.179	205243.2
72	1.5	5	0.2	23	2	23	26	8	39	1	Horizontal	89.339	198572.9
73	0.5	10	1	23	13	8	26	23	26	1	Vertical	98.746	195660.4
74	0.5	5	1	15.5	13	23	26	8	39	10	Vertical	70.708	201985.1
75	0.5	5	0.2	23	2	23	26	23	26	10	Horizontal	86.341	179641.8
76	1.5	15	0.2	15.5	13	8	13	8	39	10	Vertical	49.111	109598
77	0.5	15	0.2	23	2	8	13	15.5	26	10	Horizontal	85.731	151454.9
78	1.5	5	1	8	2	8	13	8	26	1	Horizontal	69.079	140989.8
79	0.5	15	1	8	13	8	13	8	26	1	Vertical	76.766	266997.5
80	0.5	5	0.2	23	13	8	13	8	26	1	Horizontal	73.708	222199.7

3.4.2.1 Analysis of Net Present Value Response Function

After entering the results of our design, the degree of the polynomial which fits with the equation for amount of CO_2 and net present value, needs to be confirmed with statistical calculations. By doing this, the best model for the response surfaces can be found. The Design-Expert software Version 6 (Stat-Ease Inc., 2005) is used to obtain the best model for the net present value. Table 3-11 shows the sequential model sum of squares and Table 3-12 shows the model summary statistics for NPV. These tables are produced using the Design-Expert software Version 6 (Stat-Ease Inc., 2005).

Table 3-11: Sequential Model Sum of Squares for NPV

Source	Sum of Squares	DF	Mean Square	F Value	Prob > F	
Mean	410103.1	1	410103.1061			Suggested
Linear	2281.322	11	207.3929279	0.972986	0.48	
2FI	11761.42	55	213.8439864	1.015355	0.52	
Quadratic	2656.054	10	265.6053775	2.639702	0.15	Suggested
Cubic	503.0973	5	100.6194609			Aliased
Residual	0	0				
Total	427305	82	5211.036569			

Table 3-12: Model Summary Statistics for NPV

Source	Std. Dev.	R-Squared	Adjusted R-Squared	Predicted R-Squared	PRESS	
Linear	14.59969	0.13262	-0.003682086	-0.19317	20524.78	
2FI	14.51241	0.816349	0.008282618	-8.42906	162197.7	
Quadratic	10.03093	0.970753	0.526204671	-39.3505	694105.4	Suggested

Table 3-11 suggests mean and quadratic models and Table 3-12 suggests the quadratic model. From these statistical calculations a quadratic model is chosen to build response surfaces for NPV. According to Myers et al. (2002), the caution aliased is written near the cubic model in their case because the number of runs is not abundant for a complete cubic model. Here, the same problem occurred because the number of runs is not enough for cubic model. Table 3-13 presents an analysis of variance table for the NPV response surface quadratic model. By looking at the Prob>F values shown in Table 3-13, insignificant model terms can be understood and the model can be changed to develop the design. However, for our case, the quadratic model was the best model, considering the number of runs needed.

Table 3-13: Analysis of Variance for NPV

Model	Sum of Squares	DF	Sum of Squares/DF	F Value	Prob > F
	16698.79524	76	219.7209899	2.183683	0.19
A	9.824560089	1	9.824560089	0.097641	0.77
B	3.794503065	1	3.794503065	0.037711	0.85
C	0.232662738	1	0.232662738	0.002312	0.96
D	194.4410887	1	194.4410887	1.93244	0.22
E	159.3358496	1	159.3358496	1.583549	0.26
F	2.69019814	1	2.69019814	0.026736	0.88
G	191.4429985	1	191.4429985	1.902644	0.23
H	47.9750173	1	47.9750173	0.476797	0.52
J	0.069572869	1	0.069572869	0.000691	0.98
K	790.5407663	1	790.5407663	7.856738	0.038
L	201.1549324	1	201.1549324	1.999165	0.22
A2	59.94232238	1	59.94232238	0.595733	0.48
B2	503.7688795	1	503.7688795	5.006674	0.075
C2	8.237393208	1	8.237393208	0.081867	0.79
D2	84.73856251	1	84.73856251	0.842169	0.40
E2	354.9982504	1	354.9982504	3.528127	0.12
F2	1494.186311	1	1494.186311	14.84987	0.012
G2	184.6673871	1	184.6673871	1.835305	0.23
H2	253.7721644	1	253.7721644	2.522098	0.17
J2	21.45680617	1	21.45680617	0.213247	0.66
K2	36.05758806	1	36.05758806	0.358356	0.58
AB	86.29925131	1	86.29925131	0.85768	0.40
AC	7.332987112	1	7.332987112	0.072878	0.80
AD	105.1366272	1	105.1366272	1.044894	0.35
AE	307.8395945	1	307.8395945	3.059444	0.14
AF	60.94739063	1	60.94739063	0.605722	0.47
AG	73.02688415	1	73.02688415	0.725773	0.43
AH	64.52770773	1	64.52770773	0.641304	0.46
AJ	40.28790277	1	40.28790277	0.400399	0.55
AK	0.010092877	1	0.010092877	0.0001	0.99
AL	136.9473434	1	136.9473434	1.361042	0.30
BC	175.1883898	1	175.1883898	1.741098	0.24
BD	28.75046018	1	28.75046018	0.285735	0.62
BE	224.4575938	1	224.4575938	2.230757	0.20
BF	711.1886319	1	711.1886319	7.068102	0.045
BG	353.4981508	1	353.4981508	3.513218	0.12
BH	316.7793967	1	316.7793967	3.148292	0.14

Table 3-13: Continued

Model	Sum of Squares	DF	Sum of Squares/DF	F Value	Prob > F
BJ	10.96848283	1	10.96848283	0.10901	0.75
BK	43.15536363	1	43.15536363	0.428897	0.54
BL	3.663435186	1	3.663435186	0.036409	0.86
CD	283.538468	1	283.538468	2.817929	0.15
CE	159.6033265	1	159.6033265	1.586207	0.26
CF	261.8558615	1	261.8558615	2.602438	0.17
CG	21.01086272	1	21.01086272	0.208815	0.67
CH	80.42473273	1	80.42473273	0.799296	0.41
CJ	380.5045002	1	380.5045002	3.781619	0.11
CK	549.0195808	1	549.0195808	5.456396	0.067
CL	324.092666	1	324.092666	3.220974	0.13
DE	239.7187403	1	239.7187403	2.382429	0.18
DF	369.3622284	1	369.3622284	3.670883	0.11
DG	130.4955805	1	130.4955805	1.296922	0.31
DH	480.2572523	1	480.2572523	4.773006	0.081
DJ	0.033360709	1	0.033360709	0.000332	0.99
DK	300.6383113	1	300.6383113	2.987874	0.14
DL	8.379761341	1	8.379761341	0.083282	0.78
EF	177.1308316	1	177.1308316	1.760403	0.24
EG	42.67817554	1	42.67817554	0.424154	0.54
EH	820.6247362	1	820.6247362	8.155726	0.036
EJ	263.576007	1	263.576007	2.619533	0.17
EK	323.9944592	1	323.9944592	3.219998	0.13
EL	0.550045911	1	0.550045911	0.005467	0.94
FG	328.0279261	1	328.0279261	3.260084	0.13
FH	11.07338159	1	11.07338159	0.110052	0.75
FJ	223.7310836	1	223.7310836	2.223537	0.20
FK	202.718461	1	202.718461	2.014704	0.22
FL	181.3914355	1	181.3914355	1.802747	0.24
GH	4.775000948	1	4.775000948	0.047456	0.84
GJ	226.4614234	1	226.4614234	2.250672	0.19
GK	446.9741435	1	446.9741435	4.442224	0.089
GL	16.56639708	1	16.56639708	0.164644	0.70
HJ	339.2931748	1	339.2931748	3.372043	0.13
HK	112.3702022	1	112.3702022	1.116784	0.34
HL	649.4860278	1	649.4860278	6.454875	0.052
JK	163.1189204	1	163.1189204	1.621147	0.26
KL	56.83355562	1	56.83355562	0.564837	0.49

Based on the method presented, the equation for NPV response is built. However, it must be checked by diagnostic plots shown in Figure 3-5 and Figure 3-6. If the model needs transformation, the transformation must be applied to make our design more successful. The equation for NPV without transformation is given below. The meaning for each of the coded factors is given in Table 3-8.

NPV= (3.1)

69.87642
0.737051 * A
-0.30587 * B
0.08025 * C
2.735805 * D
-2.15796 * E
0.326202 * F
2.386063 * G
-1.2024 * H
0.051695 * J
-5.98483 * K
-2.81262 * L
-7.99417 * A2
21.97606 * B2
-3.14511 * C2
8.387997 * D2
-17.067 * E2
40.54292 * F2
-17.2015 * G2
-23.9234 * H2
5.142294 * J2
-6.15959 * K2
1.642035 * A * B
-0.48129 * A * C
-2.07421 * A * D
-3.45734 * A * E
1.528381 * A * F

-1.61358 * A * G
1.453233 * A * H
1.158012 * A * J
0.025747 * A * K
-2.00716 * A * L
2.174622 * B * C
0.958841 * B * D
-4.05759 * B * E
-4.66129 * B * F
-3.58041 * B * G
3.885635 * B * H
0.680041 * B * J
1.123168 * B * K
0.312849 * B * L
3.025651 * C * D
2.127523 * C * E
-2.60039 * C * F
0.781308 * C * G
1.327986 * C * H
-3.72911 * C * J
-4.02708 * C * K
-2.85332 * C * L
2.955188 * D * E
3.93444 * D * F
-2.12697 * D * G
3.818453 * D * H
-0.03343 * D * J
-3.64199 * D * K
-0.44389 * D * L
2.527451 * E * F
-1.04649 * E * G
5.121579 * E * H
-2.7381 * E * J
-3.41487 * E * K
-0.13715 * E * L
-3.22113 * F * G

-0.56673 * F * H
2.501161 * F * J
2.69465 * F * K

As discussed before, to make the design results more accurate, transformations should be performed if needed. According to Tamhane (2009), transformations can be used to make the design robust and also to protect essential assumptions. To understand that Box-Cox plot can be used. Myers et al. (2002) stated that it is not necessary to use any transformation when lambda is equal to one. From Figure 3-5, it can be seen that the value of lambda is equal to one; therefore, transformations for NPV are not needed. Also, a normal probability plot can be used for confirmation. The normality assumption can be controlled by checking the normal plot of residuals. This assumption can also be said to be correct if the points on the normal plot of residuals build a straight line (Myers et al., 2002). According to Montgomery (1984), assumptions can be correct in small samples if there is only a small amount of variation. From Figure 3-6, it can be seen that most of the points are in a straight line; therefore; we do not need any transformation.

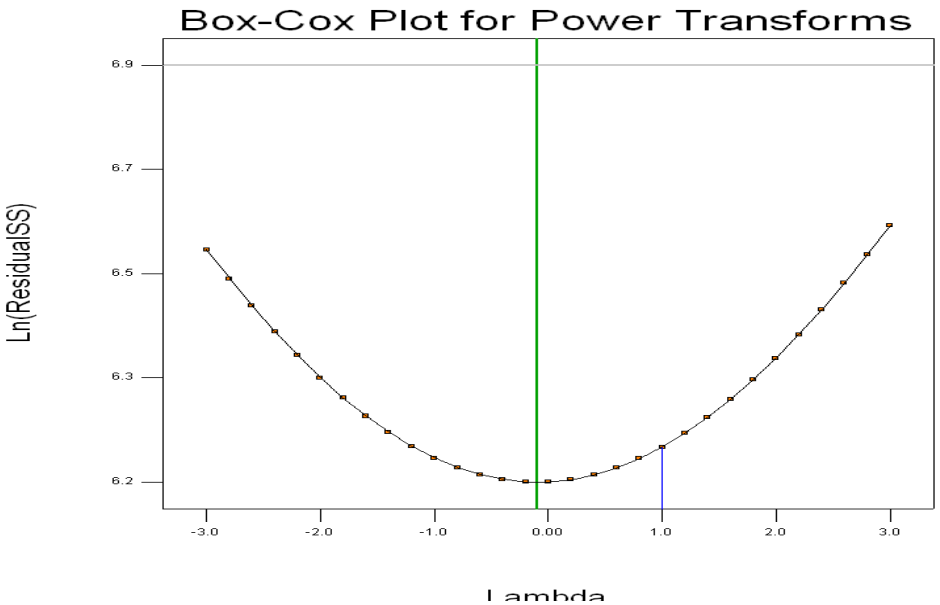

Figure 3-5: Box-Cox Plot for NPV

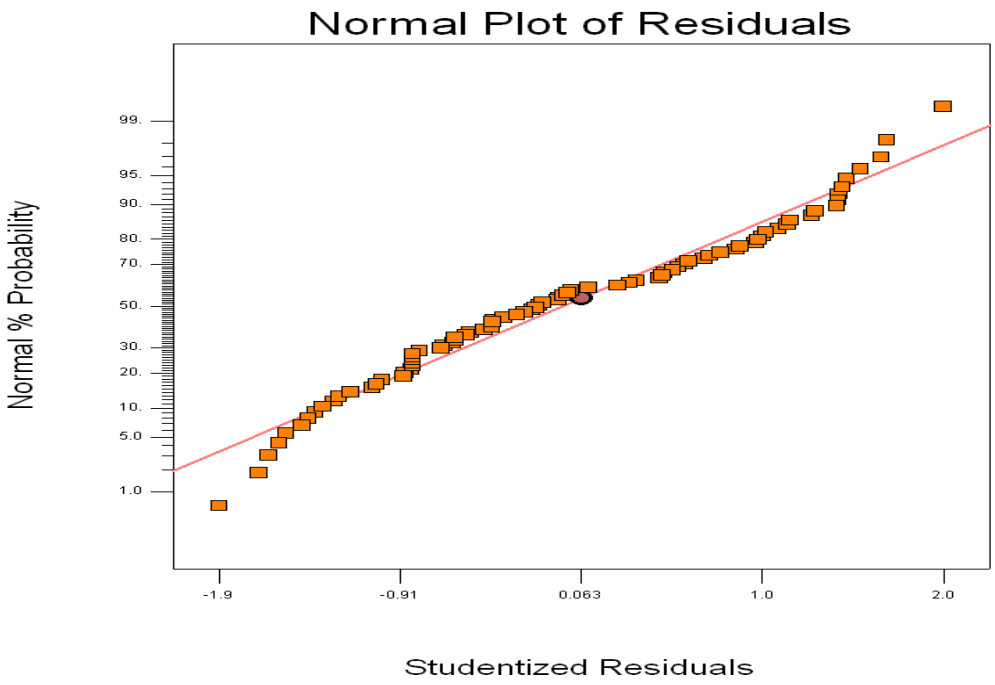

Figure 3-6: Normal Plot of Residuals for NPV

Hence, the equation for NPV response was used without any transformation. By using this equation, response surface for the net present value is built. The most appropriate conditions to maximize the net present value can be found from the equation for net present value response and these are given in Table 3-19. Figure 3-7 presents net present value versus injection rate of gas (MMscfd) and ratio of water and gas. Figure 3-8 presents net present value versus slug size, and the ratio of water and gas.

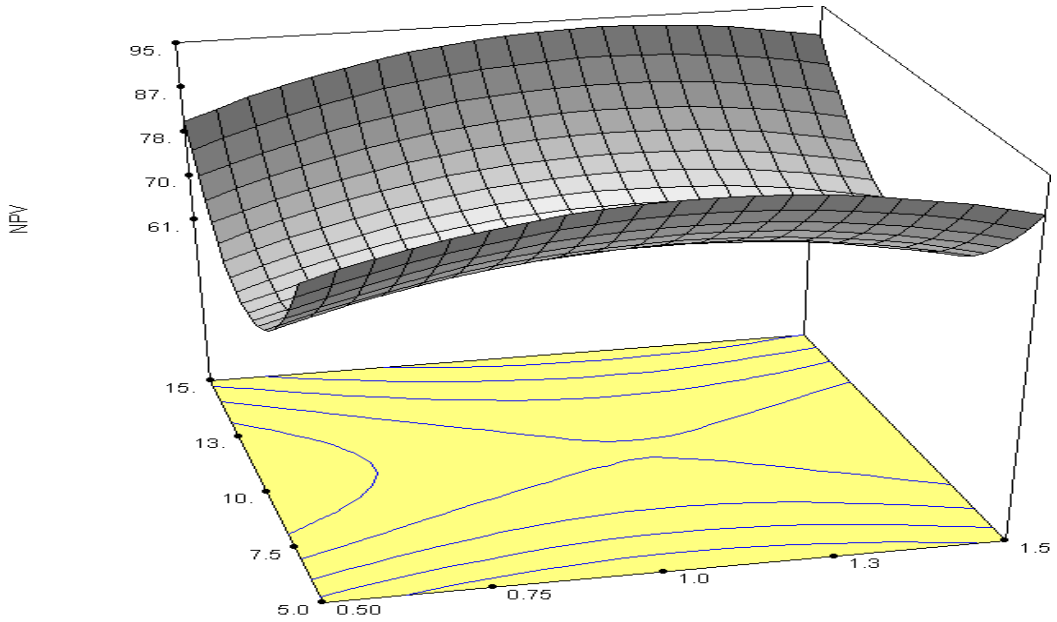

Figure 3-7: Net Present Value vs. Injection Rate and WAG

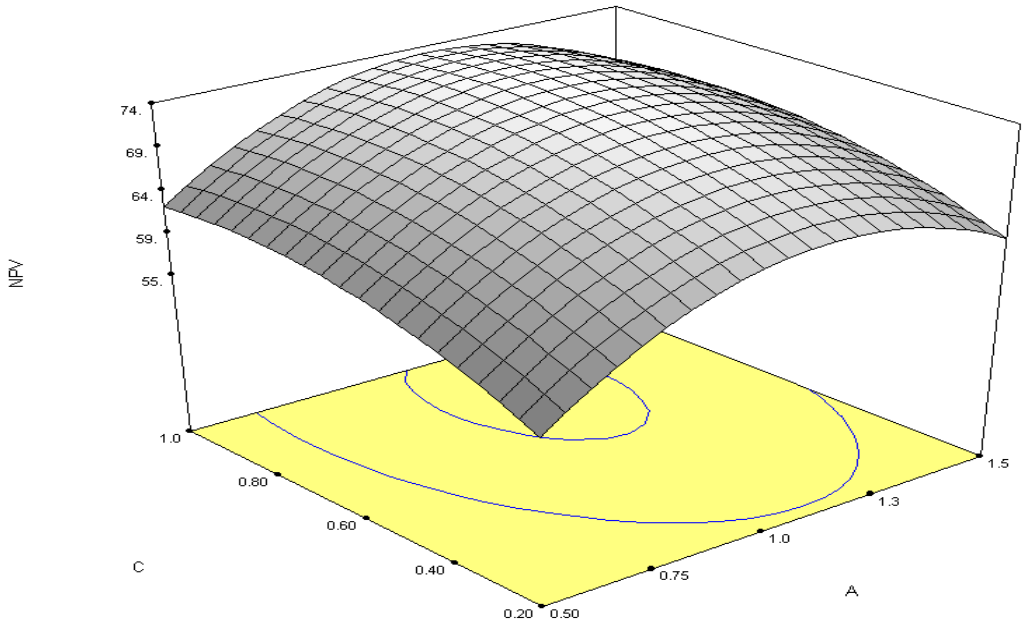

Figure 3-8: Net Present Value vs. Slug Size and WAG

3.4.2.2 Analysis of Amount of CO_2 Sequestered (ton) Response Function

In this section, the same procedure as Section 3.4.2 is followed. The quadratic model is determined as the best model which fits the equation for amount of CO_2 sequestered. The Design-Expert software Version 6 (Stat-Ease Inc, 2005) was used to find the model and obtain the outputs. The sequential model sum of squares is presented in Table 3-14 and the model summary statistics for amount of CO_2 sequestered is shown in Table 3-15. According to Table 3-14, the suggested models are mean and quadratic and Table 3-15 suggests the quadratic model. The quadratic model is accepted from these statistical calculations. Analysis of variance table is given in Table 3-16. By using Table 3-16, model terms are checked and determined that the quadratic model is appropriate for our case.

Table 3-14: Sequential Model Sum of Squares for Amount of CO_2 Sequestered (ton)

Source	Sum of Squares	DF	Mean Square	F Value	Prob > F	
Mean	2.56E+12	1	2.56E+12			Suggested
Linear	5.22E+10	11	4.74E+09	0.78087	0.66	
2FI	3.65E+11	55	6.64E+09	1.67062	0.14	Suggested
Quadratic	4.73E+10	10	4.73E+09	1.90615	0.25	
Cubic	1.24E+10	5	2.48E+09			Aliased
Residual	0	0				
Total	3.04E+12	82	3.70E+10			

Table 3-15: Model Summary Statistics for Amount of CO_2 Sequestered (ton)

Source	Std. Dev.	R-Squared	Adjusted R-Squared	Predicted R-Squared	PRESS	
Linear	77929.29	0.109296	-0.03067	-0.2544	5.99E+11	
2FI	63065.73	0.874999	0.324997	-10.497	5.49E+12	Suggested
Quadratic	49794.09	0.974025	0.579201	-15.889	8.06E+12	

Table 3-16: Analysis of Variance for Amount of CO_2 Sequestered (ton)

	Sum of Squares	DF	Mean Square	F Value	Prob > F
Model	4.65E+11	76	6.12E+09	2.46699	0.16
A	1.42E+10	1	1.42E+10	5.74147	0.062
B	12921020	1	12921020	0.00521	0.95
C	1.89E+09	1	1.89E+09	0.76229	0.42
D	1.55E+09	1	1.55E+09	0.62626	0.46
E	2.34E+09	1	2.34E+09	0.94455	0.38
F	8.85E+09	1	8.85E+09	3.56936	0.12
G	1.44E+09	1	1.44E+09	0.5821	0.48
H	8.19E+09	1	8.19E+09	3.30386	0.13
J	3.85E+10	1	3.85E+10	15.5273	0.011
K	7.78E+08	1	7.78E+08	0.31388	0.6
L	7.71E+08	1	7.71E+08	0.311	0.6
A2	87418106	1	87418106	0.03526	0.86
B2	2.43E+09	1	2.43E+09	0.98114	0.37
C2	3.38E+08	1	3.38E+08	0.13648	0.73

Table 3-16: Continued

Model	Sum of Squares	DF	Mean Square	F Value	Prob > F
D2	1.89E+10	1	1.89E+10	7.64259	0.04
E2	1.14E+10	1	1.14E+10	4.60164	0.085
F2	2.64E+09	1	2.64E+09	1.06667	0.35
G2	7.17E+08	1	7.17E+08	0.28925	0.61
H2	6.64E+09	1	6.64E+09	2.67874	0.16
J2	90933744	1	90933744	0.03668	0.86
K2	7.87E+08	1	7.87E+08	0.31744	0.6
AB	5.85E+09	1	5.85E+09	2.36103	0.19
AC	1.72E+09	1	1.72E+09	0.69253	0.44
AD	2.60E+09	1	2.60E+09	1.04779	0.35
AE	5.65E+08	1	5.65E+08	0.22773	0.65
AF	6.66E+09	1	6.66E+09	2.68443	0.16
AG	3.10E+09	1	3.10E+09	1.24845	0.31
AH	7.54E+09	1	7.54E+09	3.03948	0.14
AJ	6.78E+08	1	6.78E+08	0.27341	0.62
AK	1.47E+09	1	1.47E+09	0.59174	0.48
AL	1.13E+10	1	1.13E+10	4.54248	0.086
BC	5.52E+09	1	5.52E+09	2.2274	0.2
BD	7.52E+09	1	7.52E+09	3.03209	0.14
BE	9.65E+08	1	9.65E+08	0.38933	0.56
BF	4.84E+09	1	4.84E+09	1.95367	0.22
BG	2.81E+09	1	2.81E+09	1.13513	0.34
BH	3.37E+09	1	3.37E+09	1.35928	0.3
BJ	2.17E+10	1	2.17E+10	8.76947	0.031
BK	3.90E+08	1	3.90E+08	0.15736	0.71
BL	4.33E+09	1	4.33E+09	1.74479	0.24
CD	53994317	1	53994317	0.02178	0.89
CE	1.34E+09	1	1.34E+09	0.5387	0.5
CF	9.42E+09	1	9.42E+09	3.79825	0.11
CG	1.87E+10	1	1.87E+10	7.52993	0.041
CH	2.26E+09	1	2.26E+09	0.91114	0.38
CJ	4.04E+08	1	4.04E+08	0.16305	0.7
CK	6.53E+09	1	6.53E+09	2.6327	0.17

Table 3-16: Continued

Model	Sum of Squares	DF	Mean Square	F Value	Prob > F
CL	2.50E+09	1	2.50E+09	1.0066	0.36
DE	8.20E+09	1	8.20E+09	3.30535	0.13
DF	2.38E+09	1	2.38E+09	0.96141	0.37
DG	1.82E+09	1	1.82E+09	0.73325	0.43
DH	1.63E+10	1	1.63E+10	6.59126	0.05
DJ	1.04E+08	1	1.04E+08	0.04186	0.85
DK	6.64E+08	1	6.64E+08	0.2677	0.63
DL	4.07E+09	1	4.07E+09	1.64233	0.26
EF	6.64E+09	1	6.64E+09	2.67673	0.16
EG	2313192	1	2313192	0.00093	0.98
EH	2.20E+10	1	2.20E+10	8.87817	0.031
EJ	4.58E+09	1	4.58E+09	1.84676	0.23
EK	7.02E+09	1	7.02E+09	2.83164	0.15
EL	2.04E+09	1	2.04E+09	0.82185	0.41
FG	9.56E+09	1	9.56E+09	3.85543	0.11
FH	1.46E+09	1	1.46E+09	0.58927	0.48
FJ	3.04E+08	1	3.04E+08	0.12275	0.74
FK	3.64E+10	1	3.64E+10	14.6986	0.012
FL	1.70E+10	1	1.70E+10	6.84419	0.047
GH	3.00E+09	1	3.00E+09	1.21122	0.32
GJ	9.87E+09	1	9.87E+09	3.98007	0.1
GK	25982245	1	25982245	0.01048	0.92
GL	3.93E+08	1	3.93E+08	0.15861	0.71
HJ	7.22E+08	1	7.22E+08	0.29139	0.61
HK	3.65E+08	1	3.65E+08	0.14726	0.72
HL	4.38E+09	1	4.38E+09	1.7656	0.24
JK	1.24E+10	1	1.24E+10	5.00277	0.076
JL	7.46E+09	1	7.46E+09	3.00969	0.14
KL	2.24E+09	1	2.24E+09	0.90257	0.39

Next, the quadratic model is used to generate the equation for the amount of CO_2 sequestered response. The equation is given below. The coded factors in the equation are

our design parameters (Table 3-8). Then the assumption of normality and the value of the lambda are verified to find out if our design needs any transformation. Figure 3-8 presents the Box-Cox plot, when the value of the lambda is equal to one, the model can be used without any transformation (Myers et al., 2002). In Figure 3-9, the blue line shows the value of the lambda is one so the response surface can be generated without transformation. Figure 3-10 shows the normal plot of residuals for the amount of CO_2 sequestered. According to Myers et al. (2002), the normality assumption is valid if the points generate a straight line. The straight line generated by the points can be seen from Figure 3-9. As a result, Box-Cox plot and normal plot of residuals are checked and determined that there is no need to apply a transformation. By using the equation for the amount of CO_2 sequestered, the response surface for amount of CO_2 sequestered is built by using the Design-Expert software Version 6 (Stat-Ease Inc., 2005). The most convenient values for design parameters will be given later. Amount of CO_2 sequestered (ton) versus the injection rate of gas (MMscfd) and the ratio of water and gas is presented in Figure 3-11.

Amount of CO_2 Sequestered= (3.2)

152843.7
-28056.3 * A
564.4321 * B
7233.046 * C
7731.212 * D
8273.257 * E
18709.7 * F
-6551.46 * G
15711.97 * H
-38455.6 * J
-5938.13 * K
5506.825 * L
-9653.99 * A2

48292.33 * B2
20157.95 * C2
-125434 * D2
-96756.1 * E2
53939.19 * F2
33899.03 * G2
122389.6 * H2
10586.12 * J2
-28778.3 * K2
13524.05 * A * B
-7364.8 * A * C
10310.77 * A * D
4682.41 * A * E
15971.96 * A * F
10505.43 * A * G
15705.05 * A * H
-4750.15 * A * J
9816.658 * A * K
18202.43 * A * L
12209.79 * B * C
15505.06 * B * D
-8414.68 * B * E
-12165.1 * B * F
-10102.8 * B * G
12674.05 * B * H
30277.94 * B * J
-3377.17 * B * K
-10750.8 * B * L
1320.343 * C * D
-6154.67 * C * E
-15594.7 * C * F
-23290.2 * C * G
-7038.31 * C * H
-3843.85 * C * J
-13885.9 * C * K
-7918.09 * C * L
-17279.1 * D * E
-9995.11 * D * F
-7939.02 * D * G
-22274.7 * D * H
-1864.69 * D * J

-5411.53 * D * K
9785.192 * D * L
15470.91 * E * F
-243.635 * E * G
26525.96 * E * H
-11412.5 * E * J
-15896.5 * E * K
-8347.96 * E * L
17388.71 * F * G
6509.811 * F * H
2917.259 * F * J
-36130.3 * F * K
-22880.6 * F * L
-9895.07 * G * H
-18075.6 * G * J
886.5419 * G * K
-3164.83 * G * L
5885.283 * H * J
-3878.35 * H * K
-13580.5 * H * L
18203.87 * J * K
16118.83 * J * L
7768.496 * K * L

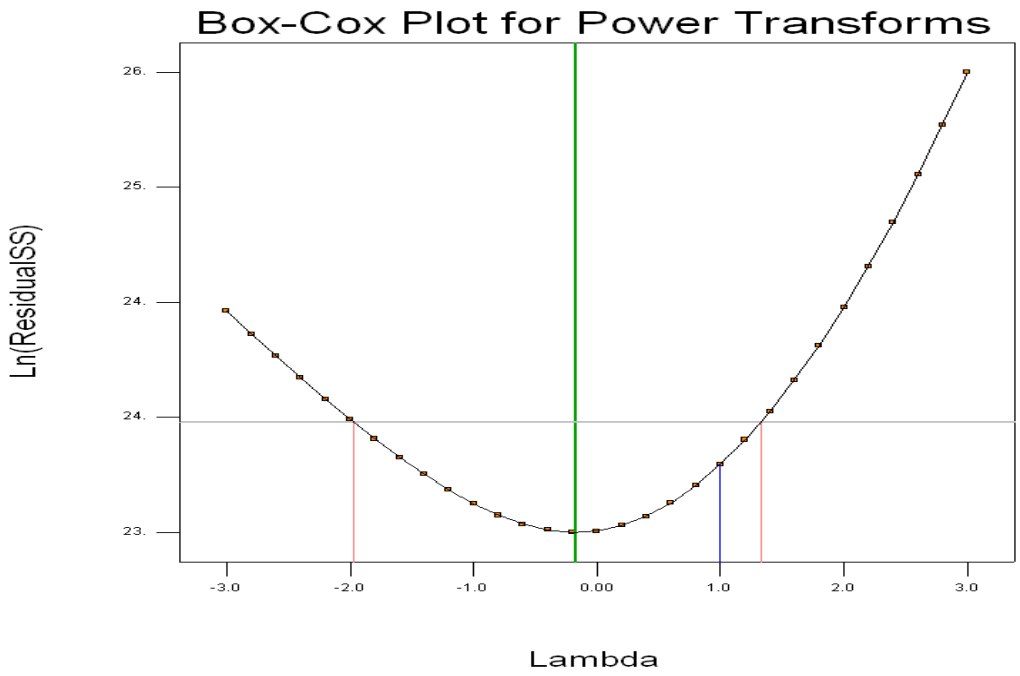

Figure 3-9 Box-Cox Plot for Amount of CO_2 Sequestered

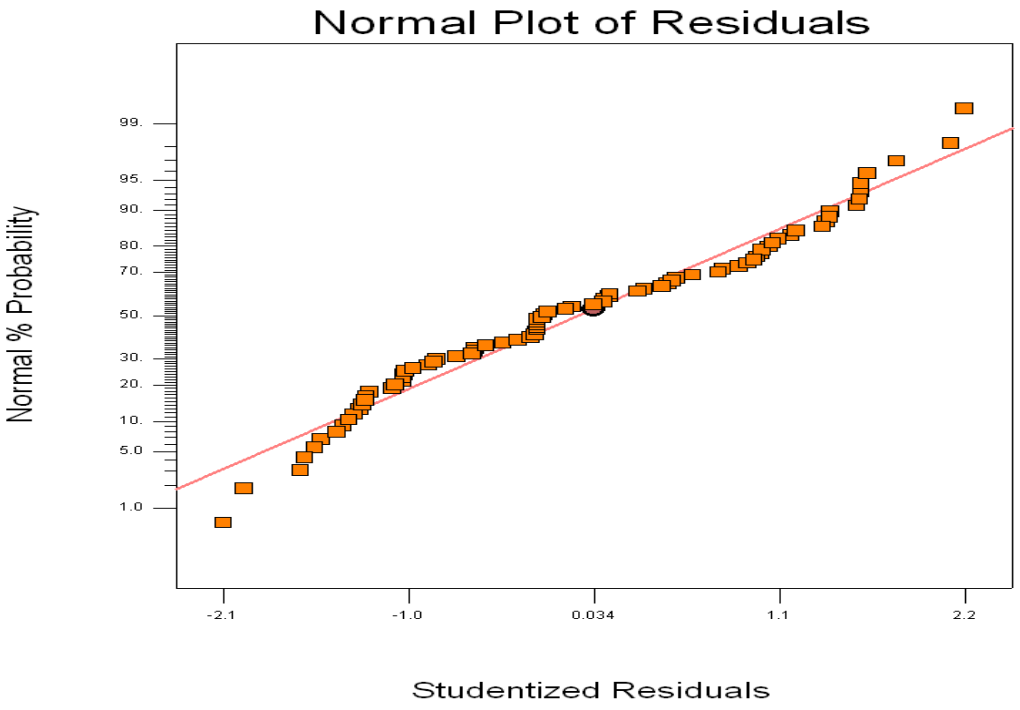

Figure 3-10 Normal Plot of Residuals for Amount of CO_2 Sequestered

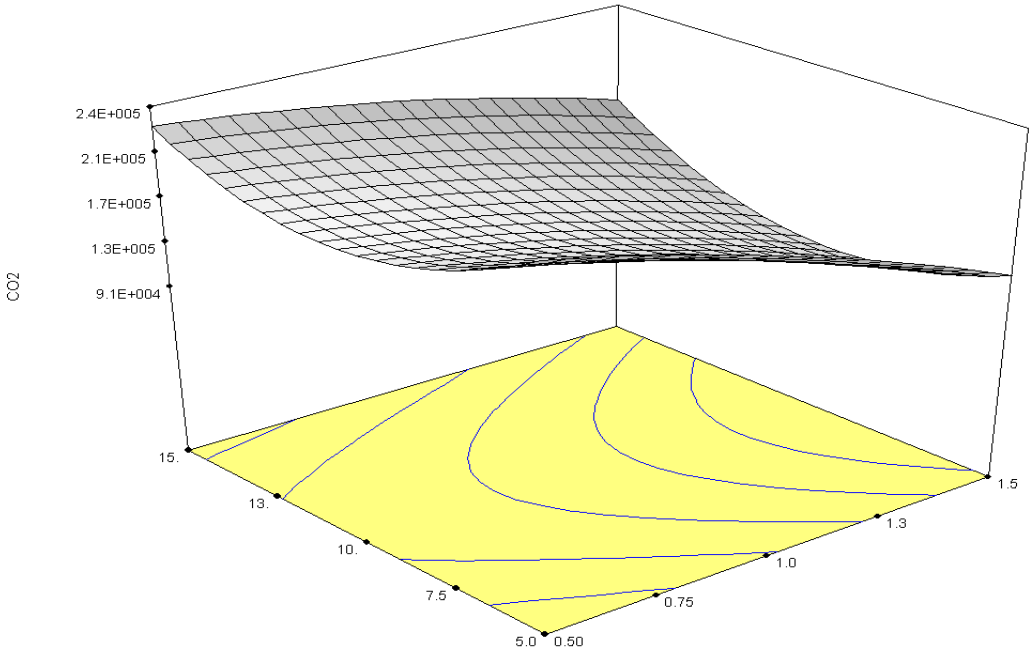

Figure 3-11 Amount of CO_2 Sequestered vs. Injection Rate and WAG

3.4.3 Co-optimization of NPV and Amount of CO_2 Sequestered by Using Desirability Functions

The co-optimization of the net present value and the amount of CO_2 sequestered is performed using desirability functions. According to Myers et al. (2002), using desirability functions is a functional technique for optimizing multiple responses. Here, the most important task is to decide the goal for each design parameter and response. As discussed before, the aim of this chapter is to maximize the net income and maximize the amount of CO_2 sequestered while using the other parameters in a given range. After deciding the goals, the next step is to generate the ideal values for each design parameter to maximize the responses. The Design-Expert software Version 6 (Stat-Ease Inc., 2005) is employed to co-optimize the response functions. Total slug size, ratio of water-gas, injection rate of gas (MMscfd), time for injector 3 (yr), well type (horizontal or vertical), and well coordinates are set in a range. Response functions, net present value and amount

of CO_2 sequestered are set as maximum. Table 3-17 shows the design goals and the limits for each design parameter. Solutions to maximize the response functions are given in Table 3-18. Twenty solutions are found using the Design-Expert software version 6 (Stat-Ease Inc, 2005). There are twenty optimum conditions for our purpose, but desirability is the most important item to verify. The range of desirability is between zero and one. Desirability is equal to one when the goal for the response functions is achieved (Myers at al., 2002). The maximum values for the NPV and amount of CO_2 sequestered are obtained from the solution one which has the highest desirability (Table 3-18). The selected solution which has the higher desirability is the optimum solution for our goals.

Table 3-17: Design Goals and Limits for Each Design Parameter

Name	Goal	Lower Limit	Upper Limit	Lower Weight	Upper Weight
Ratio of water-gas	is in range	0.5	1.5	1	1
Injection Rate of Gas, MMscfd	is in range	5	15	1	1
Total Slug Size, Pore Volume	is in range	0.2	1	1	1
Injector 1 (X)	is in range	8	23	1	1
Injector 1 (Y)	is in range	2	13	1	1
Injector 2 (X)	is in range	8	23	1	1
Injector 2 (Y)	is in range	13	26	1	1
Injector 3 (X)	is in range	8	23	1	1
Injector 3 (Y)	is in range	26	39	1	1

Table 3-17: Continued

Name	Goal	Lower Limit	Upper Limit	Lower Weight	Upper Weight
Time for injector 3, yr	is in range	1	10	1	1
Well Type	is in range	Vertical	Horizontal	1	1
Net Present Values	maximize	49	110	1	1
Amount of CO_2 Sequestered	maximize	79725.9	582045	1	1

Table 3-18: Solutions to Maximize the Response Functions

Solutions #	A	B	C	D	E	F	G	H	J	K	L	NPV	CO_2	Desirability	
1	1.3	5.0	0.31	16.	8.5	23.	24.	23.	26.	4.5	Horizontal	1.2E+002	5.5E+005	0.968065	Selected
2	0.66	5.1	0.68	16.	7.0	23.	16.	8.4	26.	3.6	Horizontal	1.1E+002	4.7E+005	0.879989	
3	0.81	15.	1.0	19.	5.6	8.0	13.	11.	37.	3.4	Horizontal	1.1E+002	4.6E+005	0.865872	
4	0.57	14.	1.0	18.	4.8	8.3	16.	9.6	27.	5.8	Vertical	1.1E+002	4.4E+005	0.850292	
5	1.1	5.0	1.0	16.	8.2	8.3	19.	23.	26.	4.8	Horizontal	1.1E+002	4.4E+005	0.841884	
6	0.91	5.0	0.84	17.	7.1	8.0	15.	8.7	26.	5.1	Vertical	1.1E+002	4.4E+005	0.841869	
7	0.98	15.	0.42	20.	8.8	23.	19.	23.	34.	2.6	Vertical	1.1E+002	4.3E+005	0.812069	
8	1.5	6.1	0.40	15.	8.6	23.	24.	12.	26.	5.6	Vertical	1.1E+002	4.0E+005	0.803123	
9	1.2	5.0	0.65	15.	9.5	23.	21.	23.	35.	4.0	Horizontal	1.1E+002	4.0E+005	0.794186	
10	0.84	5.0	0.20	18.	9.0	23.	20.	22.	36.	4.0	Vertical	1.1E+002	3.8E+005	0.779085	
11	1.2	5.0	0.51	11.	11.	8.0	25.	23.	26.	3.0	Horizontal	1.1E+002	3.9E+005	0.774901	
12	1.3	15.	1.0	16.	7.4	23.	18.	8.0	26.	5.6	Vertical	1.0E+002	4.2E+005	0.763113	

Table 3-18: Continued

Solutions #	A	B	C	D	E	F	G	H	J	K	L	NPV	CO_2	Desirability	
13	0.60	15.	1.0	17.	8.8	23.	19.	22.	39.	1.7	Horizontal	1.1E+002	3.9E+005	0.755215	
14	1.1	15.	0.80	16.	7.9	23.	13.	16.	32.	3.5	Vertical	1.2E+002	3.6E+005	0.753555	
15	0.96	5.0	1.0	17.	10.	8.0	14.	18.	26.	6.7	Vertical	1.1E+002	3.7E+005	0.738005	
16	0.81	15.	0.20	19.	7.4	23.	23.	23.	38.	7.4	Vertical	98.	4.1E+005	0.725776	
17	0.79	5.0	0.20	11.	9.4	19.	20.	22.	26.	6.2	Horizontal	92.	3.9E+005	0.665429	
18	1.0	15.	0.22	16.	4.7	8.0	25.	8.0	37.	7.4	Vertical	1.1E+002	3.1E+005	0.652593	
19	0.91	15.	0.20	16.	5.7	23.	22.	8.0	35.	5.5	Horizontal	95.	3.6E+005	0.650948	
20	0.96	8.7	0.20	15.	5.5	8.0	24.	11.	26.	5.0	Horizontal	94.	3.4E+005	0.618172	

We found the optimum values for each design parameters to maximize the net present value and amount of CO_2 sequestered. The selected solution needs to be compared with simulation results to check the reliability of the generated response surface. By using the optimum values for each parameter, a new case for the simulator is built and run. Table 3-19 presents the results from both the simulator and design. It can be seen that the calculated error is reasonable. The generated response surface give good results and shows its reliability.

Table 3-19: Design Results and Simulation Results

	Net Present Value ($ MM)	CO_2 (Ton)
Design	1.20E+02	5.50E+05
Simulation	1.09E+02	5.03E+05
Difference	0.11E+02	0.47E+05
Error	9%	8.5%

3.5 Discussion of the Simulation Results and Comparison with Previous Work

Eleven parameters are used to co-optimize the net present value and the amount of CO_2 sequestered. Eighty scenarios are run using CMG's (2008) compositional simulator. The number of required scenarios is decreased using experimental design and response surface methodology. Without using experimental design and response surface methodology, we need to run 211 = 2048 scenarios. Table 3-10 presents the simulations results. Among all of these eighty runs, a minimum net present value is 49 ($MM) and maximum value is 110 ($MM). When the average NPV values is taken for horizontal wells, it is calculated 72 ($MM). For vertical wells, the average NPV is found to be 68 ($MM). Figure 3-12 presents the net present values for each case. There are ten solutions for vertical well configuration and ten solutions for horizontal well configuration (Table 3-18). These solutions show the optimum conditions to maximize the response functions and a desired case is created by using horizontal wells. Also, the values for the amount of CO_2 sequestered are averaged according to well configuration. When the average of amount of CO_2 sequestered values is taken for horizontal wells, it is calculated 181119 (ton). For vertical wells, the average amount of CO_2 sequestered is 171704 (ton). Figure 3-13 shows the amount of CO_2 sequestered for each case. Under these circumstances, it can be stated that horizontal wells are better for this study with a small difference in net income and amount of CO_2 sequestered. However, the designer must check each case, because these values are averaged and the well configuration is a very important parameter for each specific case and may vary.

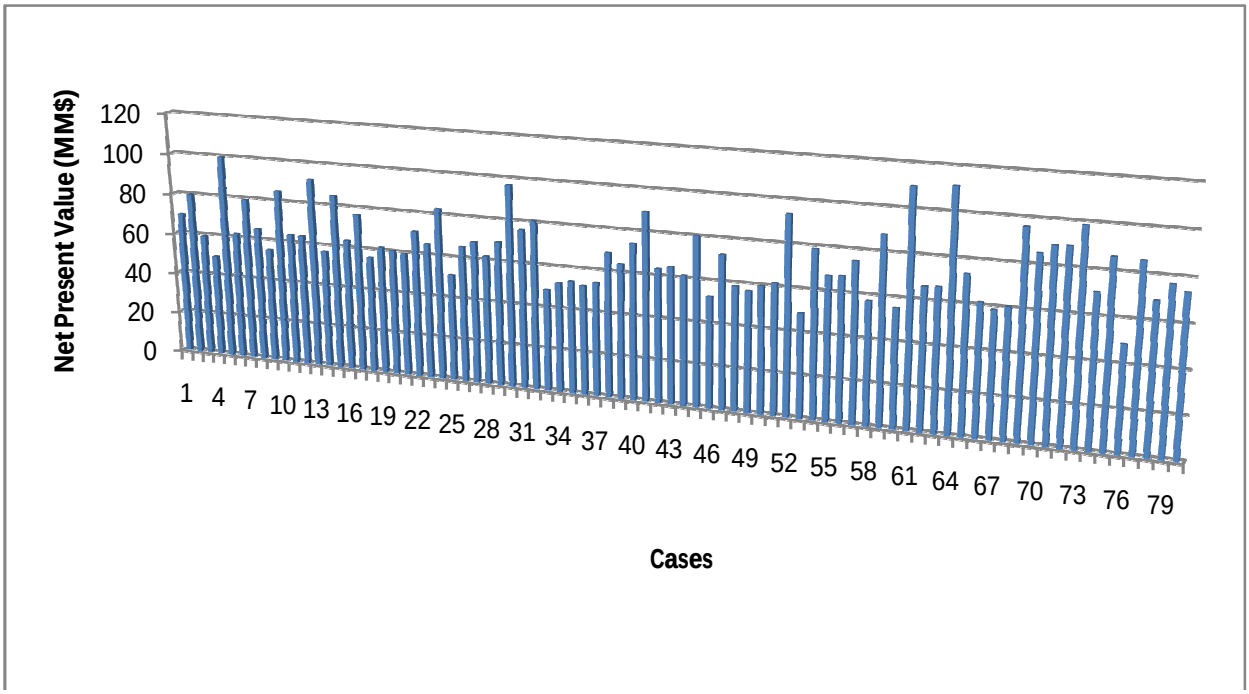

Figure 3-12 Net Present Values for Each Case

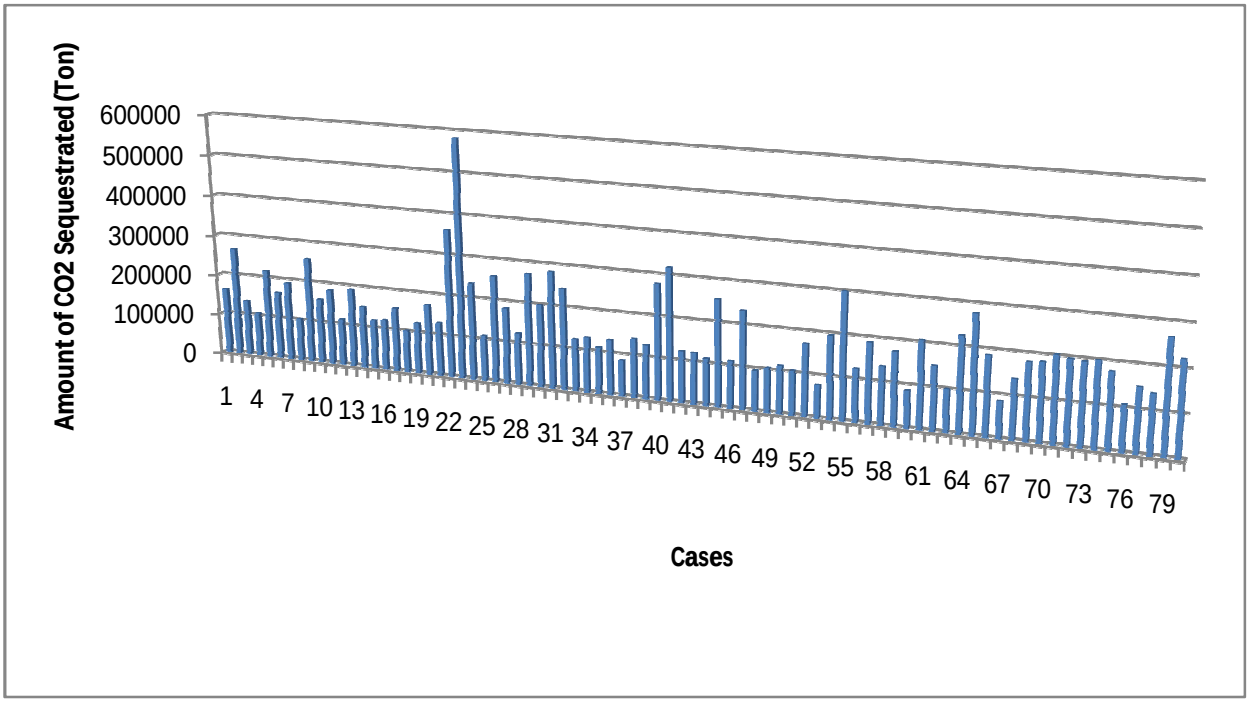

Figure 3-13 Amount of CO_2 Sequestered for Each Case

As mentioned before, this reservoir model is also used by Salazar (2009). He studied coupled CO_2 sequestration and EOR optimization using experimental design and response surface methodology. The differences between this study and Salazar's study are the equations used to calculate the NPV, economic analysis input data, and the injected fluid which is CO_2 in Salazar's study and solvent in this study (Table 3-3). His optimum condition is modified for the new version of the CMG's (2008) compositional simulator and run again. NPV is calculated using a spreadsheet, which is prepared by utilizing the equations given in Section 3.3.1. The amount of CO_2 sequestered is calculated by finding CO_2 injected minus CO_2 produced. After performing these changes and calculations, the amount of CO_2 sequestered is found to be 457517 ton and the NPVs are found to be 98 ($MM) for Salazar's modified case. This shows that the amount of CO_2 sequestered and NPV can be increased by the water alternating solvent injection method instead of the water alternating CO_2 injection method for this study.

3.6 CONCLUSION

In this study, CO_2 sequestration and oil recovery is co-optimized by using experimental design and response surface methodology. The aim of the project is to maximize both the amount of CO_2 sequestered and recovery. To achieve our aim, the water alternating solvent gas injection method is applied. The purpose of solvent injection is to decrease the minimum miscibility pressure, and hence, produce the residual oil. To decrease the number of simulations and find the optimum values, experimental design and response surface methodology is used. For the optimization, the ratio of water-gas, total CO_2 slug size, injection rate of the CO_2, coordinates of the injectors, and drilling time for the last injector are chosen as numerical factors and well design is set as a categorical factor. Net present value and the amount of CO_2 sequestered are selected as

response functions. Eighty scenarios are generated by the quadratic model build the response surface function. The amount of CO_2 sequestered is obtained from the simulator output files and net present values are calculated by the prepared spreadsheet. At the end of the study, the water alternating solvent gas injection method is compared with the water alternating pure CO_2 injection method.

According to the results of eighty simulations performed, net present value ranges between 49 ($MM) and 110 ($MM).The average net present value is 72 ($MM) for horizontal wells and 68 ($MM) for vertical wells. The amount of CO_2 sequestered is 181119 (ton) for horizontal wells and 171704 (ton) for vertical wells. Hence, the horizontal well configuration should be used instead of the vertical well configuration to maximize the net present value and amount of CO_2 sequestered. However, the well configuration should be checked for each specific scenario, because this result is obtained by considering the averaged values.

At the end of the project, result obtained from the design needs to be run by the simulator to check the reliability of the generated response surface equation. A new case is generated by using the optimum values for each parameter and run. A comparison is performed between the design and simulation results shows that the error is less than 8.5%. According to these results, experimental design and response surface methodology can be used for optimization purposes in oil fields. The reservoir model used in this study is also used by Salazar (2009). His study was about coupled CO_2 sequestration and enhanced oil recovery optimization using Experimental Design and Response surface Methodology. His optimum condition, is regenerated for the new version of the CMG's (2008) compositional simulator. The amount of CO_2 sequestered is calculated by taking the difference between injected and produced CO_2 values. Net present value is calculated by updated input values and using our spreadsheet. As a result, the water alternating CO_2

injection method maximizes the amount of CO_2 sequestered and the water alternating solvent injection method maximizes the oil recovery and the net income for the reservoir under study.

Chapter 4: Co-optimization of CO_2 Sequestration and Methane Recovery from Geopressured-Geothermal Aquifers

4.1 INTRODUCTION

Carbon dioxide injection into oil reservoirs is a common method for enhanced oil recovery used in the oil industry. However, it is known that many geopressured-geothermal aquifers contain large amounts of methane. Sequestering the CO_2 in deep geopressured-geothermal aquifers can possibly be profitable if methane recovery can be increased and the energy of these aquifers can be utilized. According to John et al. (1998), three types of energy can be obtained from geopressured-geothermal aquifers, which are chemical energy (dissolved methane), thermal energy (hot brine) and mechanical energy (excessive brine rates). These energy types can be used to offset the cost of a possible sequestration project. It is known that CO_2 is one of the greenhouse gases and one of the causes of global warming. The concentration of the CO_2 in the atmosphere increased from 315 ppm to 390 ppm between 1958 and 2011 (Tans, 2011). To achieve the aim of CO_2 sequestration, deep saline aquifers are the best candidates because of their size, environmental influence, economics, and duration. They also are convenient for three types of trapping: structural, mineral, and solubility trapping (Basbug et al., 2005). While injecting the CO_2 in geopressured-geothermal aquifers, methane can be produced by replacing it with CO_2. According to Taggart (2010), the relative solubility of the CO_2 is 5 to 10 times larger than the relative solubility of the methane.

In this chapter, experimental design and response surface methodology is used to co-optimize the recovery of the methane and storage of the CO_2. Our method is injecting CO_2 and water together at the bottom of the reservoir so that brine with dissolved methane travels upward where perforation of the production wells exists. Mobility of the

CO_2 in the reservoir can be decreased and brine with dissolved methane, which is less heavy than brine with dissolved CO_2, can be pushed upward by injecting water and CO_2 together. Recovery of the methane will be a source of income for the project; also the heat of the hot brine will be used to produce electricity, which will be an additional income for the project. Additional energy can be produced from brine by using turbines but this will decrease the flow rate, and therefore; increase the injection costs. Hence, turbines are not used in this study.

4.2 RESERVOIR DESCRIPTION AND DEVELOPMENT PLAN

4.2.1 Reservoir Description

In this section, reservoir properties of the model used to co-optimize the methane recovery and carbon dioxide sequestration are described. Most of the reservoir properties are taken from the model described in the U.S. Gulf Coast Geopressured-Geothermal Reservoir Simulation Final Report (MacDonald, et al., 1979). A three-dimensional corner point reservoir grid is built. The model consists of 3840 grid blocks, 48 in the x direction, 80 in the y direction and 1 in the z direction. In the z direction, grid size is between 160-220 ft and 660 ft in the x and y directions, respectively. The model is built by using sandstone properties for the aquifer. The average porosity of the reservoir is %19,634 and total bulk reservoir volume is 6.215E+11 res ft3. The solution gas water ratio is %34.343. Table 4-1 presents the reservoir properties and Figure 4-1 shows the cross sectional view of the three-dimensional corner point reservoir model which is created by GEM, CMG's (2008) compositional simulator. The Peng-Robinson equation of state is used to model the fluid properties. Table 4-2 shows the reservoir fluid description.

Table 4-1: Summary of the Reservoir Properties

Parameters	Values	Units
Number of cells in the x direction	28	
Number of cells in the y direction	80	
Number of cells in the z direction	1	
Number of Gridblocks	48*80*1	
x gridblock size	660	ft
y gridblock size	660	ft
z gridblock size	160-220	ft
Width	31680	ft
Length	52800	ft
Thickness	160-220	ft
Depth	15644	ft
Pressure	1.232E+04	psia
Temperature	302	F
Average Porosity	0.19634	
kv/kh	0.1	
Total Bulk Reservoir Volume	6.21E+11	res ft3
Total Pore Volume	1.22E+11	res ft3
Solution GWR	0.3434	scf/STB
OWIP	1.905E+10	STB
Dissolved Gas	6.545E+11	ft3

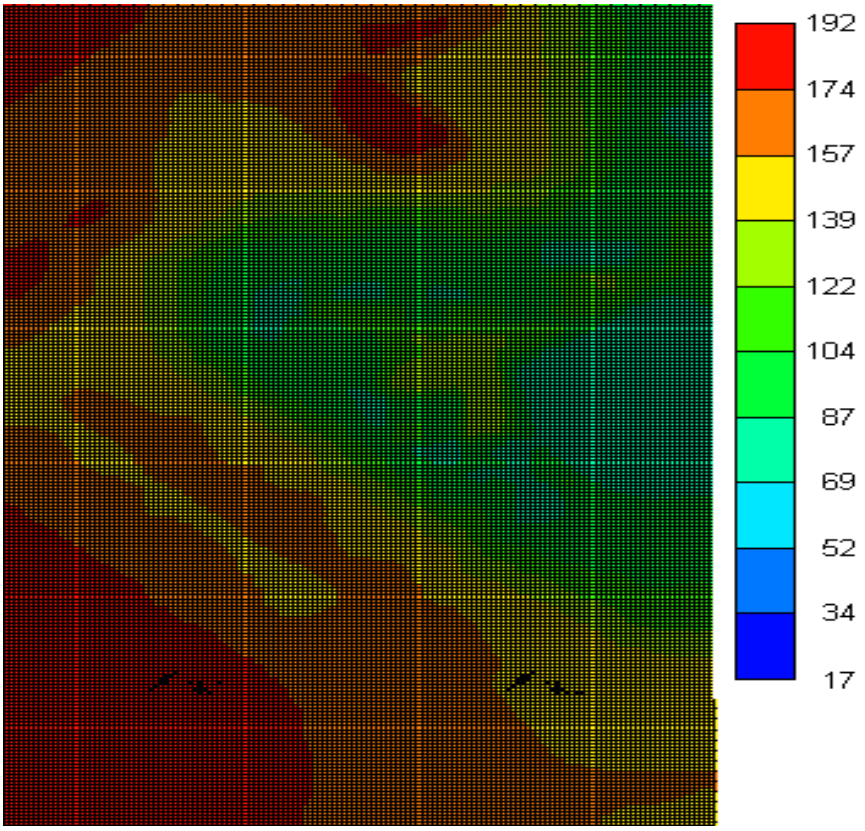

Figure 4-1: Cross Sectional View of the Three-Dimensional Corner Point Reservoir Model, Permeability

Table 4-2: Reservoir Fluid Description

Component	CO_2	C1	H2O
Pc (atm)	72.8	45.4	217.6
Tc (K)	304.2	190.6	647.3
Accentric factor	0.225	0.008	0.344
Molecular weight g/gmole	44.01	16.043	18.015
Critical Volume m3/kgmole	0.094	0.099	0.056
Omega A	0.45724	0.457235529	0.45724
Omega B	7.78E-02	7.78E-02	7.78E-02
Specific Gravity	0.818	0.3	1
Parachor	78	77	52

4.2.2 Development Plan

To decide the design parameters and their range, and as well as the injection scheme to determine the optimum well configurations, some scenarios are built and run before using the experimental design and response surface methodology. In these scenarios, the production well configuration is set as horizontal. Horizontal and vertical well configurations are used for injection wells. Horizontal injection wells are more efficient when compared with vertical injection wells due to their higher injection rate capability and their ability to increase the sweep efficiency (Gui, Jia, & Cunha, 2008). However, horizontal wells are more expensive than vertical wells and increase in the cumulative production needs to offset the cost difference for the well configuration. Also, pure carbon dioxide injection and carbon dioxide dissolved water injection schemes are used. Another aim of these scenarios is finding the most profitable case. These cases are run for 30 years or until carbon dioxide breakthrough. In the first case, one horizontal production well and one horizontal injection well are used. These two wells are drilled on the left part of the reservoir where permeability is higher. The production well is drilled at the upper part and injection well is drilled at the bottom. Figure 4-2 shows the permeability map of the model and the locations of the two wells. Figure 4-3 presents the cumulative production and daily production of methane vs. time. According to Figure 4-3, the methane production is 3.50E+10 scf and daily production rate of methane is changing between 3.20E+10 scf/day and 3.40E+10 scf/day. In the second case, two horizontal wells are drilled at the top and two injection wells are drilled at the bottom of the reservoir. Figure 4-4 shows the permeability map of the model and the locations of the four wells. According to results, the methane production is 6.50E+10 scf and daily production rate of methane is between 5.60E+10 scf/day and 6.80E+10 scf/day. Figure 4-5 presents the cumulative production and daily production of methane vs. time. To see

the areal sweep efficiency and to understand the effect of the well locations and configuration on the areal sweep efficiency, the global mole fraction of the methane is obtained from the results file. Figure 4-6 shows the global mole fraction of the methane after 30 years. In the third case, distance between the injection and production wells is decreased to understand the effect of distance between the wells on sweep efficiency and cumulative production. Figure 4-7 presents the permeability map of the model and the locations of the four wells. Figure 4-8 presents the cumulative production of methane vs. time. According to the results, cumulative methane production is 3.50E+10 scf. Figure 4-9 shows the global mole fraction of the methane after 15 years. In the fourth case, two horizontal producers and two vertical injectors are drilled to understand the effect of the vertical injectors on the sweep efficiency and production. Figure 4-10 shows the permeability map of the model and the locations of the four wells. According to the results, cumulative methane production is 6.00E+10 scf for 30 years and daily methane production is between 5.00E+10 scf/day and 6.75E+10 scf/day. Figure 4-11 presents the cumulative production and daily production of methane vs. time. Figure 4-12 shows the global mole fraction of the methane after 15 years.

In this section, the aim is to find the most profitable way to sequester more CO_2 so that methane production and electricity generation need to be increased and capital costs need to be decreased. In terms of capital investment, the only difference between cases is the number of wells and the well configurations. Capital investment decreases by decreasing the number of the wells and by using vertical wells instead of horizontal wells. Also, net income needs to be high enough to make the project profitable. Methane production is one of the parameters used while comparing the scenarios. According to the results, the highest cumulative production is achieved with the second case where four horizontal production and injection wells are drilled. The second highest production is

obtained by the fourth case; moreover the cumulative production between the second and the fourth case is not that high. In the fourth case, vertical wells are used as injectors. There is a big cost difference between horizontal and vertical wells, because these geopressured-geothermal reservoirs are very deep; hence, drilling long horizontal wells requires advanced technology. However, this will increase the cost substantially. In the first and third cases, the cumulative production is almost half of the fourth case and carbon dioxide breakthrough occurs earlier in the third case. This is not optimal due to a smaller sweep efficiency and extra cost due to carbon dioxide recycling. Considering these reasons, the second case is more appropriate for this study. Table 4-3 presents the summary of the results of the cases. Table 4-4 shows the operating properties for the production and injection wells.

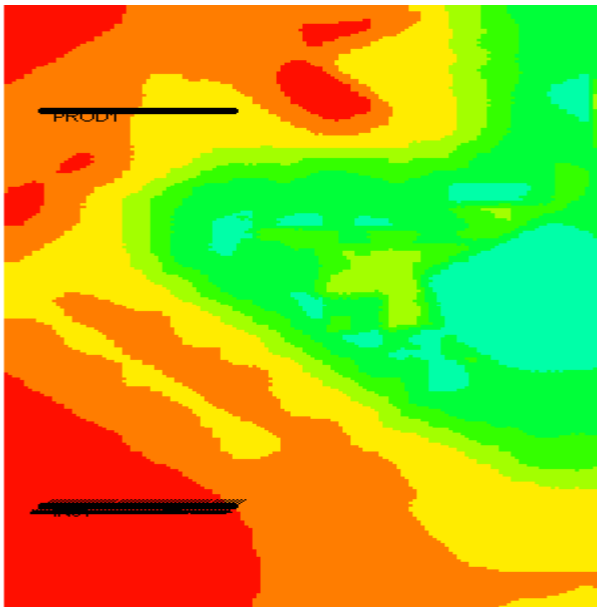

Figure 4-2: Permeability Map of the Model with Well Patterns (First Case)

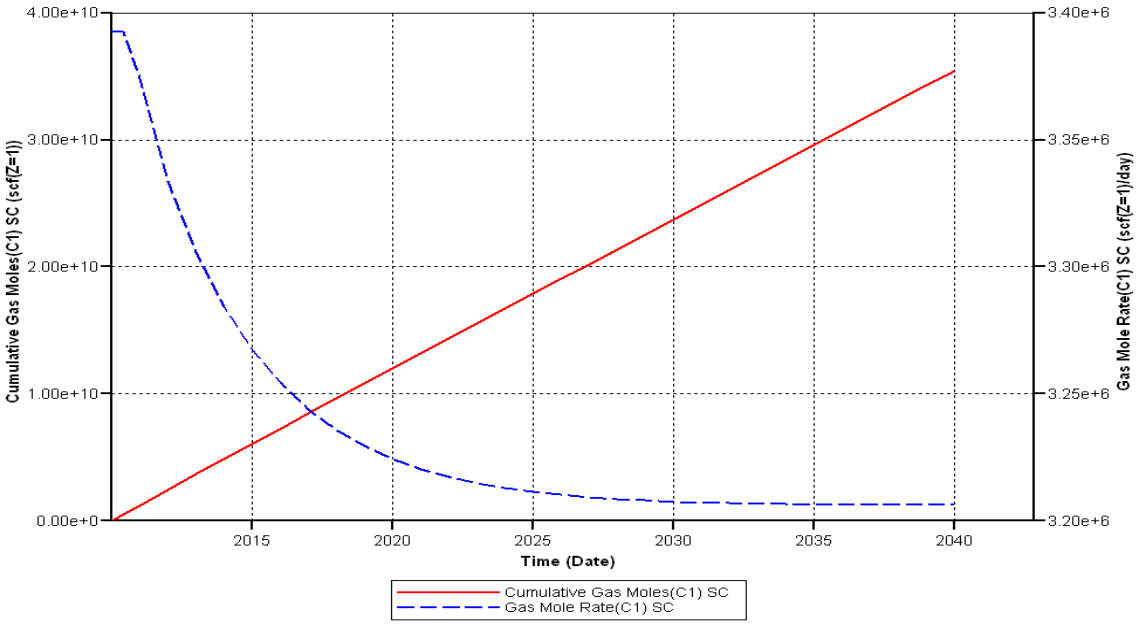

Figure 4-3: Cumulative Production and Daily Production of Methane vs. Time (First Case)

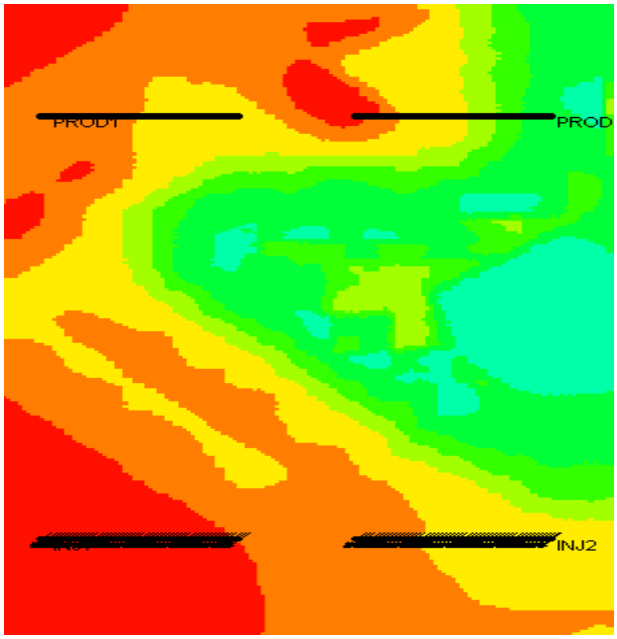

Figure 4-4: Permeability Map of the Model with Well Patterns (Second Case)

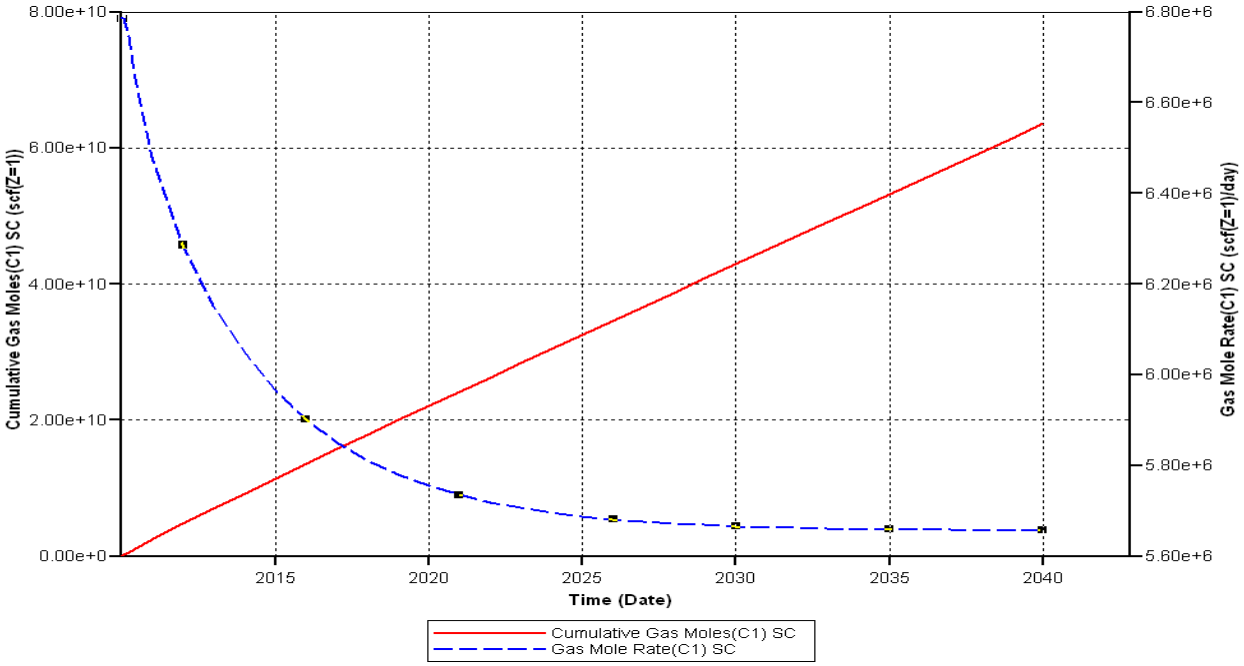

Figure 4-5: Cumulative Production and Daily Production of Methane vs. Time (Second Case)

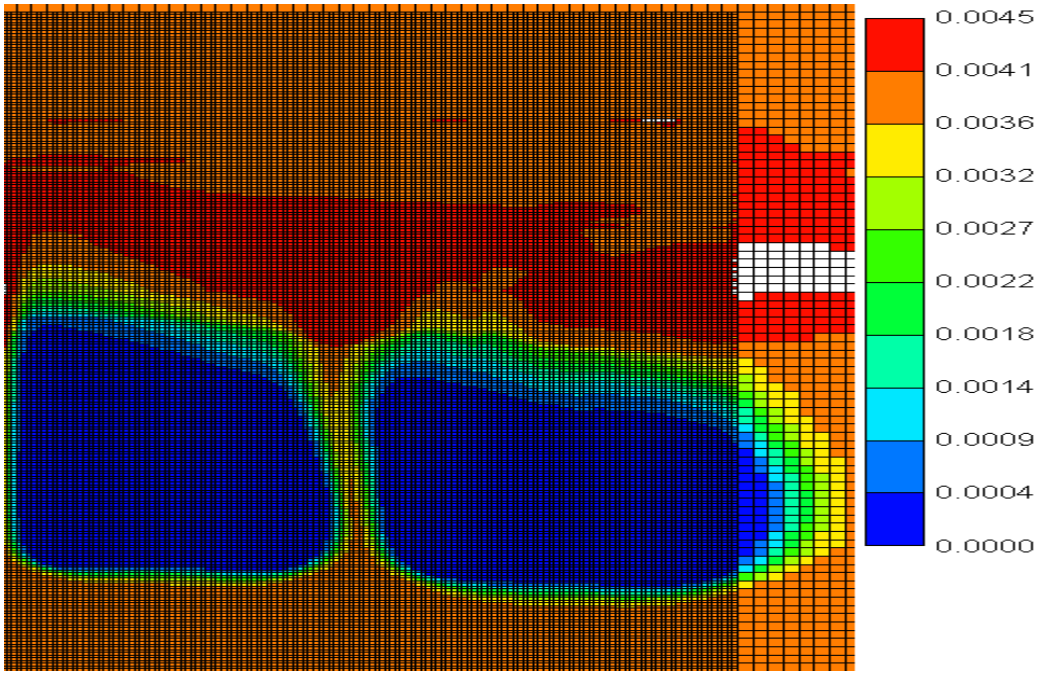

Figure 4-6: Global Mole Fraction of Methane After 30 Years (Second Case)

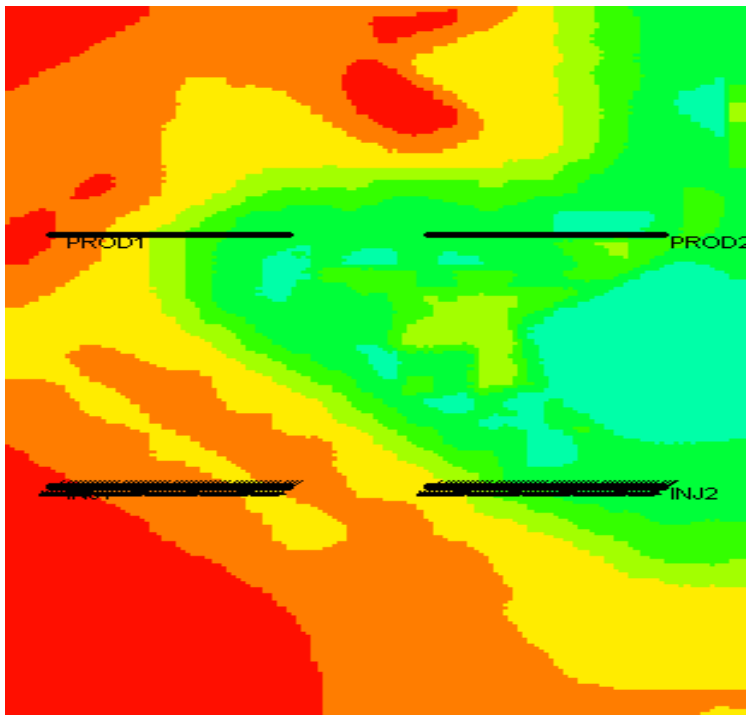

Figure 4-7: Permeability Map of the Model with Well Patterns (Third Case)

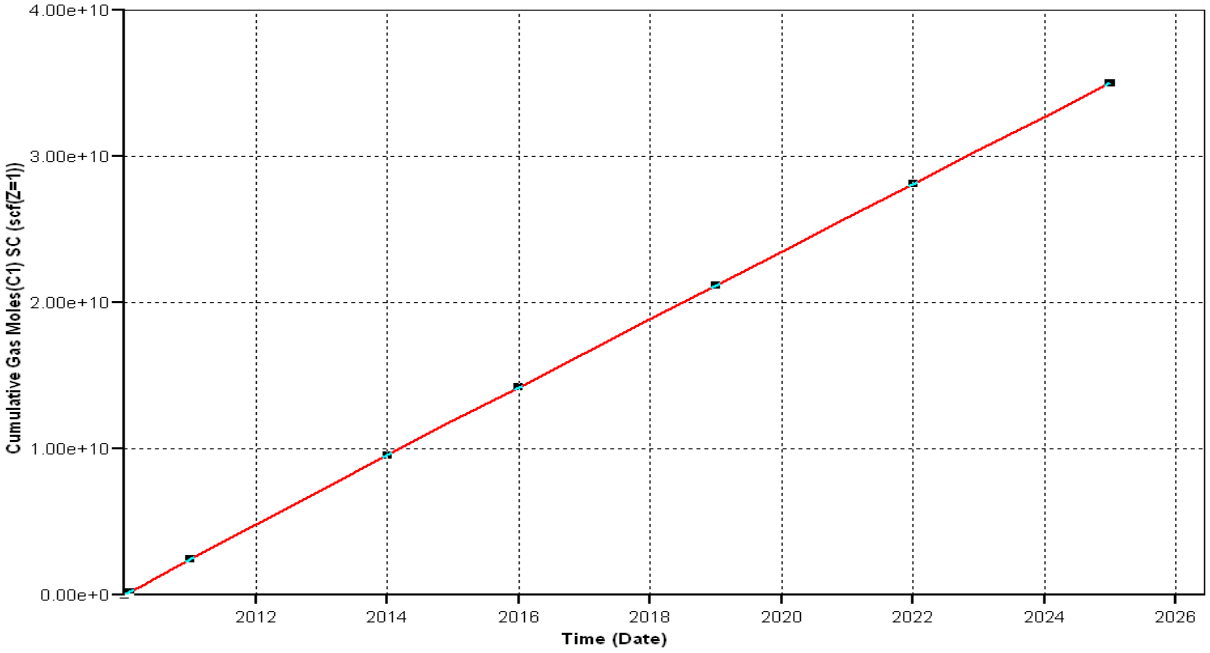

Figure 4-8: Cumulative Production of Methane vs. Time (Third Case)

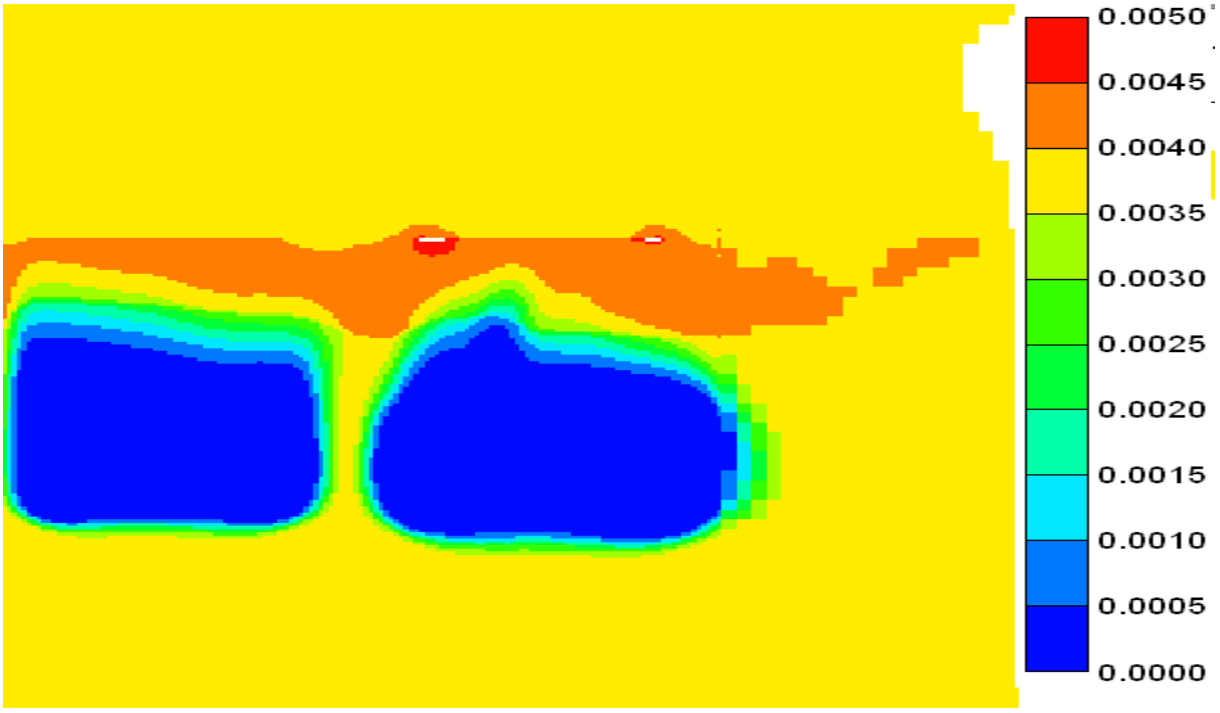

Figure 4-9: Global Mole Fraction of Methane After 15 years (Third Case)

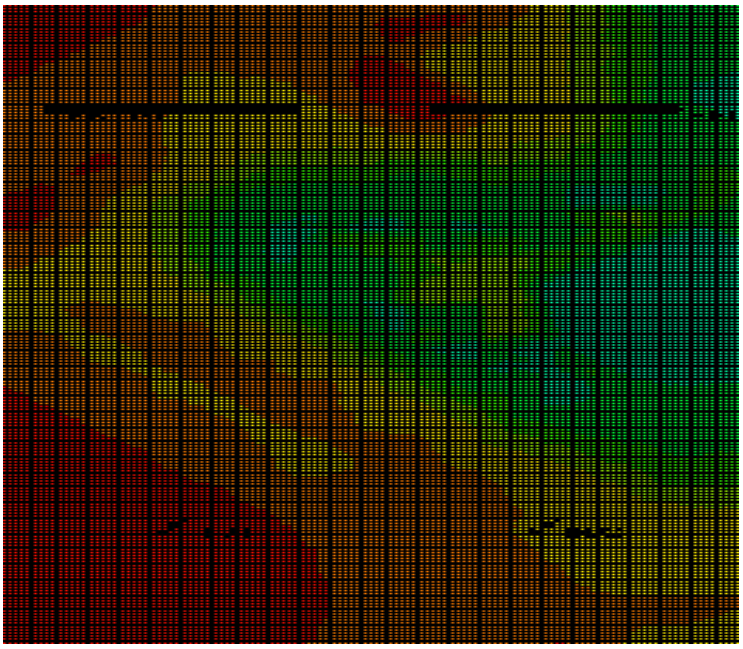

Figure 4-10: Permeability Map of the Model with Well Patterns (Fourth Case)

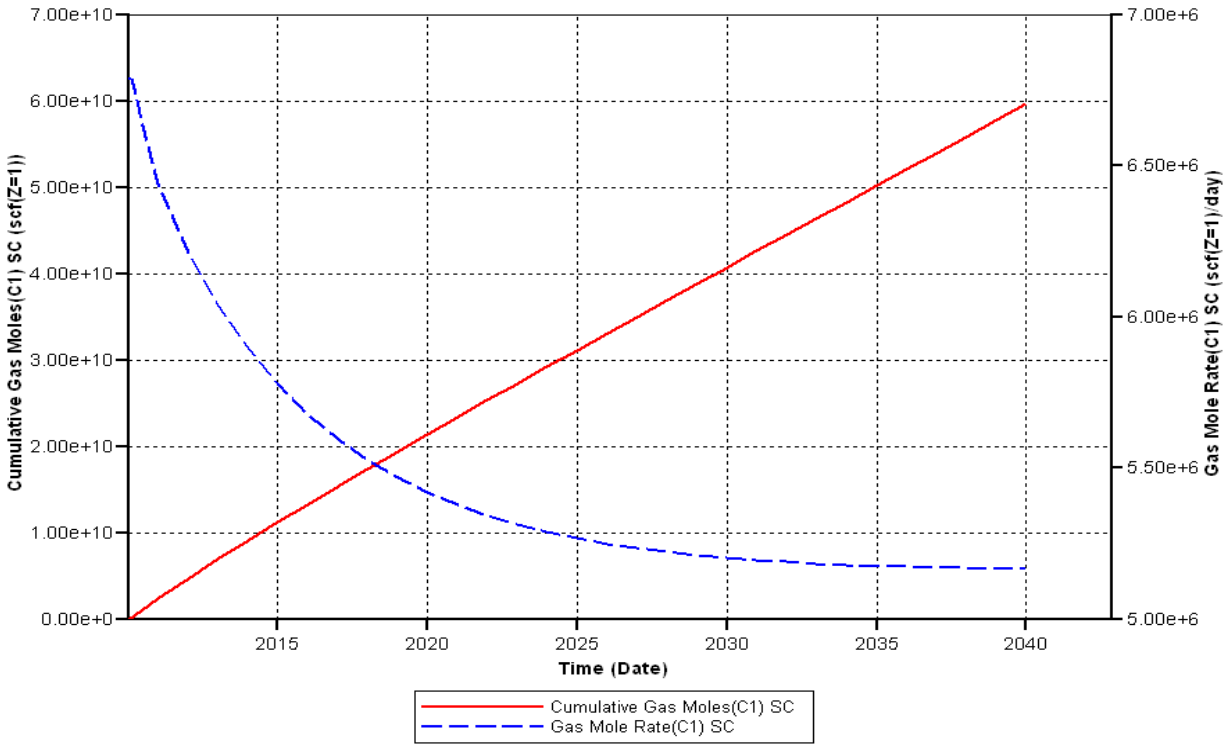

Figure 4-11: Cumulative Production Daily Production of Methane vs. Time (Fourth Case)

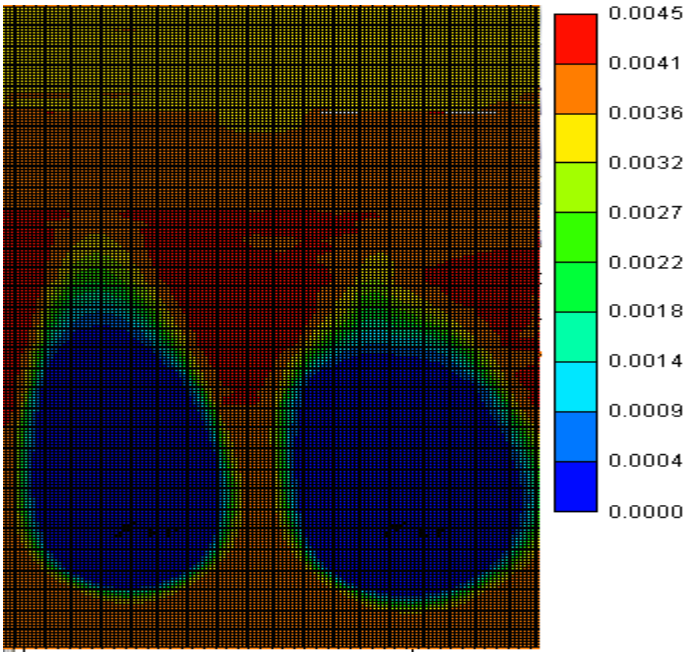

Figure 4-12: Global Mole Fraction of Methane After 30 Years (Fourth Case)

Table 4-3: Summary of the Results of the Cases

Cases	Cumulative Production (scf)	CO_2 Breakthrough Time (year)
1	3.50E+10	30
2	6.50E+10	30
3	3.50E+10	15
4	6.00E+10	30

Table 4-4: Operating Properties for the Production and Injection Wells

Production wells	Values	Units	Action
Maximum flowing bottom hole pressure	13000	psia	Continue
Injection wells			
Maximum surface liquid rate	100000	bbl/day	Continue
Maximum CO_2 component mole percent	0.0189735	fraction	Stop

4.3 METHANE RECOVERY ECONOMIC MODEL

In this section, economic analysis is used to determine the net income from CO_2 sequestration and the methane extraction project is presented. The model built to evaluate the net income from CO_2 sequestration and oil recovery is updated and used. This process requires different surface facilities which will be used to extract the methane from brine and compressed CO_2 to saturate the brine with CO_2 and generate power from the heat of the brine. In this project, all of the wells used for injection or production are drilled at the beginning of the project and all of the produced water is reinjected.

4.3.1 Capital and Operating Costs for Methane Extraction

As stated before, some of the methane is produced in a gas phase and some of it is produced by being extracted from brine. Methane extraction from the brine process needs an additional surface facility. The installation and operational costs for this additional facility depending on the flow rate are given in Table 4-5 (Griggs, 2004).

Table 4-5: Installation and Operational Costs for Methane Extraction Depending on the Flow Rate (Griggs, 2004)

Flow rate (BPD)	Costs for installation ($M)	Yearly operational expenses ($M/yr)
10,000	100	10
25,000	250	25
35,000	350	35
50,000	500	50
60,000	600	60
75,000	750	75

4.3.2 Capital and Operating Costs for Binary Cycle Power Plant and Power Generation

The aim of this project is to maximize the net income and amount of CO_2 sequestered; therefore the use of additional facilities to generate power from the geothermal-geopressured aquifer while sequestering the CO_2 and producing methane is included in the design. Electricity can be produced from high temperature brine by using binary cycle power plants. The working principle of the plant is shown in Figure 4-13 (http://www1.eere.energy.gov/geothermal/powerplants.html#binarycycle). When produced brine goes through the heat exchanger, it will heat the other fluids which have a lower boiling point. Then the heated fluid will vaporize and turn the turbines. These plants are one of the best candidates for electricity generation because they can also produce power from lower temperature fluids with 225 °F-360 °F.A benefit of this option is that air emissions are not generated

(http://www.seco.cpa.state.tx.us/re_geothermal.htm). Installation costs, operational expenses, and electric generation for different flow rates and reservoir temperatures used in this economic model are given in Table 4-6 (Griggs, 2004).

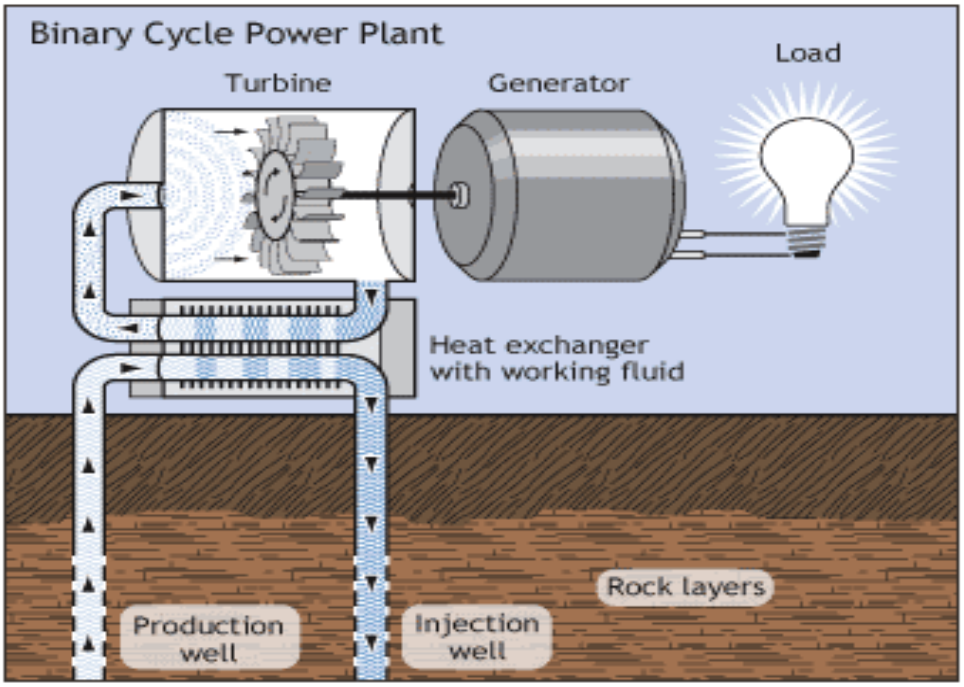

Figure 4-13 Binary Cycle Power Plant
(http://www1.eere.energy.gov/geothermal/powerplants.html#binarycycle 11/16/2010)

Table 4-6: Installation Costs, Operational Expenses, and Electricity Generation for Binary Cycle Plants (Griggs, 2004)

	Reservoir Temperature (212 F)			Reservoir Temperature (266F)		
Flowrate (BPD)	Electric Output (MW)	Installation Cost ($M)	Operational Expenses ($M)	Electric Output (MW)	Installation Cost ($M)	Operational Expenses ($M)
50,000	0.58	580	58	1.75	1750	175
60,000	0.7	700	70	2.25	2250	225
75,000	0.8	800	80	2.5	2500	250

4.3.3 Input and Output Data

Methane production, water production, water injection, carbon dioxide production, and carbon dioxide injection data are obtained from the simulation results. Economic input data is entered into a prepared spreadsheet. Input data from the simulator is presented in Table 4-7 and economic input data are presented in Table 4-8. After entering the input data into Excel spreadsheet, output data is calculated for each run. Output data are shown in Table 4-9.

Table 4-7: Input Data from the Simulator

	Units	Symbol
Methane Production	ft3/day	Mpro
Water Production	bbl/day	Wpro
Water Injection	bbl/day	Winj
CO_2 Production	ft3/day	CO_2pro
CO_2 Injection	ft3/day	CO_2inj

Table 4-8: Economic Input Data

	Units	Symbol	Low	Base	High
Total Investment	MM$	Tinv		16.5	
Intangible Drilling Costs for 4 Wells	MM$	IDC		9.142	
Methane Price	$/mcf	MP		4	
Methane Price Nominal Growth	fraction/year	OPI	0	0.02	0.05
Royalty	fraction	ROY		0.125	
Discount Rate	fraction/year	DR		0.08	
Fed Tax Rate	fraction	FTR	0.2	0.32	0.45
Local/State (Production) Taxes (sev)	$/STB	SEV	0	0.05	0.1
Lift Cost	$/bbl	LC	0.1	0.25	0.50
Lift Cost Nominal Growth	fraction/year	OCI	0	0.02	0.05
CO_2 Price	$/mcf	CO_2P	0	1	2
CO_2 Price Inflation	fraction/year		0	0.02	0.05
Recycle Cost for CO_2	$/mcf	RecCO_2	0.25	0.75	1.25

Table 4-8: Continued

	Units	Symbol	Low	Base	High
CO_2 Recycle Cost Inflation	fraction/year		0	0.02	0.05
CO_2 Injection Cost (compressor)	$/mcf	Included in Total Gas & Water Recycling & Operational Costs			
CO_2 Injection Cost Inflation	fraction/year				
Methane Extraction Cost	$/bbl (yearly)	Mec		1	
Methane Extraction Cost Inflation	fraction/year			0.02	
Electricity price	c/kwh	Ep		5.44	
Water Injection Cost	$/bbl	WIC		0.5	
Water Injection Cost Inflation	fraction/year		0	0.02	0.05

Table 4-9: Output Data

	Units	Symbol
Methane Revenue	mm$/yr	Mrev
CO_2 Purchase Price	mm$/yr	CO_2PP
Electricity Revenue	mm$/yr	Erev
Total Gas Recycling & Operational Cost	mm$/yr	TGROPC
Water Injection Cost	mm$/yr	WIC
Lift Cost	mm$/yr	LC
M Income Before Tax	mm$/yr	MCIBT
Cumulative NCF Before Tax	mm$	CNCFBT
Depreciation	mm$/yr	Dep
Fed Income Tax	mm$/yr	FIT
M Income After Tax	mm$/yr	MCIAT
Cumulative NCF After Tax	mm$	CNCFAT
Discounted Cumulative NCF After Tax	mm$	DCNCFAT

4.3.4 Calculation Algorithm

The net income from the methane recovery and CO_2 sequestration project needs to be calculated for each run to determine the most profitable case. To do that, an excel spreadsheet is prepared by the equations given below. In this project, no credit is applied for CO_2 sequestration. Revenue is calculated on a daily basis and then converted to a yearly basis by using 365.25 as a conversion factor. Methane production, water production, water injection, CO_2 production, CO_2 injection, and time is imported from the simulator and entered after post-processing. Methane production is converted to ft3/day to bbl/day.

Methane Revenue (mm$/yr) =

$$\frac{\text{Methane Production(mbbl/day)}*365.25*\text{Methane Price(\$/bbl)}*(1\text{-Royalty})*\left((\text{Methane Price Inflation}+1)^{t}\right)}{1000}$$

CO_2 Purchase Cost (mm$/yr) =

$$\frac{Max\left((CO2Inj(mmscf/day)-CO2\ \text{Pro(mmscf/day)}),0\right)*365.25*CO2\ \text{Price(\$/mcf)}}{1000}$$

Total Gas & Water Recycling & Operational Cost (mm$/yr) =

$$\left(\frac{\left(\text{CO2 Pro(mmscf/day)}*\text{Recycle Cost}^{CO2}(\$/\text{mcf})+\text{Methane Pro(mbbl/day)}*\text{Methane Extraction Cost(\$/bbl)}\right)}{1000}\right.$$

$$+\frac{\text{Water Pro(mbbl/day)}*Electricity\ \text{Generation Cost(\$/bbl)}}{1000}$$

$$\left.+\frac{\text{Water Pro(mbbl/day)}*\text{Recycle Cost}^{Water}(\$/bbl)}{1000}\right)$$

$$*\left((\text{Operational Cost Inflation}+1)^{t}\right)*365.25$$

Water Injection Cost (mm$/yr) =

$$\frac{\left(\text{Water Inj(mstb/day)}*365.25*\text{Water Inj Cost(\$/stb)}\right)*\left((\text{Operational Cost Inflation}+1)^{t}\right)}{1000}$$

CO_2 Injection Cost (mm$/yr)=

$$\frac{\left(\text{CO2 Inj(mmscf/day)}*365.25*\text{CO2 Inj Cost(\$/mmscf)}\right)*\left((\text{Operational Cost Inflation}+1)^{t}\right)}{1000}$$

Lift Cost (mm$/yr) =

$$\frac{\left(\text{Water Pro(mstb/day)}\right)*365.25*\text{Lift Cost(\$/stb)}*\left(\text{(Operational Cost Inflation+1)}^{t}\right)}{1000}$$

Production Taxes (state, Texas), (mm$/yr)=
Methane Revenue(mm$/yr)*Production Tax(fraction)

Taxable Income (No Credit), (mm$)=
For the first calculation;
=

$$\begin{aligned}&(\text{Methane Revenue(mm\$/yr)}+\text{Electricity Revenue(mm\$/yr)})*\text{t(yr)}\\&-\text{Intangible Drilling \& Comp Costs(mm\$)}\\&-\text{Production Taxes(mm\$/yr)}*\text{t(yr)}\\&-\left(\begin{array}{l}\text{Lift Cost(mm\$/yr)}+\text{CO2 Injection Cost(mm\$/yr)}\\+\text{Water Injection Cost(mm\$/yr)}+\text{Gas \& Water Recycle \& Operation Cost(mm\$/yr)}\\+\text{CO2 Purchase Price(mm\$/yr)}+\text{Depreciation(mm\$/yr)}\end{array}\right)\\&*\text{t(yr)}\end{aligned}$$

For other calculations (at time= t_i);
=

$$\begin{aligned}&\text{Methane Revenue(mm\$/yr)}*(\text{t}_i\text{(yr)}-\text{t}_{i-1}\text{(yr)})+\text{Electricity Revenue(mm\$/yr)}*(\text{t}_i\text{(yr)}-\text{t}_{i-1}\text{(yr)})\\&-\text{Production Taxes(mm\$/yr)}*(\text{t}_i\text{(yr)}-\text{t}_{i-1}\text{(yr)})\\&-\left(\begin{array}{l}\text{Lift Cost(mm\$/yr)}+\text{CO2 Injection Cost(mm\$/yr)}\\+\text{Water Injection Cost(mm\$/yr)}+\text{Gas \& Water Recycle \& Operation Cost(mm\$/yr)}\\+\text{CO2 Purchase Price(mm\$/yr)}+\text{Depreciation(mm\$/yr)}\end{array}\right)\\&*(\text{t}_i\text{(yr)}-\text{t}_{i-1}\text{(yr)})\end{aligned}$$

Federal Income Tax (for Non-Credit Option) (mm$) =
Taxable Income (No Credit), (mm$)*Federal Tax Rate
After Tax Income (for Non-Credit Option) (mm$) =
Taxable Income (No Credit), (mm$) - Federal Income Tax (mm$)
After Tax Cash Flow to Equity (mm$) (for Non-Credit Option) =
For the first calculation;
=After Tax Income (for Non-Credit Option) (mm$) + (Depreciation (mm$/yr)* t(yr)
For other calculations (at time= t_i);
=After Tax Income (mm$) (for Non-Credit Option) + (Depreciation (mm$/yr)*
$(\text{t}_i\text{(yr)}-\text{t}_{i-1}\text{(yr)})$

Discounted Cash Flow (for Non-Credit Option) (mm$) =

$$\frac{\text{AfterTax Cash Flow to Equity } (\text{mm\$}) \ (\text{for Non}-\text{Credit Option})}{(\text{Discount Rate}+1)^{t_i}}$$

Cumulative Discounted Cash Flow (for Non-Credit Option) (mm$)=
For the first calculation;
= Discounted Cash Flow (for Non-Credit Option) (mm$) – Capital Investment (mm$)
For other calculations (at time= t_i);
= Discounted Cash Flow $(\text{for Non}-\text{Credit Option})(\text{mm\$})_i$
+ Discounted Cash Flow $(\text{for Non}-\text{Credit Option})(\text{mm\$})_{i-1}$

4.4 CO_2 SEQUESTRATION AND METHANE RECOVERY FROM GEOPRESSURED-GEOTHERMAL AQUIFERS CO-OPTIMIZATION

In this section, to co-optimize the CO_2 sequestration and methane recovery from geopressured-geothermal aquifers, experimental design and response surface methodology is applied. The purpose of this work is to maximize the CO_2 sequestration and methane recovery from geopressured-geothermal aquifers. Factors are selected to understand the impact of reservoir properties, well type and well configuration on storage and recovery. Some of these factors are eliminated in the development section. It is concluded that vertical wells are more profitable for injection wells and horizontal wells are more efficient for production wells for a thirty-year production period. The reservoir is divided into four parts in which two injectors are drilled at the lower part and two producers are drilled at the top. Range of the coordinates of the wells is set based on these zones. Coordinates of the injectors and producers are selected as numerical factors. A total of eight parameters are chosen for the design. The amount of carbon dioxide sequestered and the cumulative methane production are set as response functions to find the optimum conditions to maximize the recovery and storage. Factors used in the design and the range of these factors are presented in Table 4-10.

Table 4-10: Design Variables

Factors	Type	Min	Max
Injector 1 (X)	Numerical	2	10
Injector 1 (Y)	Numerical	133	167
Injector 2 (X)	Numerical	26	32
Injector 2 (Y)	Numerical	133	167
Producer 1 (X)	Numerical	2	10
Producer 1 (Y)	Numerical	93	127
Producer 2 (X)	Numerical	26	32
Producer 2 (Y)	Numerical	93	127

4.4.1 Design

After deciding the design parameters, ranges, and objective functions, the D-optimal design method is selected to determine the response function and to build the response surface. As stated before, there are eight design parameters and two response functions. Without using the experimental design and response surface methodology, we need to run at least 28 cases. However; by using this method, the number of runs is reduced to 55. To do this, the Design-Expert software version 6 (Stat-Ease Inc, 2005) is employed. The next step is to build these 55 scenarios to determine the amount of carbon dioxide sequestered and the cumulative methane production for each run. D-optimal design with a quadratic model is shown in Table 4-11.

Table 4-11: D-optimal Design with the Quadratic Model

	Factor 1	Factor 2	Factor 3	Factor 4	Factor 5	Factor 6	Factor 7	Factor 8
Run	A:Inj-1 (x)	B:Inj-1 (y)	C:Inj-2 (x)	D:Inj-2 (y)	E:Pro-1 (x)	F:Pro-1 (y)	G:Pro-2 (x)	H:Pro-2 (y)
1	10	167	32	133	10	127	32	127
2	2	167	29	133	10	127	32	127
3	2	133	32	167	2	127	26	127
4	2	167	26	133	10	127	26	93

Table 4-11: Continued

	Factor 1	Factor 2	Factor 3	Factor 4	Factor 5	Factor 6	Factor 7	Factor 8
Run	A:Inj-1 (x)	B:Inj-1 (y)	C:Inj-2 (x)	D:Inj-2 (y)	E:Pro-1 (x)	F:Pro-1 (y)	G:Pro-2 (x)	H:Pro-2 (y)
5	2	167	32	167	10	93	32	127
6	10	167	26	167	6	93	32	127
7	10	133	32	167	10	93	26	127
8	2	133	26	167	10	127	26	127
9	2	167	26	167	2	93	26	110
10	2	133	32	150	2	93	32	93
11	2	167	32	167	10	127	32	93
12	2	167	32	167	10	93	26	93
13	10	133	29	133	10	127	26	127
14	10	167	26	133	2	127	26	127
15	10	133	29	133	10	127	26	127
16	6	167	26	133	2	93	32	93
17	10	167	32	133	2	127	26	93
18	2	133	32	133	2	127	32	93
19	10	133	26	133	10	93	32	127
20	2	167	26	167	10	93	29	127
21	10	133	26	167	10	127	26	110
22	2	133	26	133	2	93	32	127
23	2	133	26	167	2	127	32	93
24	10	167	26	167	10	93	26	93
25	2	133	26	133	2	127	26	127
26	10	167	32	167	2	93	29	93
27	10	167	32	167	10	127	26	127
28	2	167	32	167	2	127	26	93
29	2	133	32	167	10	127	32	127
30	10	133	26	133	6	127	32	93
31	6	133	32	167	2	93	26	93
32	10	150	32	133	2	93	26	93
33	10	150	26	167	2	127	26	93
34	10	133	26	167	2	93	32	93
35	10	133	32	167	2	127	32	93
36	10	133	32	133	2	93	32	127
37	6	133	32	167	2	93	26	93
38	10	133	32	133	10	93	32	93
39	2	167	32	133	6	93	32	93

Table 4-11: Continued

	Factor 1	Factor 2	Factor 3	Factor 4	Factor 5	Factor 6	Factor 7	Factor 8
Run	A:Inj-1 (x)	B:Inj-1 (y)	C:Inj-2 (x)	D:Inj-2 (y)	E:Pro-1 (x)	F:Pro-1 (y)	G:Pro-2 (x)	H:Pro-2 (y)
40	10	167	26	167	10	127	32	93
41	2	167	32	167	2	127	32	127
42	10	133	26	167	2	127	32	127
43	10	167	26	167	2	93	26	127
44	2	133	26	133	2	93	26	93
45	10	133	32	167	10	93	26	127
46	10	133	32	167	2	127	32	93
47	10	133	32	150	2	127	26	127
48	10	167	26	133	2	110	32	93
49	10	133	26	133	10	93	26	93
50	10	167	26	133	2	110	32	93
51	2	133	32	133	10	93	26	110
52	6	150	29	150	6	93	29	110
53	2	133	32	167	10	127	26	93
54	2	167	32	133	2	93	26	127
55	2	133	26	167	10	93	32	93

4.4.2 Analysis of the Response Functions

Design-Expert software version 6 (Stat-Ease Inc, 2005) is used to analyze the response functions methane production and amount of carbon dioxide sequestered. Fifty five different scenarios are built and run by GEM, CMG's (2008) compositional simulator. Before analyzing the results, outputs from the simulator need to be entered for each case. Cumulative production data for the methane and cumulative injection and production data for the carbon dioxide were obtained from the simulator. The amount of carbon dioxide sequestered is obtained by taking the difference between cumulative carbon dioxide production and cumulative carbon dioxide injection from the field for thirty years period. Table 4-12 presents the D-optimal design results and the results of the response functions.

Table 4-12: D-optimal Design with Response Functions

Run	Inj-1 (x)	Inj-1 (y)	Inj-2 (x)	Inj-2 (y)	Pro-1 (x)	Pro-1 (y)	Pro-2 (x)	Pro-2 (y)	Methane Production (mmmscf)	Amount of CO_2 Sequestered (mmmscf)
1	10	167	32	133	10	127	32	127	5.14E+01	2.76E+02
2	2	167	29	133	10	127	32	127	4.93E+01	2.62E+02
3	2	133	32	167	2	127	26	127	4.40E+01	2.38E+02
4	2	167	26	133	10	127	26	93	5.16E+01	2.83E+02
5	2	167	32	167	10	93	32	127	6.22E+01	3.60E+02
6	10	167	26	167	6	93	32	127	6.24E+01	3.62E+02
7	10	133	32	167	10	93	26	127	6.35E+01	3.59E+02
8	2	133	26	167	10	127	26	127	5.16E+01	2.83E+02
9	2	167	26	167	2	93	26	110	5.71E+01	3.50E+02
10	2	133	32	150	2	93	32	93	5.94E+01	3.62E+02
11	2	167	32	167	10	127	32	93	6.28E+01	3.62E+02
12	2	167	32	167	10	93	26	93	5.42E+01	3.46E+02
13	10	133	29	133	10	127	26	127	2.89E+01	1.39E+02
14	10	167	26	133	2	127	26	127	5.08E+01	2.71E+02
15	10	133	29	133	10	127	26	127	2.89E+01	1.39E+02
16	6	167	26	133	2	93	32	93	5.64E+01	3.49E+02
17	10	167	32	133	2	127	26	93	6.35E+01	3.58E+02
18	2	133	32	133	2	127	32	93	4.39E+01	2.31E+02
19	10	133	26	133	10	93	32	127	5.33E+01	2.92E+02
20	2	167	26	167	10	93	29	127	6.23E+01	3.60E+02
21	10	133	26	167	10	127	26	110	4.45E+01	2.43E+02
22	2	133	26	133	2	93	32	127	5.29E+01	2.89E+02
23	2	133	26	167	2	127	32	93	4.50E+01	2.48E+02
24	10	167	26	167	10	93	26	93	5.45E+01	3.48E+02
25	2	133	26	133	2	127	26	127	3.05E+01	1.47E+02
26	10	167	32	167	2	93	29	93	5.49E+01	3.49E+02
27	10	167	32	167	10	127	26	127	6.64E+01	3.77E+02
28	2	167	32	167	2	127	26	93	6.31E+01	3.62E+02
29	2	133	32	167	10	127	32	127	5.26E+01	2.90E+02
30	10	133	26	133	6	127	32	93	4.06E+01	2.15E+02
31	6	133	32	167	2	93	26	93	5.97E+01	3.65E+02
32	10	150	32	133	2	93	26	93	5.76E+01	3.54E+02
33	10	150	26	167	2	127	26	93	5.78E+01	3.25E+02
34	10	133	26	167	2	93	32	93	5.98E+01	3.67E+02

Table 4-12: Continued

Run	Inj-1 (x)	Inj-1 (y)	Inj-2 (x)	Inj-2 (y)	Pro-1 (x)	Pro-1 (y)	Pro-2 (x)	Pro-2 (y)	Methane Production (mmmscf)	Amount of CO_2 Sequestered (mmmscf)
35	10	133	32	167	2	127	32	93	4.25E+01	2.34E+02
36	10	133	32	133	2	93	32	127	5.12E+01	2.77E+02
37	6	133	32	167	2	93	26	93	5.97E+01	3.65E+02
38	10	133	32	133	10	93	32	93	5.94E+01	3.56E+02
39	2	167	32	133	6	93	32	93	5.51E+01	3.40E+02
40	10	167	26	167	10	127	32	93	6.31E+01	3.64E+02
41	2	167	32	167	2	127	32	127	6.63E+01	3.74E+02
42	10	133	26	167	2	127	32	127	4.37E+01	2.38E+02
43	10	167	26	167	2	93	26	127	6.27E+01	3.62E+02
44	2	133	26	133	2	93	26	93	5.93E+01	3.53E+02
45	10	133	32	167	10	93	26	127	6.35E+01	3.59E+02
46	10	133	32	167	2	127	32	93	4.25E+01	2.34E+02
47	10	133	32	150	2	127	26	127	4.16E+01	2.20E+02
48	10	167	26	133	2	110	32	93	5.87E+01	3.50E+02
49	10	133	26	133	10	93	26	93	5.96E+01	3.58E+02
50	10	167	26	133	2	110	32	93	5.87E+01	3.50E+02
51	2	133	32	133	10	93	26	110	5.78E+01	3.30E+02
52	6	150	29	150	6	93	29	110	6.03E+01	3.64E+02
53	2	133	32	167	10	127	26	93	5.46E+01	3.02E+02
54	2	167	32	133	2	93	26	127	4.55E+01	2.44E+02
55	2	133	26	167	10	93	32	93	5.91E+01	3.64E+02

4.4.2.1 Analysis of the Cumulative Methane Production Response Function

The cumulative methane production response function first needs to be analyzed. To find the most appropriate model to build the response surfaces, the degree of the polynomial which fits with the equation for the cumulative methane production needs to be validated. The sequential model sum of squares is presented in Table 4-13 and the model summary statistics is shown in Table 4-14, generated by Design-Expert software version 6 (Stat-Ease Inc, 2005). According to Table 4-13 and Table 4-14, the suggested model for the design is 2FI. As explained before, the number of runs required for the

cubic model is very high; therefore fifty-five runs is not suitable for the cubic model. Thus, aliased is written near the cubic model. For the cumulative methane production response function, the suggested 2FI model is used. The analysis of variance table for cumulative methane production is shown in Table 4-15. This table can be used to see the trivial parameters by reviewing the Prob>F. After the parameters are checked, it is decided that the 2FI model is the best model for our case. After finding the convenient model for the design, the equation for cumulative methane production is built. As discussed in Section 4.4.2.1, the generated equation needs to be checked by diagnostic plots to make the design more accurate, which is shown in the next section. Equation 4.1 presents the generated equation for cumulative methane production.

Table 4-13: Sequential Model Sum of Squares for Cumulative Methane Production

Source	Sum of Squares	DF	Mean Square	F Value	Prob > F	
Mean	159546.9358	1	159546.9358			
Linear	2373.77239	8	296.7215487	6.392173	< 0.0001	
2FI	2060.643908	28	73.5944253	17.74464	< 0.0001	Suggested
Quadratic	50.55040294	8	6.318800368	2.621573	0.078	
Cubic	24.10308982	5	4.820617964	63660000	< 0.0001	Aliased
Residual	0	5	0			
Total	164056.0056	55	2982.836466			

Table 4-14: Model Summary Statistics for Cumulative Methane Production

Source	Std. Dev.	R-Squared	Adjusted R-Squared	Predicted R-Squared	PRESS	
Linear	6.813186385	0.526443923	0.444086344	0.318711253	3071.979	
2FI	2.036520627	0.983443704	0.950331113	0.747369289	1139.13	Suggested
Quadratic	1.552516983	0.994654532	0.971134471	0.065683875	4212.897	

Table 4-15: Analysis of Variance for Cumulative Methane Production

	Sum of Squares	DF	Sum of Squares/DF	F Value	Prob > F
Model	4434.416298	36	123.1782305	29.69999	< 0.0001
A	0.025447489	1	0.025447489	0.006136	0.94
B	333.7484738	1	333.7484738	80.47142	< 0.0001
C	5.420570965	1	5.420570965	1.306975	0.27
D	655.4739547	1	655.4739547	158.0439	< 0.0001
E	0.083199731	1	0.083199731	0.020061	0.89
F	281.2748778	1	281.2748778	67.8193	< 0.0001
G	0.176850649	1	0.176850649	0.042641	0.84
H	56.85106974	1	56.85106974	13.70759	0.0016
AB	20.20199501	1	20.20199501	4.870983	0.041
AC	2.636336222	1	2.636336222	0.635657	0.44
AD	2.334188251	1	2.334188251	0.562805	0.46
AE	16.40799126	1	16.40799126	3.956196	0.062
AF	0.939222161	1	0.939222161	0.22646	0.64
AG	2.63494429	1	2.63494429	0.635322	0.44
AH	1.929227396	1	1.929227396	0.465164	0.50
BC	0.044412536	1	0.044412536	0.010708	0.92
BD	4.782775352	1	4.782775352	1.153194	0.30
BE	13.21693102	1	13.21693102	3.186787	0.091
BF	974.2879842	1	974.2879842	234.9144	< 0.0001
BG	12.07621101	1	12.07621101	2.911743	0.11
BH	17.96912862	1	17.96912862	4.332608	0.052
CD	11.93675665	1	11.93675665	2.878119	0.11
CE	13.27109131	1	13.27109131	3.199846	0.090
CF	12.5734637	1	12.5734637	3.031638	0.099
CG	0.457990856	1	0.457990856	0.110428	0.74
CH	1.481136084	1	1.481136084	0.357123	0.56
DE	14.51408423	1	14.51408423	3.499548	0.078
DF	43.42478698	1	43.42478698	10.47032	0.0046
DG	14.45315791	1	14.45315791	3.484858	0.078
DH	284.6468073	1	284.6468073	68.63232	< 0.0001
EF	0.772626297	1	0.772626297	0.186291	0.67
EG	1.187618067	1	1.187618067	0.286351	0.60
EH	4.523988469	1	4.523988469	1.090797	0.31
FG	2.766536479	1	2.766536479	0.667051	0.42
FH	23.4163959	1	23.4163959	5.64602	0.029
GH	9.637419253	1	9.637419253	2.323716	0.14

Cumulative Methane Production= (4.1)

574.7128597	
1.014329238	* Inj-1 (x)
-2.724116955	* Inj-1 (y)
1.345721721	* Inj-2 (x)
-0.844429497	* Inj-2 (y)
-2.075566269	* Pro-1 (x)
-3.457978359	* Pro-1 (y)
-0.052625404	* Pro-2 (x)
-1.797565854	* Pro-2 (y)
0.012076346	* Inj-1 (x) * Inj-1 (y)
-0.023001596	* Inj-1 (x) * Inj-2 (x)
-0.004004921	* Inj-1 (x) * Inj-2 (y)
-0.047089364	* Inj-1 (x) * Pro-1 (x)
-0.002317424	* Inj-1 (x) * Pro-1 (y)
-0.022261732	* Inj-1 (x) * Pro-2 (x)
-0.003467607	* Inj-1 (x) * Pro-2 (y)
-0.000729254	* Inj-1 (y) * Inj-2 (x)
0.00140073	* Inj-1 (y) * Inj-2 (y)
-0.010455482	* Inj-1 (y) * Pro-1 (x)
0.019069975	* Inj-1 (y) * Pro-1 (y)
0.011287786	* Inj-1 (y) * Pro-2 (x)
0.002550548	* Inj-1 (y) * Pro-2 (y)
-0.011357779	* Inj-2 (x) * Inj-2 (y)
0.051321827	* Inj-2 (x) * Pro-1 (x)
0.011289285	* Inj-2 (x) * Pro-1 (y)
-0.012759112	* Inj-2 (x) * Pro-2 (x)
-0.004046395	* Inj-2 (x) * Pro-2 (y)
0.010669239	* Inj-2 (y) * Pro-1 (x)
0.004013812	* Inj-2 (y) * Pro-1 (y)
-0.012079145	* Inj-2 (y) * Pro-2 (x)
0.009777083	* Inj-2 (y) * Pro-2 (y)
-0.002066318	* Pro-1 (x) * Pro-1 (y)
0.015113067	* Pro-1 (x) * Pro-2 (x)
0.005586052	* Pro-1 (x) * Pro-2 (y)
-0.005236245	* Pro-1 (y) * Pro-2 (x)
-0.003012394	* Pro-1 (y) * Pro-2 (y)
0.010769708	* Pro-2 (x) * Pro-2 (y)

After finding the appropriate model for the design, the Box-Cox plot and Normal Plot of Residuals need to be checked to see whether the design requires transformation or not. As stated before, when lambda is equal to one, are not needed transformation for the design (Myers et al., 2002). Figure 4-14 presents the Box-Cox plot for cumulative methane production. The blue vertical line shows that the value of the lambda is equal to one. Figure 4-15 shows the normal plot of residuals for cumulative methane production. It can be seen that most of the points are on the straight line which means that the normality assumption for the design is correct. So the equation generated for the cumulative methane production response function can be used without applying any transformation.

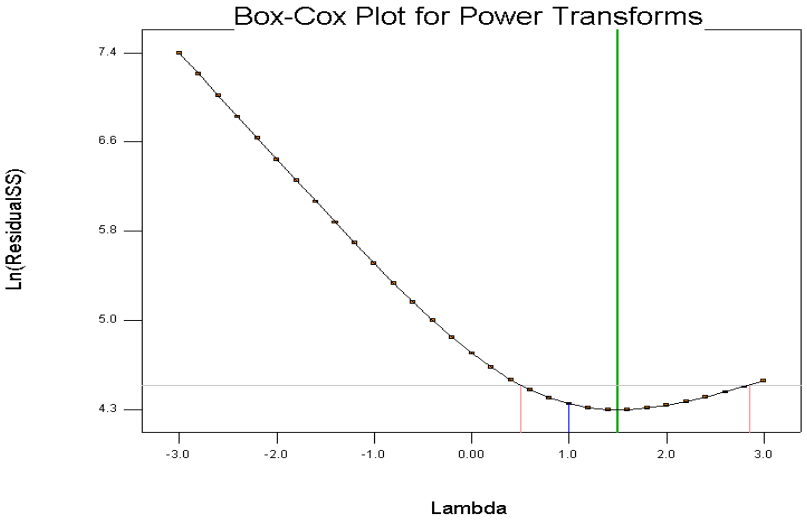

Figure 4-14: Box-Cox Plot for Cumulative Methane Production

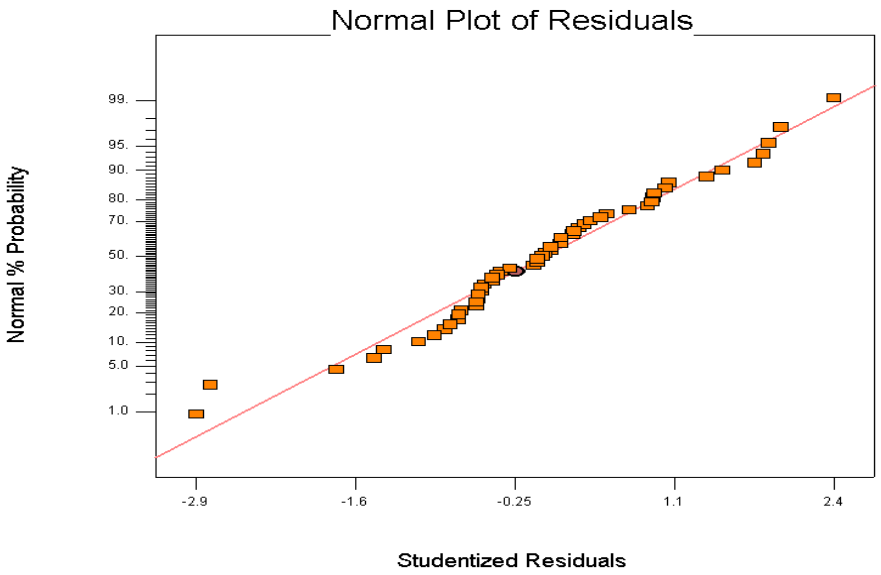

Figure 4-15: Normal Plot of Residuals for Cumulative Methane Production

4.4.2.2 Analysis of Amount of CO_2 Sequestered Response Functions

The same steps performed for the analysis of cumulative methane production are followed in this section. Table 4-16 presents the sequential model sum of squares for the amount of carbon dioxide sequestered and Table 4-17 shows the model summary statistics for the amount of carbon dioxide sequestered. It can be seen that the suggested model for the design is 2FI model. Aliased is written near cubic model because the number of experiments is not enough for the cubic model. The 2FI model is used to build the equation for the amount of carbon dioxide sequestered. Also the analysis of variance table for the amount of carbon dioxide sequestered (Table 4-18) shows the parameters which do not have great impact on the response function. The next step is to check whether the design requires any transformation or not. This can be done by looking at the Box-Cox plot and Normal Plot of Residuals to see if the lambda value is equal to one or if the points on the normal plot of residuals figure are on the straight line, the design does not require transformation. Figure 4-16 presents the Box-Cox plot for the amount of

carbon dioxide sequestered where lambda is equal to one. Figure 4-17 shows the normal plot of residuals for the amount of carbon dioxide sequestered and it can be seen that most of the points are on the straight line. This supports our design without the use of transformations. Equation 4.2 is the equation for the amount of carbon dioxide sequestered.

Table 4-16: Sequential Model Sum of Squares for Amount of CO_2 Sequestered (mmmscf)

Source	Sum of Squares	DF	Mean Square	F Value	Prob > F	
Mean	5252580.006	1	5252580.006			
Linear	151667.2207	8	18958.40259	11.98580284	< 0.0001	
2FI	69792.76138	28	2492.598621	15.12092752	< 0.0001	Suggested
Quadratic	2022.176999	8	252.7721248	2.674779862	0.074	
Cubic	945.0202929	5	189.0040586	63660000	< 0.0001	Aliased
Residual	0	5	0			
Total	5477007.186	55	99581.94883			

Table 4-17: Model Summary Statistics for Amount of CO_2 Sequestered (mmmscf)

Source	Std. Dev.	R-Squared	Adjusted R-Squared	Predicted R-Squared	PRESS	
Linear	39.7710728	0.675797027	0.619413902	0.53258336	104901	
2FI	12.8391703	0.986778797	0.960336391	0.822724559	39785.43	Suggested
Quadratic	9.721215422	0.99578919	0.977261624	0.269409377	163964.4	

Table 4-18: Analysis of Variance for Amount of CO_2 Sequestered (mmmscf)

	Sum of Squares	DF	Sum of Squares/DF	F Value	Prob > F
Model	221459.9821	36	6151.66617	37.31804	< 0.0001
A	10.81527592	1	10.81527592	0.065609	0.80
B	17226.91123	1	17226.91123	104.5041	< 0.0001
C	132.0819314	1	132.0819314	0.801253	0.38

Table 4-18: Continued

	Sum of Squares	DF	Sum of Squares/DF	F Value	Prob > F
D	33507.08798	1	33507.08798	203.2651	< 0.0001
E	1.184878843	1	1.184878843	0.007188	0.93
F	25084.32677	1	25084.32677	152.1698	< 0.0001
G	31.9556458	1	31.9556458	0.193854	0.66
H	10584.88441	1	10584.88441	64.21141	< 0.0001
AB	828.6240258	1	828.6240258	5.026707	0.038
AC	73.94209245	1	73.94209245	0.448557	0.51
AD	209.5391571	1	209.5391571	1.271134	0.27
AE	574.6789109	1	574.6789109	3.486192	0.078
AF	7.502051419	1	7.502051419	0.04551	0.83
AG	114.1880438	1	114.1880438	0.692702	0.42
AH	88.92475826	1	88.92475826	0.539447	0.47
BC	2.49965786	1	2.49965786	0.015164	0.90
BD	209.8977689	1	209.8977689	1.273309	0.27
BE	393.8690835	1	393.8690835	2.38934	0.14
BF	32634.37604	1	32634.37604	197.9709	< 0.0001
BG	376.6056238	1	376.6056238	2.284614	0.15
BH	263.5838721	1	263.5838721	1.598987	0.22
CD	380.7087035	1	380.7087035	2.309505	0.15
CE	484.5521966	1	484.5521966	2.939454	0.10
CF	530.1642436	1	530.1642436	3.216152	0.090
CG	27.36683609	1	27.36683609	0.166016	0.69
CH	87.12884534	1	87.12884534	0.528552	0.48
DE	452.8346846	1	452.8346846	2.747045	0.11
DF	1511.820204	1	1511.820204	9.171201	0.0072
DG	526.3694733	1	526.3694733	3.193131	0.091
DH	10967.7871	1	10967.7871	66.53422	< 0.0001
EF	23.53761945	1	23.53761945	0.142787	0.71
EG	23.57070452	1	23.57070452	0.142988	0.71
EH	163.064266	1	163.064266	0.989202	0.33
FG	63.06544439	1	63.06544439	0.382576	0.54
FH	58.0912194	1	58.0912194	0.352401	0.56
GH	309.7075508	1	309.7075508	1.878788	0.19

Amount of CO_2 Sequestered= (4.2)

3619.08	
6.98889	* Inj-1 (x)
-15.1035	* Inj-1 (y)
8.160824	* Inj-2 (x)
-5.09137	* Inj-2 (y)
-12.1323	* Pro-1 (x)
-23.5994	* Pro-1 (y)
1.177448	* Pro-2 (x)
-13.0049	* Pro-2 (y)
0.077342	* Inj-1 (x) * Inj-1 (y)
-0.12182	* Inj-1 (x) * Inj-2 (x)
-0.03795	* Inj-1 (x) * Inj-2 (y)
-0.27868	* Inj-1 (x) * Pro-1 (x)
-0.00655	* Inj-1 (x) * Pro-1 (y)
-0.14655	* Inj-1 (x) * Pro-2 (x)
-0.02354	* Inj-1 (x) * Pro-2 (y)
-0.00547	* Inj-1 (y) * Inj-2 (x)
0.009279	* Inj-1 (y) * Inj-2 (y)
-0.05708	* Inj-1 (y) * Pro-1 (x)
0.110368	* Inj-1 (y) * Pro-1 (y)
0.063036	* Inj-1 (y) * Pro-2 (x)
0.009769	* Inj-1 (y) * Pro-2 (y)
-0.06414	* Inj-2 (x) * Inj-2 (y)
0.310112	* Inj-2 (x) * Pro-1 (x)
0.073307	* Inj-2 (x) * Pro-1 (y)
-0.09863	* Inj-2 (x) * Pro-2 (x)
-0.03104	* Inj-2 (x) * Pro-2 (y)
0.059595	* Inj-2 (y) * Pro-1 (x)
0.023683	* Inj-2 (y) * Pro-1 (y)
-0.0729	* Inj-2 (y) * Pro-2 (x)
0.06069	* Inj-2 (y) * Pro-2 (y)
-0.0114	* Pro-1 (x) * Pro-1 (y)
0.067329	* Pro-1 (x) * Pro-2 (x)
0.033537	* Pro-1 (x) * Pro-2 (y)

-0.025 * Pro-1 (y) * Pro-2 (x)
0.004745 * Pro-1 (y) * Pro-2 (y)
0.061052 * Pro-2 (x) * Pro-2 (y)

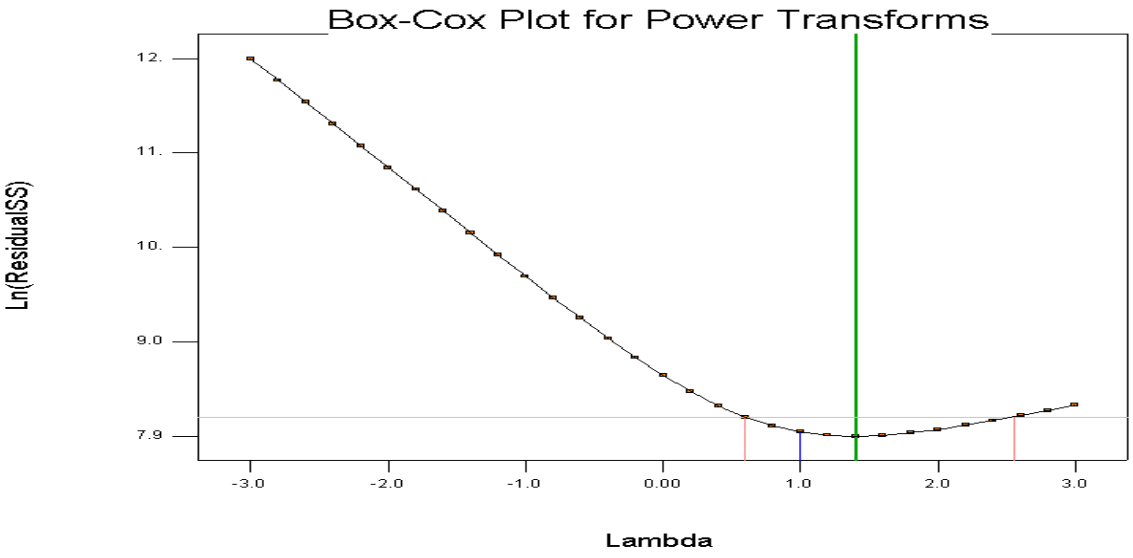

Figure 4-16: Box-Cox Plot for Amount of CO_2 Sequestered (mmmscf)

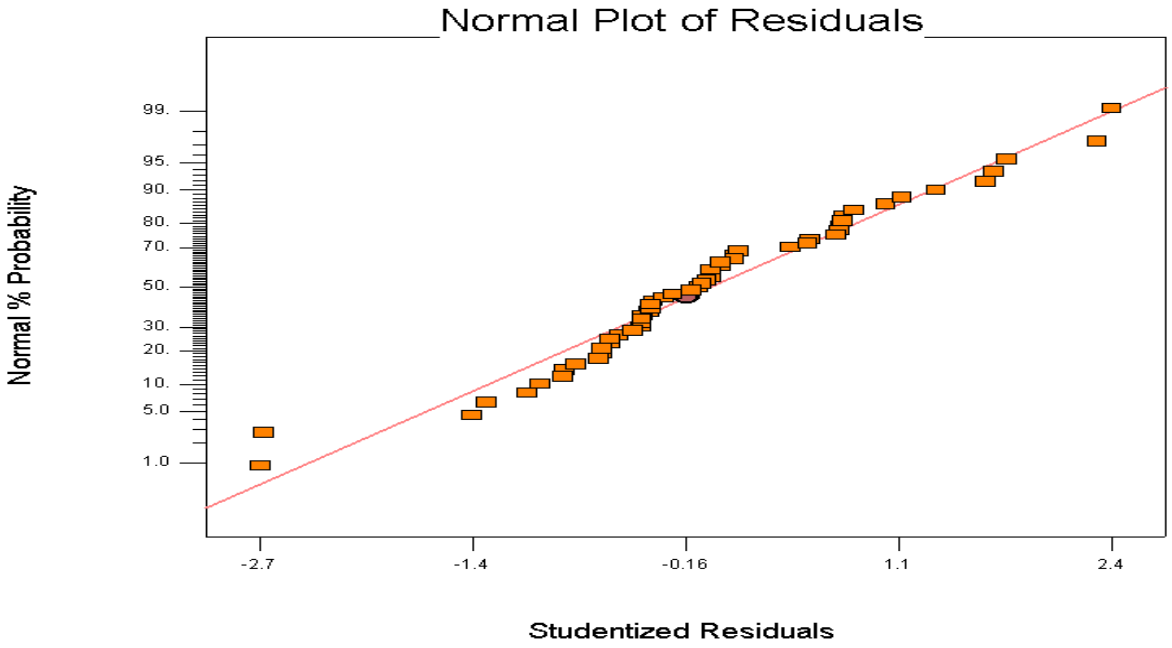

Figure 4-17: Normal Plot of Residuals for Amount of CO_2 Sequestered (mmmscf)

4.4.3 Co-Optimization of Cumulative Methane Production and Amount of CO_2 Sequestered, by Using Desirability Functions

Desirability functions are used to co-optimize the cumulative methane production and the amount of carbon dioxide sequestered response functions. In this study, the aim is to find the optimum conditions to maximize both cumulative methane production and the amount of carbon dioxide sequestered. Hence, to find the optimum values for the parameters, design parameters are used in a given range and response functions are set as the maximum. To co-optimize the response functions, the Design-Expert software version 6 (Stat-Ease Inc, 2005) is used. Design goals and the limits for each parameter and response function are presented in Table 4-19. After setting the goals and limits, the next step is finding the optimum solutions. By using the Design-Expert software version 6 (Stat-Ease Inc, 2005) ten solutions are generated. According to Myers et al. (2002), the goal is achieved when the value of the desirability is equal to one. Table 4-20 presents the solutions. According to Table 4-20, first solution has the highest desirability, which means that maximum recovery and storage goal can be achieved by using first solution. However, the results need to be checked by simulating the solution to see the reliability of the design.

Table 4-19: Design Goals and Limits for Each Parameter

Name	Goal	Lower Limit	Upper Limit
Inj-1 (x)	is in range	2	10
Inj-1 (y)	is in range	133	167
Inj-2 (x)	is in range	26	32
Inj-2 (y)	is in range	133	167
Pro-1 (x)	is in range	2	10
Pro-1 (y)	is in range	93	127
Pro-2 (x)	is in range	26	32
Pro-2 (y)	is in range	93	127
Methane Production	maximize	28.8846	66.3507
Amount of CO_2 Sequestered	maximize	138.906	377.182

Table 4-20: Solutions to Maximize the Response Functions

Solutions	Inj-1 (x)	Inj-1 (y)	Inj-2 (x)	Inj-2 (y)	Pro-1 (x)	Pro-1 (y)	Pro-2 (x)	Pro-2 (y)	Methane Production (mmmscf)	Amount of CO_2 Sequestered (mmmscf)	Desirability
1	3.8	1.7E+002	26.	1.7E+002	6.8	1.3E+002	30.	1.3E+002	66.	3.8E+002	0.9943
2	2.0	1.7E+002	28.	1.7E+002	10.	1.2E+002	32.	1.2E+002	65.	3.7E+002	0.967624
3	3.2	1.4E+002	27.	1.7E+002	10.	93.	26.	1.1E+002	64.	3.8E+002	0.967341
4	4.4	1.7E+002	31.	1.7E+002	10.	1.3E+002	28.	96.	65.	3.7E+002	0.962955
5	2.0	1.7E+002	32.	1.7E+002	10.	1.2E+002	28.	1.0E+002	64.	3.7E+002	0.954849
6	6.2	1.3E+002	26.	1.7E+002	6.4	93.	26.	1.0E+002	63.	3.8E+002	0.948712
7	9.9	1.7E+002	32.	1.7E+002	7.5	1.2E+002	30.	1.1E+002	64.	3.7E+002	0.944246
8	9.9	1.7E+002	26.	1.7E+002	4.8	1.1E+002	26.	1.1E+002	63.	3.7E+002	0.939805
9	6.7	1.3E+002	32.	1.4E+002	10.	94.	26.	93.	61.	3.7E+002	0.914963
10	3.8	1.3E+002	27.	1.5E+002	7.2	93.	26.	1.0E+002	61.	3.7E+002	0.905112

After finding the best solution that gives the maximum cumulative methane production and the maximum amount of carbon dioxide sequestered, it must be checked by simulation results. A new case is generated based on this solution and run using CMG's (2008) compositional simulator. Figure 4-18 presents the optimum well locations and Table 4-21 shows the design results, simulation results, and the difference between them. According to Table 4-21, the difference between the design and simulation results is very small, which means that our design is reliable. Equations generated for the design can be used for future studies. Also, the experimental design and response surface

methodology showed its success in a carbon dioxide sequestration and methane production for a geopressured-geothermal aquifer study.

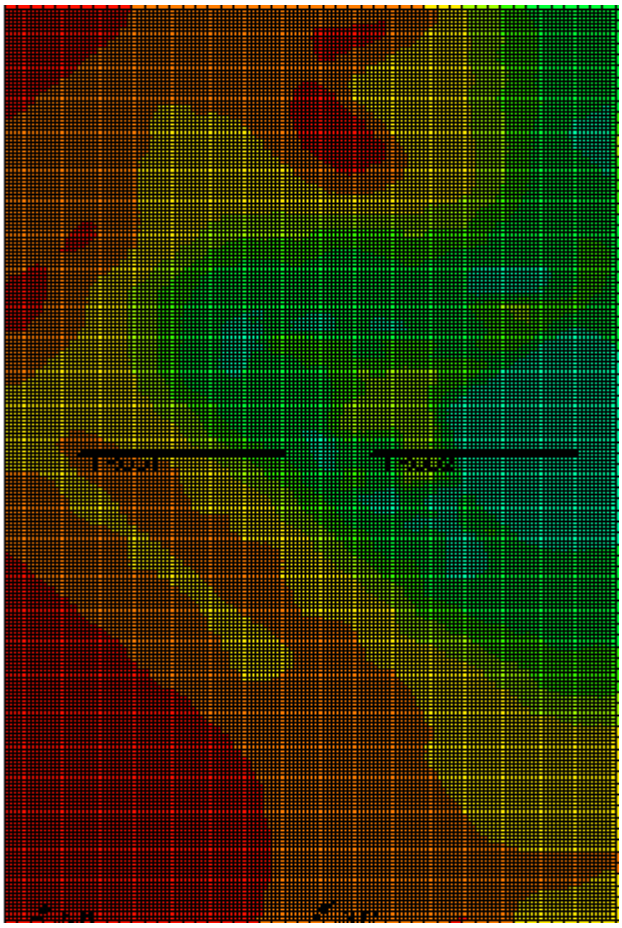

Figure 4-18: Optimized Well Locations, Permeability

Table 4-21: Design Results with Simulation Results

	Cumulative Methane Production (mmmscf)	Amount of CO_2 Sequestered (mmmscf)
Design	66	3.80E+02
Simulation	66.98	3.76E+02
Difference	-0.98	4.00E+00

4.4.4 Economic Investigation of the Co-optimized CO_2 Sequestration and Methane Recovery from Geopressured-Geothermal Aquifers

Co-optimization of carbon dioxide sequestration and methane production is presented in this section. As previously discussed, another aim of this study is to understand whether the project is profitable or not for different scenarios. The economic model used to calculate the net income from the project is given in Section 4.3 and solution to maximize the objective functions is given in Table 4-20. The first and the best solution in Table 4-20 is used to build a new case and run by GEM, CMG's (2008) compositional simulator. Methane price, energy price, horizontal, and vertical well costs are selected as variables to calculate the net income for different scenarios. Allowing it to will be possible to see the profit of the project for different conditions. By using the economic model given in Section 4.3, a code is written in Excel to find the net income and output of the solution, obtained from the simulator, is entered in a spreadsheet. Two different cases are generated based on the well cost. Table 4-22 shows the low case for the lower well cost and Figure 4-19 presents the three-dimensional surface chart for the low case. Horizontal well costs are approximately 10 ($MM) and vertical well costs are approximately 7.5 ($MM) for the low case. It can be seen that the net income is positive when the total of the energy and methane price is more than six dollars. Table 4-23 presents the high case for the higher well cost and Figure 4-20 shows the three-dimensional surface chart for the high case. Horizontal well cost is assumed as 20 ($MM) and vertical well cost is assumed as 15 ($MM) in the high case. For the high case, it is found that there is positive cash flow when the total of the methane price and energy price is higher than eight dollars.

Table 4-22: Low Case for Lower Well Cost

Energy Price ($/BTU) / Methane Price ($/mcf)	2	3	4	5	6
2	-40	-27.0112	-7.39955	12.21212	31.82379
3	-29.0598	-9.44809	10.16358	29.77525	49.38692
4	-11.4966	8.115048	27.72672	47.33839	66.95006
5	6.066512	25.67818	45.28985	64.90152	84.51319
6	23.62965	43.24132	62.85299	82.46466	102.0763

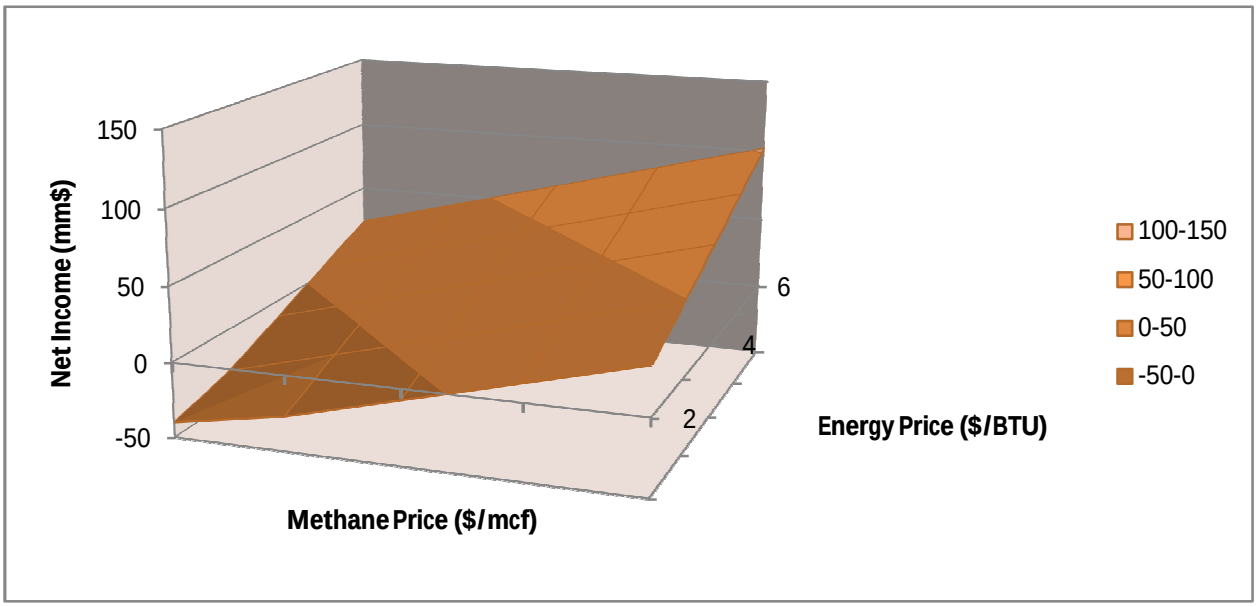

Figure 4-19: Three Dimensional Surface Chart for the Low Case

Table 4-23: High Case for Higher Well Cost

Energy Price ($/BTU) / Methane Price ($/mcf)	2	3	4	5	6
2	-75	-62.0112	-42.3995	-22.7879	-3.17621
3	-64.0598	-44.4481	-24.8364	-5.22475	14.38692
4	-46.4966	-26.885	-7.27328	12.33839	31.95006
5	-28.9335	-9.32182	10.28985	29.90152	49.51319
6	-11.3704	8.241316	27.85299	47.46466	67.07633

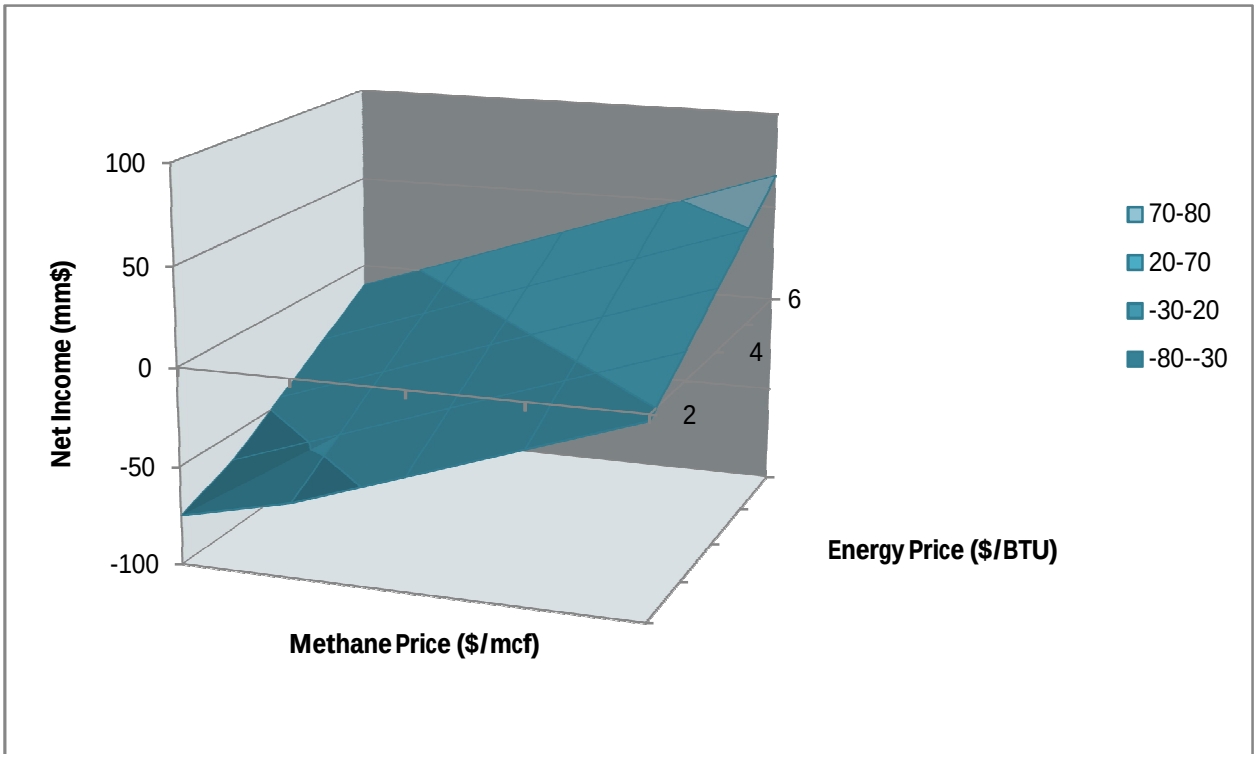

Figure 4-20: Three-Dimensional Surface Chart for the High Case

4.5 CONCLUSION

In this study, carbon dioxide sequestration and methane recovery is co-optimized by using experimental design and response surface methodology. The aim of the project is to maximize both carbon dioxide sequestration and cumulative methane production. Before deciding the design parameters, some scenarios were generated and ran in the development section. Based on these simulation results, it is decided to use horizontal wells for the production to increase the production and vertical wells for the injection to decrease the well cost. For the injection scheme, it is decided to inject the carbon dioxide into the water at the surface, and then inject the water into the aquifer. Coordinates of the injection and production wells are chosen as parameters for the design. The reservoir is

divided into four parts and the range of each well coordinate is determined. The amount of carbon dioxide sequestered and cumulative methane production are set as response functions. The quadratic model is used and fifty-five cases are generated. Results of these cases are obtained from the simulator and used in the design to build response surface functions. After completing the design, the cumulative methane production is 66 (mmmscf) and amount of carbon dioxide sequestered is 3.80E+02 (mmmscf) by using optimized values for the well coordinates. The optimized solution is compared with simulation results and it is determined that error is very small, which demonstrates that the experimental design and response surface methodology is reliable and can be used in co-optimizing carbon dioxide sequestration and methane recovery processes.

Another aim of this study is to understand under which conditions carbon dioxide sequestration and methane recovery project is profitable. To offset the project costs, electricity is generated from produced hot water. An excel spreadsheet is prepared to calculate the net income. Two different cases are generated by changing the well costs and seventy-two different cases are generated by changing the methane price and energy price. Conditions needed to make the project profitable are found and are presented in Section 4.4.4.

Chapter 5: Conclusions

In this study, two different approaches to sequester carbon dioxide are examined. These are sequestering the carbon dioxide into a mature oil field and a geopressured-geothermal aquifer which are located in Texas. The aims of these two studies are to find the best strategies to sequester the maximum amount of carbon dioxide and to obtain the maximum profit.

In the first part of this study, experimental design and response surface methodology is used to co-optimize the carbon dioxide sequestration and net income from the project. The water alternating pure carbon dioxide injection method is modified and solvent is used instead of pure carbon dioxide. In this section, for the optimization purposes, total slug size, ratio of water and gas, injection rate, well configuration, well configuration and time for drilling the third well are selected as parameters which are need to be optimized to find the best strategy for the above mentioned task. The optimum result from the design is run by using a simulator and is compared with design results. According to the results, the experimental design and response surface methodology is an efficient method and can be used for the oil field designs. Also, by using this method, the required number of simulations is decreased from $2^{11} = 2048$ to 80, which is a much less expensive and more time-efficient method. After finding the best strategy, optimized results were compared with the water alternating gas injection method used for the same model developed by Salazar (2009). It is concluded that by using the water alternating solvent injection method, the profit for the project can be increased and by using the water alternating pure carbon dioxide injection method, more carbon dioxide can be sequestered.

In the second part of this study, a geopressured-geothermal reservoir model was built and used to co-optimize the amount of carbon dioxide sequestered, methane recovery, and income from the project. To offset the project costs it was assumed that electricity was generated from the hot brine while extracting the methane. Before deciding the design parameters, different scenarios were built by changing the well locations and well constraints. It is concluded that using horizontal wells for the producers and using vertical wells for the injectors is more profitable, while using horizontal wells for the injectors increases the amount of carbon dioxide that can be sequestered. After deciding the well configuration, the reservoir is divided into four parts. The results show that drilling the injectors at the bottom of the lower part of the reservoir and drilling the producers at the top of the above part of the reservoir have better sweep efficiency allowing more carbon dioxide to be sequestered. To find the optimum locations for the wells and to maximize the methane recovery and carbon dioxide storage, the experimental design and response surface methodology is used. The optimum solution is found by using the experimental design method and then compared with the simulation results. The error was very small so that it can be concluded that experimental design and response surface methodology is a reliable method to be used for such studies. In the last part of this work, net income was calculated for different conditions. Methane price, energy price, and well costs are used as parameters. Conditions required to make the project profitable are given in Section 4.4.4.

Bibliography

Akinnikawe, O., Chaudhary, A., Vasquez, O., Enih, C., and Ehlig-Economides, C. 2010. Increasing CO_2-Storage Efficiency through a CO_2-Brine Displacement Approach. Paper SPE 139467 presented at the SPE International Conference on CO_2 capture, Storage, and Utilization, New Orleans, Louisiana, USA, 10-12 November.

Bachu, S. 2000. Climate Change and Sequestration of CO_2 in Geological Media: a Viable Option for the Energy Industry. Presented at the 16th World Petroleum Congress, Calgary, Canada, June 11 - 15.

Basbug, B., Gumrah, F., and Oz, B. 2005. Simulating the Effects of Deep Saline Aquifer on CO_2 Sequestration. Presented at the Petroleum Society's 6th Canadian International Petroleum Conference (56th Annual Technical Meeting), Calgary, Alberta, Canada, June 7 – 9.

Bayliss, B. 1972. Introduction to Geothermal Energy. Paper SPE 4176 presented at the 43rd Annual SPE California Regional Meeting, Bakersfield, California, November 8-10.

Budd, C. F. 1984. Geothermal Energy for Electrical Generation. Journal of Petroleum Technology, 36(2), 189–195.

Burton, M. and Bryant, S. 2007. Eliminating Buoyant Migration of Sequestered CO_2 Through Surface Dissolution: Implementation Costs and Technical Challenges. Paper SPE 110650 presented at the SPE Annual Technical Conference and Exhibition, Anaheim, California, USA, November 11-14.

Chen, S., Li, H., Yang, D., and Tontiwachwuthikul, P. 2009. Optimal Parametric Design for Water- Alternating-Gas (WAG) Process in a CO_2 Miscible Flooding Reservoir. Journal of Canadian Petroleum Technology, Vol. 49, No. 10, p. 75-82.

Chen, S., Li, H., and Yang, D. 2010. Optimization of Production Performance in a CO_2 Flooding Reservoir under Uncertainty. Journal of Canadian Petroleum Technology, Vol. 49, No. 2, p. 71-78.

Design-Expert, Version 6.0.11, Stat-Ease, Inc., 2005.

Doscher, T., Osborne, R., Wilson, T., Rhee, S., Cox, D., and Kuuskraa, V. 1979. The Technology and Economics of Methane Production from Geopressured Aquifers. Journal of Petroleum Technology, Vol. 31, No. 12, p. 1502-1514.

Ennis-King, J. and Lincoln, P. 2002. Engineering Aspects of Geological Sequestration of Carbon Dioxide. Paper SPE 77809 presented at the Asia Pacific Oil and Gas Conference and Exhibition, Melbourne, Australia, October 8-10.

Forooghi, A., Hamouda, A., and Eilertsen, T. 2009. Co-optimization of CO_2 EOR and Sequestration Process in a North Sea Chalk Reservoir. Paper SPE 125550 presented at the SPE/EAGE Reservoir Characterization and Simulation Conference, Abu Dhabi, UAE, October 19-21.

Freund, P. 2000. Progress in Understanding the Potential Role of CO_2 Storage. Presented at the Fifth International Conference on Greenhouse Gas Control Technologies.

Gallo, Y., Couillens, P., and Manai, T. 2002. CO_2 Sequestration in Depleted Oil or Gas Reservoirs. Paper SPE 74104 presented at the International Conference on Health, Safety and Environment in Oil and Gas Exploration and Production, Kuala Lumpur, Malaysia, March 20-22.

GEM, Advanced Compositional Reservoir Simulator, Computer Modeling Group Ltd., 2008.

Ghomian, Y. 2008. Reservoir Simulation Studies for Coupled CO_2 Sequestration and Enhanced Oil Recovery. Ph.D. dissertation, The University of Texas at Austin, Austin, Texas.

Griggs, J. S. 2004. A Re-Evaluation of Geopressured-Geothermal Aquifers as an Energy

Resource. M.S. Thesis, Louisiana State University.

Gui, P., Jia, X., Cunha, J., and Cunha L. 2008. Economic Analysis for Enhanced CO_2 Injection and Sequestration Using Horizontal Wells. Journal of Canadian Petroleum, Vol. 47, No. 11.

Hammershaimb, E. and Kuuskraa, V. 1984. The Economic Potential of Reinjection into Geopressured Aquifers. Journal of Petroleum Technology, Vol. 36, No. 7, p. 1164-1170.

Hawkins, M. F. and Parmigiano, J. M. 1973. Geopressured Water as an Energy Resource.

Hoffert, M.I. 2002. Advanced Technology Paths to Global Climate Stability: Energy for a Greenhouse Planet, Science 298, 981-987.

Hydrothermal Power Systems. (2010). http://www1.eere.energy.gov/geothermal/powerplants.html#binarycycle.

John, C. J., Maciasz, G., and Harder, B. J. 1998. Gulf Coast Geopressured-Geothermal Program Summary Report Compilation Executive Summary.

Karsner, A., 2007. Texas Geothermal Energy, U.S. Department of Energy.

http://www.seco.cpa.state.tx.us/re_geothermal.html.

Kartikasurja, D. O., Rds, H., Lin, T. G., Sukahar, M. W., and Viratno, B. 2008. Study of Produced CO_2 Storage into Aquifer in an Offshore Field , Malaysia. Paper SPE 114553 presented at the 2008 SPE Asia Pacific Oil & Gas Conference and Exhibition, Perth, Australia, October 20-22.

Keeling C.D., Whorf T.P., Wahlen M., and Vanderplicht J. 1995. Interannual Extremes in the Rate of Atmospheric Carbon Dioxide Since 1980. Nature 1995; 375(6533):666–70.

Kovcek, A.R., and Cakici, M.D. 2005. Geologic Storage of Carbon Dioxide and Enhanced Oil Recovery. II. Cooptimization of Storage and Recovery. Journal of Energy Conversion and Management, Vol. 46, (11-12), p. 1941-1956.

Kumar, A., Noh, M., Pope, G. A., Sepehrnoori, K., Bryant, S., and Lake, L. W. 2004. Reservoir Simulation of CO_2 Storage in Deep Saline Aquifers. Paper SPE 89343 presented at SPE/DOE Fourteenth Symposium on Improved Oil Recovery, Tulsa, Oklahoma, April 17-21.

Lee, K. S., and Kyonggi, U. 2000. Analysis on the Depletion and Recovery Behavior of a Geopressured/Geothermal Reservoir. Paper SPE 64516 presented at the SPE Asia Pacific Oil and Gas Conference and Exhibition, Brisbane, Australia, October 16-18.

MacDonald, R., Ohkuma, H., AND Sepehrnoori, K. 1979. U.S. Gulf Coast Geopressured-Geothermal Reservoir Simulation Final Report (Year 4).

Matthews, C. S. 1981. Possibilities of Enhancing Gas Production from Geopressured Aquifers.

McCarthy J. J., Canziani, O.F., Leary, N.A., Dokken D.J., and White K.S. 2001. IPCC 2001b, Climate Change 2001: Impacts, Adaptation and Vulnerability, Contribution of Working Group II to the Third Assessment Report of the Intergovernmental Panel on Climate Change, Cambridge University Press.

Montgomery, D. C. 1984. Design and Analysis of Experiments (2nd Ed.), John Wiley & Sons, New York.

Myers, R. H. and Montgomery, D. C. 2002. Response Surface Methodology: Process and Product Optimization Using Designed Experiments (2nd Ed.), John Wiley & Sons, New York.

Nguyen, D. 2003. Carbon Dioxide Geological Sequestration: Technical and Economic Reviews. Paper SPE 81119 presented at SPE/EPA/DOE Exploration and Production Environmental Conference, San Antonio, Texas, March 10-12.

Odi, U. and Gupta, A. 2010. Optimization and Design of Carbon Dioxide Flooding. Paper SPE 138684 presented at the Abu Dhabi International Petroleum Exhibition and Conference, Abu Dhabi, UAE, November 1-4.

Ozah, R., Lakshminarasimhan, S., Pope, G., Sepehrnoori, K., and Brynt, S. 2006. Numerical Simulation of CO_2 and CO_2/H_2S Storage in Deep Saline Aquifers. Journal of Petroleum Technology, Vol. 58, No. 8, p. 68–70.

Petrusak, R., Riestenberg, D., Goad, P., Schepers, K., Pashin, J., Esposito, R., and Trautz, R. 2009. World Class CO_2 Sequestration Potential in Saline Formations, Oil and Gas Fields, Coal, and Shale: The US Southeast Regional Carbon Sequestration Partnership Has It All. Paper SPE 126619 presented at SPE International Conference on CO_2 Capture, Storage, and Utilization, San Diego, California, November 2-4.

Righi, E., Royo, J., Gentil, P., Castelo, R., Monte, A., and Bosco, S. 2004. Experimental Study of Tertiary Immiscible WAG Injection. Paper SPE 89360 presented at SPE/DOE Symposium on Improved Oil Recovery, Tulsa, Oklahoma, April 17-21.

Rogers, J. and Grigg, R. 2001. A Literature Analysis of the WAG Injectivity Abnormalities in the CO_2 Process. Presented at SPE/DOE Improved Oil Recovery Symposium, Tulsa, Oklahoma, April 3-5.

Salazar, J.E.R. 2009. Coupled CO_2 Sequestration and Enhanced Oil Recovery Optimization Using Experimental Design and Response Surface Methodology. M.S. thesis, The University of Texas at Austin, Austin, Texas.

Sanchez, N. 1999. Management of Water Alternating Gas (WAG) Injection Projects. Paper SPE 53714 presented at Latin American and Caribbean Petroleum Engineering Conference, Caracas, Venezuela, April 21-23.

Schneider, C. and Shi, W. 2005. A Miscible WAG Project Using Horizontal Wells in a Mature Offshore Carbonate Middle East Reservoir. Paper SPE 93606 presented at SPE Middle East Oil and Gas Show and Conference, Kingdom of Bahrain, March 12-15.

Taheri, A. and Sajjadian, V. A. 2006. WAG Performance in a Low Porosity and Low Permeability Reservoir. Paper SPE 100212 presented at SPE Asia Pacific Oil & Gas Conference and Exhibition, Adelaide, Australia, September 11-13.

Taggart, I. 2010. Extraction of Dissolved Methane in Brines by CO_2 Injection: Implication for CO_2 Sequestration. Journal of SPE Reservoir Evaluation & Engineering, Vol. 13, No. 5, p. 791-804.

Tamhane, A. C. 2009. Statistical Analysis of Designed Experiments: Theory and Applications, John Wiley & Sons, New Jersey.

Tans, P., 2011. NOAA/ESRL, http://www.esrl.noaa.gov/gmd/ccgg/trends.

Torabi, F., Jamaloei, B. Y., Zarivnyy, O., and Paquin, B. A. 2010. Effect of Oil Viscosity, Permeability and Injection Rate on Performance of Waterflooding , CO_2 Flooding and WAG Process in Recovery of Heavy Oils. Paper SPE 138188 presented at Canadian Unconventional Resources and International Petroleum Conference, October 19-21, Calgary, Alberta, Canada.

Vidiuk, K., and Cunha, L. B. 2007. A Simulation Study of Effects of Operational Procedures in CO_2 Flooding Projects for EOR and Sequestration. Presented at Canadian International Petroleum Conference, Jun 12 - 14, Calgary, Alberta.

Wu, X., Ogbe, D. O., Zhu, T., and Khataniar, S. 2004. Critical Design Factors and Evaluation of Recovery Performance of Miscible Displacement and WAG Process. Presented at Canadian International Petroleum Conference, June 1 - 8, Calgary, Alberta.

Vita

Serdar Bender was born on October 16, 1985, the son of Kaplan and Sati Bender, in Ankara, Turkiye. He has a younger sister named Simay Bender. He received his B.S. in Petroleum and Natural Gas Engineering from Middle East Technical University in 2008. He worked for Turkish Petroleum Corporation (TPAO) as a production engineer from 2008 to 2009. In 2009, he received a scholarship from the Turkish Petroleum Corporation to study M.S. in Petroleum & Geosystems Engineering at The University of Texas at Austin.

Permanent address: 490. Sokak 3/13 Birlik Mahllesi Cankaya-Ankara/Turkiye

This thesis was typed by the author.